COHERENT RESONANT INTERACTION AND HARMONIC GENERATION IN ATOMIC VAPORS

DISSERTATION

Presented to the Graduate Council of the
North Texas State University in Partial
Fulfillment of the Requirements

For the Degree of

DOCTOR OF PHILOSOPHY

By

Nandini Mukherjee, M.Sc., M.S.
Denton, Texas

August, 1987

Mukherjee, Nandini, Coherent Resonant Interaction and Harmonic Generation in Atomic Vapors. Doctor of Philosophy (Physics), August, 1987, 243 pages, 4 tables, 60 illustrations, bibliography, 32 titles.

This work examines the use of higher order multiphoton resonances in higher harmonic generation together with judicious exploitation of coherent interaction properties to achieve efficient harmonic generation. A detailed experimental study on third harmonic generation in two photon resonant coherent interaction and a theoretical study on four photon resonant coherent interaction have been conducted.

Two photon resonant coherent propagation in lithium vapor (2S-4S and 2S-3D interaction) has been studied in detail as a function of phase and delay of the interacting pulse sequence. Under coherent lossless propagation of 90° phase shifted pulse pair, third harmonic generation is enhanced. A maximum energy conversion efficiency of 1% was measured experimentally. This experiment shows that phase correlated pulse sequence can be used to control multiphoton coherent resonant effects.

A larger two photon resonant enhancement does not result in more efficient harmonic generation, in agreement with the theoretical prediction.

An accurate (to at least 0.5 Å) measurement of intensity dependent Stark shift has been done with the newly developed "interferometric wavemeter." Stark shifts as big as

several pulse bandwidths (of picosecond pulses) result in a poor tuning of multiphoton resonance and become a limiting factor of resonant harmonic generation.

A complete theory has been developed for harmonic generation in a four photon resonant coherent interaction. A numerical application of the theory to the Hg atom successfully interprets the experimental observations in terms of the phase dependent stimulated Raman scattering. With the intensity required for four photon resonant transition, the calculation predicts a dramatic Stark shift effect which completely destroys the resonance condition. This model provides a basis for the development of future schemes for efficient higher order coherent upconversion.

TABLE OF CONTENTS

LIST OF TABLES

LIST OF ILLUSTRATIONS

CHAPTER I

INTRODUCTION

With the development of the ultrashort light pulses of picosecond (ps, 10^{-12} sec) and femtosecond (fs, 10^{-15} sec) duration[1,2] a new door has opened in the field of light matter interaction. Such time scales are comparable to or even shorter than the phase memory time of atomic and molecular system. As a result, the polarisation induced in the medium by the short optical pulses retains a definite phase relationship with the inducing field. Under such circumstances the internal dynamics of the atom such as absorption or emission process can be controlled by controlling the phase of the incident pulse. Such phase correlated phenomena are called "coherent interaction." A simple minded picture of the coherent interaction can be drawn from the "Bohr model"of atom shown in FigI.1a. The stationary orbits of an atom are like clocks of different frequencies. The difference between the two clock frequencies corresponds to the transition frequency between the two stationary orbits. Initially the atom is in the ground state and the electron is following the clock of the lowest orbit 1 (clock frequency is ω_1). With an outward force $\vec{F}$ provided by the incident laser field in resonance with I1><——>I2> transition,the electron can be thrown to the outer orbit 2 following an absorption of energy from the

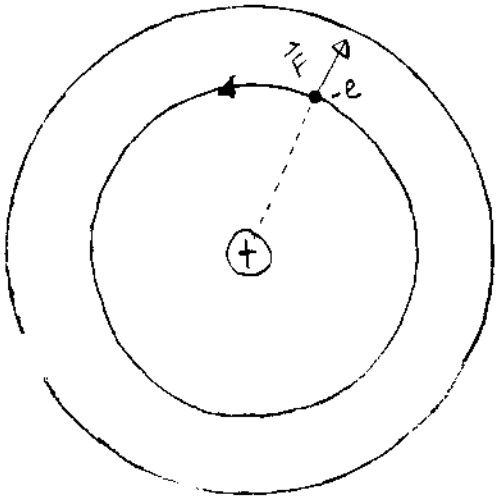

(a)

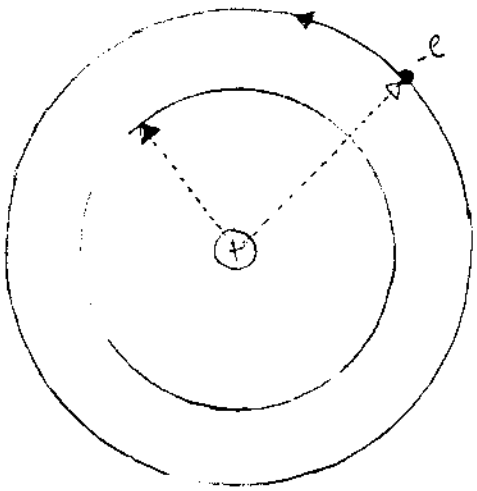

(b)

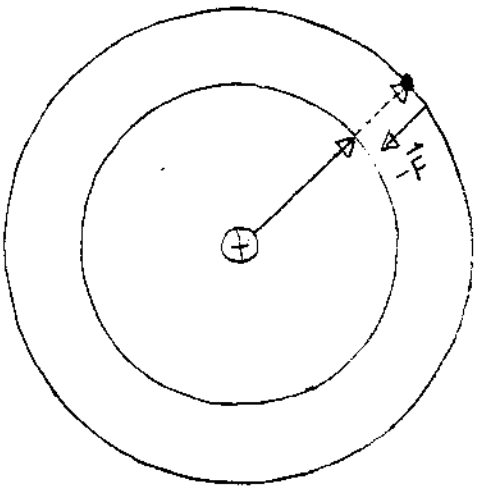

(c)

Fig I.1

incident light. The electron now follows the clock of the outer orbit, Fig I.1b (of clock frequency ω_2). In the absence of incoherent losses the two clocks come to the phase at time interval of $T = \frac{2\pi}{\omega_{21}}$. When the two clocks come to the same phase the electron can be brought back to the old orbit with a reverse force $-\vec{F}$ provided by a properly phase shifted input pulse (Fig I.1c),and the energy absorbed in the earlier process will be emitted back to the field. The idea of coherent interaction is to follow the atomic clocks with short light pulses of frequency equal to the difference frequency of two of the clocks. When the atomic clocks are followed, the absorption and emission processes in atomic transitions can be controlled. The experiments of self-induced transparency[3] and photon-echo[4] have revealed the striking features of coherent interaction of light with matter. The "vector model" of Feynman et al[5] has been successfuly applied to understand the atomic phase correlated interaction with optical pulses. Soon the study of such coherent interaction has been extended to multiphoton processes[6-11] where in presence of higher order nonlinearity many new effects such as multiphoton ionization, dynamic Stark shift, harmonic generation were observed which were absent in one photon processes. Coherent resonant multiphoton processes are extremely important for harmonic generation. The nonlinear susceptibility responsible for harmonic generation is enhanced by resonance condition. For instance third harmonic susceptibility is enhanced if the

medium has single ,two or three photon resonance with the incident field. The depletion of the pump wave by absorption (single or multiphoton) associated with these resonances limits the conversion efficiency that can generaly be achieved. Resonant absorption changes the index of refaction of the medium by changing the population of the resonant levels and under this circumstances phase matching becomes impossible. Coherent propagation effect can be used to keep all the energy in the radiation field even in the condition of resonance. For instance if a sequence of 90° phase shifted pulses is sent through a two photon resonant medium ,the energy absorbed from the first pulse can be returned back to the following pulse by two photon stimulated emission. Longer propagation length results in a stronger third harmonic generation. In crystals the absorption edge near 200nm limits the efficient harmonic generation. For this reason atomic vapors are very important sources of shorter wavelength VUV light. This work examines the use of higher order multiphoton resonances in higher harmonic generation together with judicious exploitation of coherent interaction properties to achieve efficient harmonic generation. The complexity of the interaction increases dramatically with the order of the multiphoton interaction. A four photon resonant interaction is not merely an extension of the two photon case. In view of the increasing phenomena of various order (single,two,three photon ionisation, quadratic and quartic Stark shift) a

general study is no longer possible. Therefore we have chosen a specific model (Hg) to carry out the study of the four photon resonant interaction. In this thesis an effort has been made to investigate and understand both theoretically and experimentally the new phenomena in multiphoton resonance processes.

The remainder of the thesis is composed in the following manner. Chapter II briefly discusses the basic idea of two photon resonant third harmonic generation (THG) under coherent excitation. Chapter III discusses an experiment of two photon resonant THG in Li vapor and analyses its interesting results. Chapter IV presents a theory of harmonic generation in a four photon resonant (FPR) coherent interaction. Chapter V shows an application of the FPR theory in Hg atom. The thesis concludes in Chapter VI with a brief summary of the work.

CHAPTER BIBLIOGRAPHY

1. Diels et al.,"intracavity pulse compression with glass," Optics Letters 8, 4 (1983).
2. Diels et al.,"Control and measurement of ultrashort pulse shapes," Applied Optics 24, 1270 (1985).
3. McCall S. L. and Hahn E. L.,"Self-induced transparency by pulsed coherent light," Physical Review Letters 18, 908 (1967).
4. Abella et al.,"Photon echoes," Physical Review 141, 391 (1966).
5. Feynmann et al., J.Appl.Phys. 28 ,49 (1957).
6. Diels.J.C., "Two-photon coherent propagation ,transmission of 90° phase shifted pulses.", Optical and Quantum Electronics 8, (1976) 513-522.
7. Belenov et al.,"Coherent effects in propagation of ultrashort light pulses in a medium with two-photon resonance absorption." Soviet Physics JEPT 29 , 754 (1969).
8. Grischkowsky et al.,"Adibatic following model for two photon transition." Physical Review A 12, 2514 (1975).
9. Georges et al.,"Theory of third harmonic generation in metal vapor under two photon resonant conditions." Physical Review A, 15, 300 (1977).

10. Diels et al.,"Coherent two photon resonant third and fifth harmonic generation in metal vapors." Physical Review A 19, 1589 (1979).

11. Mukherjee et al.,"Coherent multiphoton interaction using sequence of of picosecond pulses." Technical digest XIV International quantum electronics conference (IQEC ,86), p.78.

CHAPTER II

TWO PHOTON RESONANT THIRD HARMONIC GENERATION

A third harmonic susceptibility is enhanced in presence of intermediate two photon resonance (TPR). Two photon coherent as opposed to steady state excitation is required for efficient harmonic generation. Exact solution of Schroedinger and Maxwell's equations are needed for a complete description of resonant third harmonic generation (THG). Solution of Schroedinger equation gives the induced polarisation as a function of time and field strengths at a certain point in space. Using the induced polarisation Maxwell's equation determines the fields at the next point in space. Schroedinger's equation describes the local behavior while Maxwell's equation describes the propagation effect of the incident and the generated fields. Two photon coherent effects has been studied in detail by many people.[1-4] An extensive description of two photon resonance THG would be found in Ref 5. In this chapter a brief introduction of the subject will be given.

Third Harmonic Susceptibility of an Off Resonant System

The third harmonic polarisation induced in a system under off resonant excitation condition, is given by:

$$P_3 = \chi_3 E_1^3 \qquad \text{(II.1)}$$

where

E_1 = incident field at the fundamental frequency ω

P_3 = third harmonic polarisation at 3ω

χ_3 = third harmonic susceptibility of the medium

$$\chi_3 \sim \frac{\mu_{1f}\,\mu_{fk}\,\mu_{kl}\,\mu_{l1}}{(\omega_{f1}-\omega)(\omega_{k1}-2\omega)(\omega_{l1}-3\omega)} \qquad \text{(II.2)}$$

Summation is implied over the repeated indices. $|1\rangle$ is the ground state of the atom . $|f\rangle, |k\rangle, |l\rangle$ are the intermediate states (see Fig II.1). μ_{ij} and ω_{ij} are the dipole matrix elements and transition frequency of $|i\rangle \langle\!\rightarrow |j\rangle$ transition. Third harmonic emission takes place from a virtual level. This virtual level is created through the couplings of intermediate levels. χ_3 is enhanced by approaching any one of the intermediate resonances. In presence of an intermediate resonance χ_3 goes to infinity, in

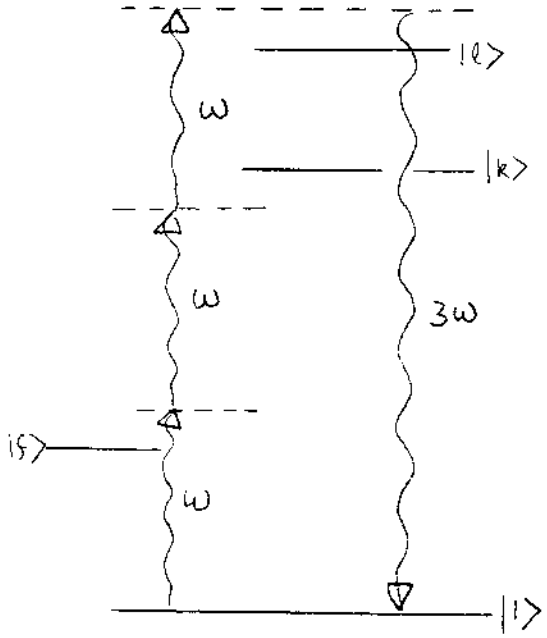

Fig II·1

other words equation (II.1) will no longer be a valid expression for P_3 . In case of resonance, an exact solution of Schroedinger's equation is needed to find the correct expression for P_3 . For THG one and three photon resonances are not particularly interesting as they will limit the efficiency of THG by introducing strong one photon absorption loss for the input first harmonic and generated fields. A two photon absorption on the other hand will have less loss. For higher intensities required to achieve the maximum conversion, depletion of the fundamental by two photon absorption limits the highest achievable conversion efficiency.[6]

Fig II.2 shows the two photon resonant system we are going to study. I1> is the ground state, I2> is the excited state, I1> and I2> states are connected by two photons from the incident first harmonic field. The third photon goes to the continuum. In this case the third harmonic level coincides with a real level in the ionisation continuum. As a result THG is accompanied by an inevitable two photon resonant three photon ionisation.

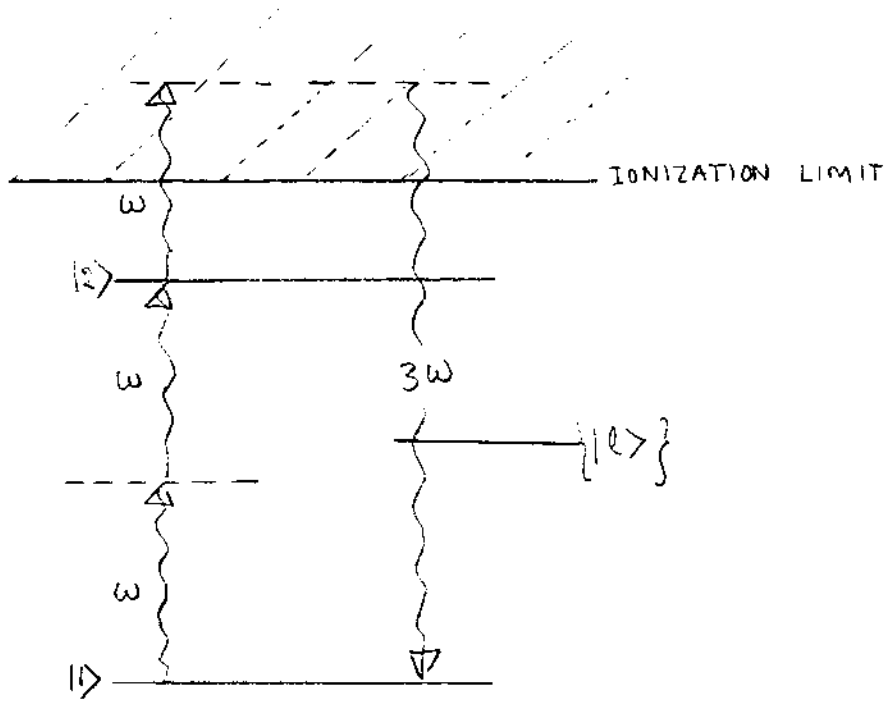

Fig II·2

Maxwell-Bloch Equation in a Two Photon Resonant Medium

An equivalent two level model has been developed for a TPR system.[1-5] A TPR system is then described by a 2X2 resonant density matrix ρ .

In presence of an electric field $\vec{E}$ given by

$$\vec{E} = \vec{\mathcal{E}}_1(z,t)\, e^{i(\omega t - Kz)} + \vec{\mathcal{E}}_3(z,t)\, e^{i3(\omega t - Kz)} + C.C. \qquad \text{(II.3)}$$

(where $\mathcal{E}_1(z,t)$ and $\mathcal{E}_3(z,t)$ are the slowly varying amplitudes of the first and third harmonic fields respectively) and with

$$\rho_{12} = \sigma_{12}\, e^{i2(\omega t - Kz)}$$

$$\rho_{11} = \sigma_{11}$$

$$\rho_{22} = \sigma_{22}$$

we have the two photon Bloch equation:

$$\frac{\partial \sigma_{12}}{\partial t} + i(2\omega - \omega_{21} - \delta\omega_{21})\sigma_{12} + \left(\frac{1}{T_2} + \frac{\gamma_1+\gamma_2}{2}\right)\sigma_{12}$$

$$= i(\sigma_{22} - \sigma_{11})\left[\frac{r_{12}}{\hbar^2}\mathcal{E}_1^2 + \frac{\xi_{21}^*}{\hbar^2}\mathcal{E}_1^*\mathcal{E}_3\right] \qquad \text{(II.4)}$$

$$\frac{\partial \sigma_{22}}{\partial t} + \left(\frac{1}{T_1} + \gamma_2\right)\sigma_{22}$$

$$= -2\,\mathrm{Im}\left\{\left(\frac{r_{12}}{\hbar^2}\mathcal{E}_1^{*2} + \frac{\xi_{21}}{\hbar^2}\mathcal{E}_1\mathcal{E}_3^*\right)\sigma_{12}\right\} \qquad \text{(II.5)}$$

$$\frac{\partial}{\partial t}(\sigma_{22} + \sigma_{11}) = -\gamma_1\sigma_{11} - \gamma_2\sigma_{22} \qquad \text{(II.6)}$$

ω_{21} = zero-field resonance frequency of 2<—>1 transition.

$\delta\omega_{21}$ = laser induced Stark-shift

γ_1 = intensity dependent ionization rate from level $|1\rangle$

γ_2 = intensity dependent ionization rate from level $|2\rangle$

T_1 = population relaxation time of level $|2\rangle$

T_2 = tranverse relaxation time, accounts phenomenologicaly for the decay of coherence due to both radiation damping and phase interrupting elastic collision.

$$\delta\omega_{21} = \frac{1}{\hbar}\left[\alpha_1'(\omega) - \alpha_2'(\omega)\right]|\mathcal{E}_1|^2 + \frac{1}{\hbar}\left[\alpha_1'(3\omega) - \alpha_2'(3\omega)\right]|\mathcal{E}_3|^2 \qquad \text{(II.7)}$$

$$\gamma_1 = \gamma_1^{3\omega} = \frac{2}{\hbar}\alpha_1''(3\omega)|\mathcal{E}_3|^2 \qquad \text{(II.8)}$$

$$\gamma_2 = \gamma_2^{\omega} + \gamma_2^{3\omega} = \frac{2}{\hbar}\left[\alpha_2''(\omega)|\mathcal{E}_1|^2 + \alpha_2''(3\omega)|\mathcal{E}_3|^2\right] \qquad \text{(II.9)}$$

there is 3 photon ionization $\gamma_1^{3\omega}$ from level I1> and 1 and 3 photon ionization γ_2^{ω} and $\gamma_2^{3\omega}$ from level I2>. The intensity dependent dynamic Stark shift as well as intensity dependent ionization are functions of space and time. Dynamic Stark shift is a special effect in multiphoton interaction. There is no such Stark shift in single photon case. Due to the space time dependent Stark shift resonance condition changes both in time and space. In order to have two photon absorption over a certain distance a constant intensity of the pulse has to be maintained. Only under loss-less coherent propagation TPR condition will be maintained over longer distance. Ionization is an incohernt loss mechanism and is a limiting factor of harmonic generation.

$\alpha_j(m\omega)$ = the atomic polarisability of j^{th} level at frequency $m\omega$

$$\alpha_j(m\omega) = \alpha_j'(m\omega) - i\,\alpha_j''(m\omega)$$

$$= \frac{1}{\hbar}\sum_{\ell}\left[\frac{|\mu_{\ell j}|^2}{(\omega_{\ell j} - m\omega)} + \frac{|\mu_{\ell j}|^2}{(\omega_{\ell j} + m\omega)}\right] \qquad \text{(II.10)}$$

where,

$\mu_{\ell j}$ and $\omega_{\ell j}$ are the matrix element and frequency of the transition $I\ell\rangle\langle\longrightarrow Ij\rangle$.

γ_{i2} = two photon transition matrix = $\sum_{\ell}\frac{\mu_{i\ell}\,\mu_{\ell 2}}{(\omega_{\ell 2} + \omega)}$ (II.11)

ξ_{21} = third harmonic coupling coefficient

$$= \sum_{\ell}\left(\frac{\mu_{2\ell}\,\mu_{\ell 1}}{\omega_{\ell 1} - 3\omega} + \frac{\mu_{2\ell}\,\mu_{\ell 1}}{\omega_{\ell 2} + 3\omega}\right) \qquad \text{(II.12)}$$

The summation over ℓ implies summation over all levels bound or free. Eq(II.6)is the probability conservation Equation for the eqivalent two level atom. Eq(II.4) and Eq(II.5) describe the two photon resonant trnsition. $\frac{\gamma_{i2}\,\xi_1^2}{\hbar^2}$ is the two photon Rabi frequency. $\xi_{21}^*\,\xi_1^*\,\xi_3$ is a resonant raman scattering term. Eqs(II.4) to (II.6) are called "two photon Bloch equation",because of their analogy with the equations derived by Bloch for the precession of a spin in a resonant radio frequency field..

Dipole moment of the TPR atom is calculated from $P=Tr(\rho\mu)$. The dipole-moment oscilating at the first harmonic frequency is given by :[4]

$$P_1(z,t) = \tilde{P}_1(z,t)\, e^{i\omega t - ikz} + c.c$$

$$= \left\{ \left(\alpha_1(\omega)\sigma_{11} + \alpha_2(\omega)\sigma_{22}\right)\mathcal{E}_1 + 2\frac{r_{12}\sigma_{12}\mathcal{E}_1^*}{\hbar} + \frac{\mathcal{E}_{f2}}{\hbar}\sigma_{12}^*\mathcal{E}_3 \right\} e^{i\omega t - ikz} + C.C. \qquad \text{(II.13)}$$

Dipole-moment at third harmonic frequency:

$$P_3(z,t) = \tilde{P}_3(z,t)\, e^{i3(\omega t - kz)} + C.C.$$

$$= \left\{ \left(\alpha_1(3\omega)\sigma_{11} + \alpha_2(3\omega)\sigma_{22}\right)\mathcal{E}_3 + \frac{\mathcal{E}_{f1}}{\hbar}\sigma_{12}\mathcal{E}_1 \right\} \times e^{i3(\omega t - kz)} + C.C. \qquad \text{(II.14)}$$

These dipole moments will drive the Maxwell's Equation to generate fields at the next point in space.

Following Ref2. Maxwell's Equation in "slowly varying envelope approximation" written in reduced time frame ($t_r = t - z/c$):

$$\frac{\partial \mathcal{E}_m}{\partial z} = -i \frac{N \omega_m}{2 c \epsilon_0} \mathcal{P}_m \qquad (II.15)$$

$$m=1,3$$

where N=density of atoms

c=velocity of light in vacuum

ϵ_0 =vacuum permittivity.

Equation II.15 together with Eqs(II.4) to (II.6) are called Maxwell-Bloch equations . From coupled solution of Maxwell-Bloch equation we get $\mathcal{E}_1(z,t)$ and $\mathcal{E}_3(z,t)$ for all space time points.

For a TPR medium we have,

$$\mathcal{P}_3 = \frac{\rho_{21}}{n} \sigma_{12} \mathcal{E}_1 \qquad \text{instead of} \quad \mathcal{P}_3 = \chi_3 \mathcal{E}_1^3$$

To get larger $\mathcal{P}_3$ we must look for larger ρ_{21} and σ_{12}. ρ_{21} is fixed for a given transition. Larger σ_{12} implies stonger TPR interaction . From Eq(II.13) it follows that the term $\sigma_{12} \mathcal{E}_1^*$ is responsible for pump depletion due to TPR absorption. Larger σ_{12} implies stronger pump depletion. In presence of pump depletion the generation length is reduced. Resonance absorption reduces the efficiency.

For efficient harmonic generation we need

1. not only resonance enhancement of χ_3

   but also

2. A loss free propagation through the absorbing medium.

Apparently contradicting conditions 1 and 2 can be satisfied simultaniously only in case of coherent interaction.

Two Photon Vector Model and Anomalous Pulse Propagation

From the two photon Bloch equations a two photon vector model can be drawn.[2-5] In absence of ionization, Stark shift and harmonic generation, we can define a "pseudo vector" $\vec{R}$.

$$\vec{R} = W\,\hat{e}_1 + \frac{\sigma_{12}}{i}\,\hat{e}_2 \qquad \text{(II.16)}$$

where $$W = \frac{\sigma_{22} - \sigma_{11}}{2} \qquad \text{(II.17)}$$

In presence of an input square pulse of constant amplitude $\mathcal{E}_1$ (in resonance with the two photon transition) the vector $\vec{R}$ rotates about a vector $\vec{\Omega}$, in the pseudo space spanned by $\hat{e}_1$, $\hat{e}_2$ and $\hat{e}_3$ (see fig II.3).

$\vec{\Omega}$ = angular velocity vector in the pseudo space.

$$\vec{\Omega} = \frac{2\,\gamma_{12}}{\hbar^2}\,\mathcal{E}_1^2\,\hat{e}_3 \qquad \text{(II.18)}$$

An illustrative description of this vector model can be found from Ref 5.

Angle of rotation $\theta(t) = \int_0^t \Omega(t')\,dt'$

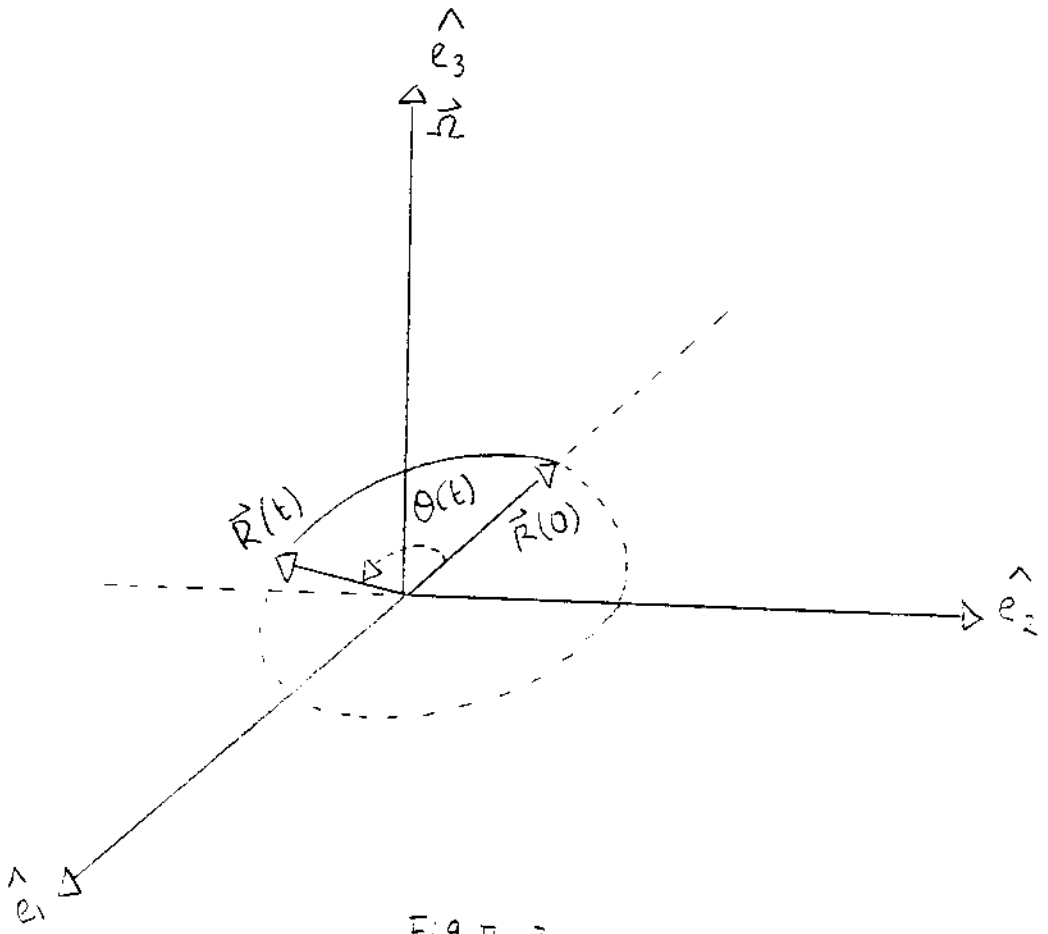

Fig II·3

The net angle of rotation due to a pulse, is given by

$$\theta_2 = \frac{2\gamma_{12}}{\hbar^2} \int_{-\infty}^{-\infty} \mathcal{E}_1^2 \, dt \qquad \text{(II.19)}$$

θ_2 is called two photon "area" of the pulse in analogy with single photon area $\int_{-\infty}^{+\infty} \mathcal{E}\, dt$ defined for one photon resonant medium. Two photon area of the pulse is determined by the energy of the pulse. For instance for $\theta_2 = \pi$ the pulse is called a "π pulse" and so on.

Suppose the pulse is applied at time t=0

at $t \leq 0$, $\sigma_{11} = 1$, $\sigma_{22} = 0$ and $\sigma_{12} = 0$

from Eq(II.16) $R(0) = -1/2\ \hat{e}_1$.

With time as $\vec{R}$ rotates σ_{22} and σ_{11} grows and two photon absorption takes place. For a π -pulse ($\theta_2 = \pi$) we have $\sigma_{22} = 1$ (atom is inverted) at the end of the pulse. Similarly for a 2π -pulse the atom is first inverted and then returns back to the ground state at the end of the pulse. The energy absorbed from the front part of the 2π pulse is returned back by the atom which is added coherently to the trailing edge of the pulse. In absence of ionization ,Stark shift and harmonic generation a 2π pulse propagates without absorption through a resonant medium.

Replacing θ by $-\theta$ (or Ω by $-\Omega$) we can change the

direction of rotation of the pseudo vector $\vec{R}$. If $\mathcal{E}_1$ is replaced by $\mathcal{E}_1 e^{i\pi/2}$, θ becomes $-\theta$ and $\vec{R}$ rotates back reversing an absorption into an emission process. For example if a square pulse is followed by a $\frac{\pi}{2}$ phase shifted second square pulse, the energy absorbed during the first pulse will be emitted back during the second pulse. Due to this phase dependent stimulated emission a pair of 90° phase shifted pulses can have absorption free propagation. Total energy of the pulse pair is conserved. Since two-photon emission (field at 2ω) is dipole forbidden no energy is emitted between the pulses. Only requirement is that the total interaction time has to be less than the relaxation times T_1 and T_2. Since for efficient harmonic generation our idea is to get loss free propagation through the resonant medium, we are left with two choices: either to use a 2π-pulse or to use a pair of 90° phase shifted pulses. In a real two photon resonant system with ionization Stark shift etc. a pair of phase shifted pulses are more favorable than a 2π pulse. It should be noted that in presence of phase modulation or with non negligible Stark shifts, the pulse energy is no longer proportional to the tipping angle of the "pseudopolarisation" vector. A 2π pulse with higher energy will have more ionization, more Stark-shift and will tend to be more unstable than a pair of low energy phase shifted pulses. The theoretical calculation of Diels et al[4] shows that a 2π pulse suffers considerable phase modulation

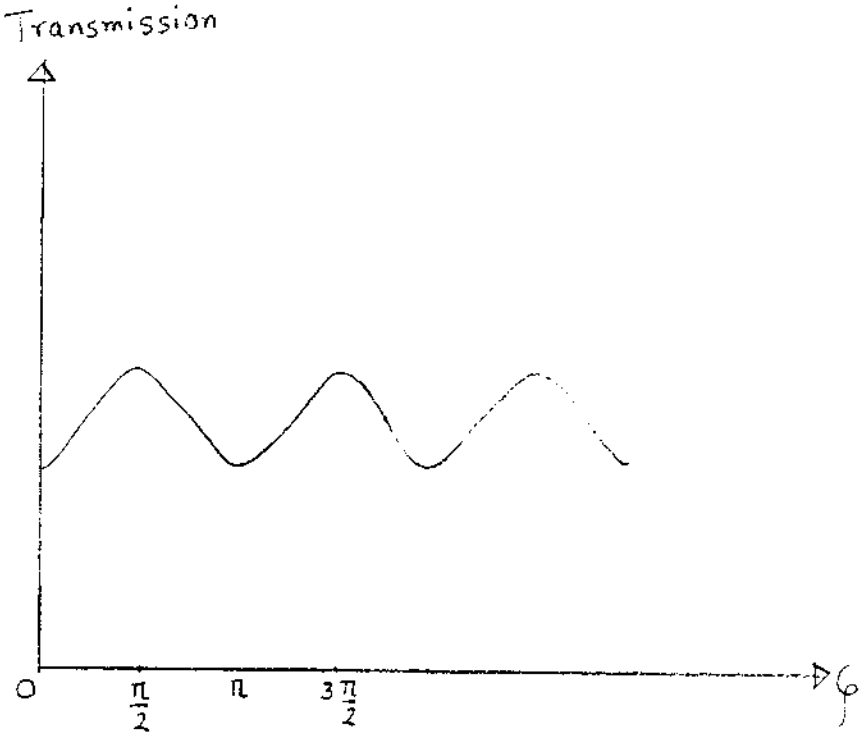

Fig II · 4

and both the fundamental and third harmonic pulses are broadened in frequency. From the above simple minded picture of the TPR atom it follows that the transmission of a pair of phase shifted pulses would be a funtion of their relative phase. We would expect the transmission to be maximum at odd multiples of $\frac{\pi}{2}$ as shown in figII.4. The anomalous propagation of a pair of 90° phase shifted pulses will have longer generation length. Theoretical analysis of Diels et al.[4] predicts a maximum energy conversion efficiency up to 8% in an ideal phase matched condition, for a plane wave of infinite transverse dimension.

Transient Phase Matching

Efficient harmonic generation demands efficint phase matching between the first and third harmonic field. Phases of the first and third harmonic field are determined by their respective single-photon susceptibilities. Single photon susceptibilities for the two fields follow from the expression of P_1 and P_3 (EqII.13 and II.14):

$$\chi_1(\omega) = \{\alpha_1(\omega)\sigma_{11} + \alpha_2(\omega)\sigma_{22}\}N \qquad \text{(II.20)}$$

$$\chi_1(3\omega) = \{\alpha_1(3\omega)\sigma_{11} + \alpha_2(3\omega)\sigma_{22}\}N \qquad \text{(II.21)}$$

Where,

$\chi_1(n\omega)$ =single photon susceptibilty of the n^{th} harmonic field.

Phase matching requires $\chi_1(\omega)$to be equal to $\chi_1(3\omega)$. This condition is achieved by adding an off-resonant vapor so that the total susceptibilities become equal for the two harmonics.

Suppose,

$\alpha_N(\omega)$ =single-photon polarizability of the off-resonant vapor at the frequency ω .

$\alpha_N(3\omega)$ =single-photon polarizability of the off-resonant vapor at 3ω .

f = ratio of the off-resonant to on-resonant atoms in the vapor.

single-photon susceptibility of the mixed vapors at ω :

$$\chi_T(\omega) = N\left\{\alpha_1(\omega)\,\sigma_{11} + \alpha_2(\omega)\,\sigma_{22}\right\} + N f\,\alpha_N(\omega) \tag{II.22}$$

single-photon susceptibilty of the mixture at 3ω :

$$\chi_T(3\omega) = N\left\{\alpha_1(3\omega)\,\sigma_{11} + \alpha_2(3\omega)\,\sigma_{22}\right\} + N f\,\alpha_N(3\omega) \tag{II.23}$$

Phase matching requires:

$$\chi_T(\omega) = \chi_T(3\omega) \tag{II.24}$$

For coherent interaction both σ_{11} and σ_{22} are functions of time, and Eq(II.24) can not be satisfied for all times. For weak interaction however we can find a time independent phase matching condition. For weak interaction we have $\sigma_{11} \simeq 1$, $\sigma_{22} \simeq 0$

and Eq(II.24) becomes:

$$N\alpha_1(\omega) + Nf\alpha_N(\omega) = N\alpha_1(3\omega) + Nf\alpha_N(3\omega) \tag{II.25}$$

Condition expressed by equation (II.25) is called "linear phase matching". Linear phase matching is only good for off resonant interaction. For resonant coherent interaction the susceptibilities (given in Eqs.(II.22) and (II.23)) are functions of time and no time-independent phase matching condition exists. In this situation the best we can have is an approximate phase-matching for optimum third harmonic generation. For example we may phase match not over the whole pulse but for a certain region of the pulse where third harmonic generation is maximum. In this case Eq(II.24) is satisfied with certain values of σ_{11} and σ_{22} corresponding to maximum third harmonic generation. The value of the ratio f giving maximum third harmonic would be very different from the value satisfying Eq(II.25). Optimum value of the phase matching ratio has to be found dynamicaly either by a real experiment or by a numerical experiment. The optimum phase matching for resonant transient interaction will be referred to as "transient phase matching". Due to windowing, the phase matching time, the third harmonic will be narrowed in time and broadened in frequency. Due to Stark shift the resonance

condition is a function of the pulse intensity. The "transient phase matching", true for certain values of σ_{11} and σ_{22} will be effective over a reasonable distance only if the pulse intensity is maintained constant over that distance. In otherwords "transient phase matching" requires that a certain condition of anomalous (enhanced) transmission be met. Although a pair of 90° phase shifted pulses seems to be useful for this purpose ,only a real experiment can prove it's utility. In the next chapter we are going to discuss an experiment which puts the above idea into real tests.

CHAPTER BIBLIOGRAPGY

1. Grischkosky et al.,"Adibatic following model for two photon transition." Physical Rev. A 12, 2514 (1975).

2. Diels.J.C., "Two-photon coherent propagation, transmission of 90° phase shifted pulses." Optical and quantum electronics 8, (1976) 513-522.

3. Georges et al., "Theory of third harmonic generation in metal vapor under two photon resonant conditions". Physical rev. A, 15, 300 (1977).

4. Diels et al.,"Coherent two photon resonant third and fifth harmonic generation in metal vapors." Physical Rev.A ,19, 1589 (1979).

5. Mukherjee.A., Ph.D Thesis, NTSU (1987).

6. Diels J.C. "Coherent propagation and harmonic generation," proceeding of the VI Vavilov Conference on Coherence and Nonlinear Optics, Novosibirsk, (june, 1979).

7. McCall S. L.and Hahn E. L.,"Self-induced transparency by pulsed coherent light," Physical review letter 18, 909 (1967).

CHAPTER III

TWO PHOTON RESONANT THIRD HARMONIC GENERATION IN LITHIUM VAPOR

In this chapter we study two photon resonant(TPR) third harmonic generation(THG) in lithium vapor. A level diagram of lithium atom[1] is shown in fig III.1. We have studied two different resonances in lithium atom. In one case the incident light was in two photon resonance with the 2s-4s transition and in the other case the light was in two photon resonance with 2s-3d transition. In both cases the third harmonic levels coincide with a P-level($\ell=1$) in the continuum. In the first part of this chapter we will study the two resonant cases individually and after that we will discuss the significant differences between the two transitions.

In chapter II we have learned that a pair of 90° phase shifted pulses propagate through a two photon resonant medium without absorption loss when the pulse duration is much shorter than the relaxation times of the medium. This idea is exploited in all our experiments to get longer length for third harmonic generation and for phase matching.

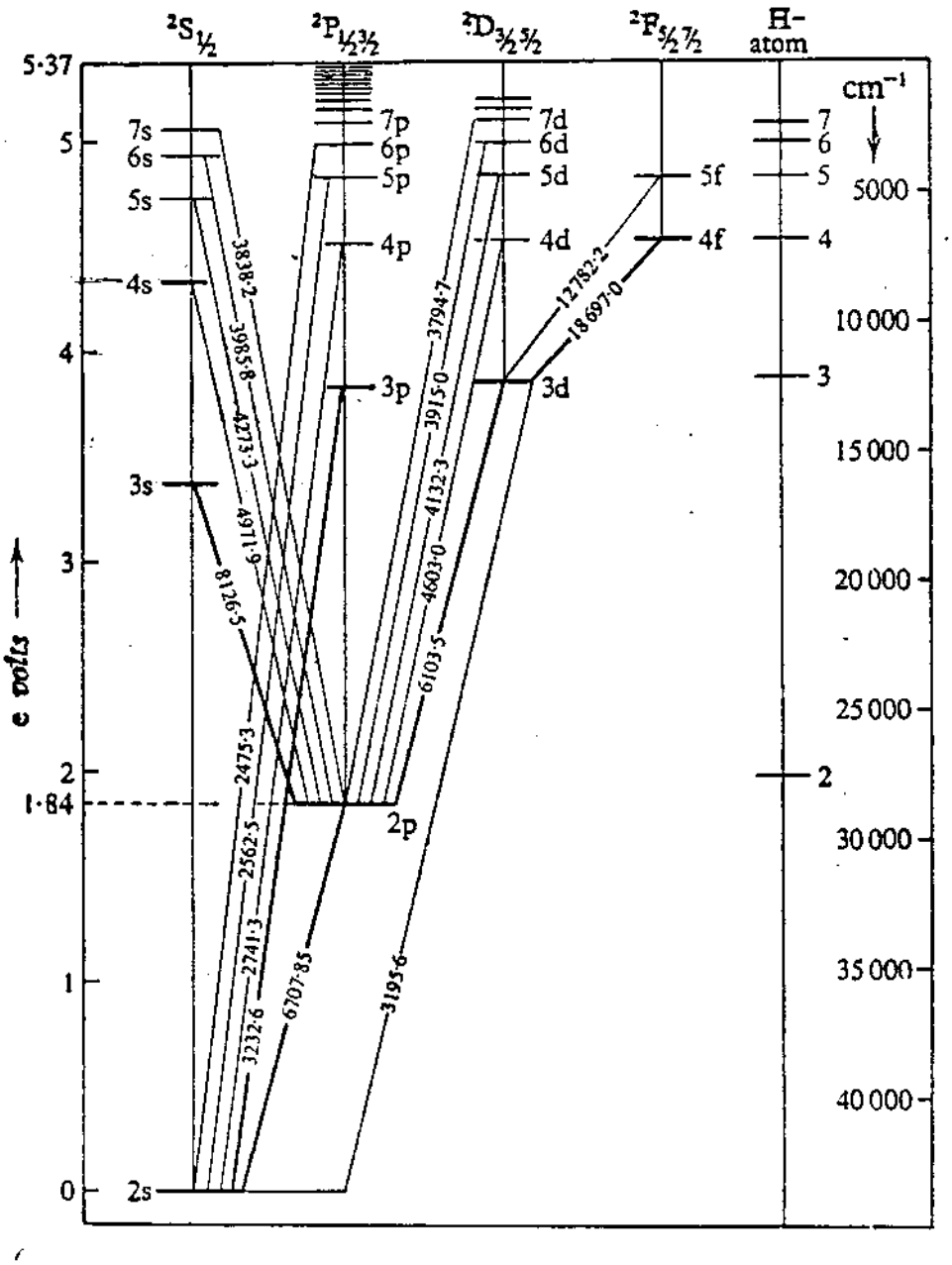
$^2S_{1/2}$
$^2P_{1/2,3/2}$
$^2D_{3/2,5/2}$
$^2F_{5/2,7/2}$
H-atom
cm^{-1}
5·37
5
4
3
2
1·84
1
0
e volts
7s
6s
5s
4s
3s
2s
7p
6p
5p
4p
3p
2p
7d
6d
5d
4d
3d
5f
4f
7
6
5
4
3
2
5000
10 000
15 000
20 000
25 000
30 000
35 000
40 000
3838·2
3965·8
4273·3
4971·9
8126·5
2475·3
2562·5
2741·3
3232·6
6707·85
3195·6
3794·7
3915·0
4132·3
4603·0
6103·5
12782·2
18697·0

FIG III · 1

The experiment was done with a pair of delayed and phase shifted pump pulses, tuned to a two photon resonant transition in lithium atom. The delay and phase were varied smoothly. The third harmonic signal was found to be enhanced when delay and phase were ideal for coherent loss free propagation. Up to 1% efficiency was obtained when phase matching was optimized. Third harmonic signal was recorded as a funtion of phase and delay of the input pulse pair for each tuning. The second harmonic of the transmitted pulse pair was also recorded as a function of their relative phase and delay. Before we discuss the experimental data it is important to define some of the parameters of TPR medium.

Efficiency coefficient: η

From Eq(II.4) & Eq(II.5) we find that $\left(\xi_{21}/\gamma_{12}\right)$ determines the relative strength of third harmonic generatin and two photon absorption. We define the efficiency coefficient

$$\eta = \frac{\xi_{21}}{\gamma_{12}} \qquad \text{(III.1)}$$

η is a measure of the largest possible third harmonic conversion.

Two Photon characteristic length ℓ_2 :[6]

From Eq(II.13) the TPR first harmonic plarisation

$$P_1 = \frac{2\gamma_{12}}{\hbar} \sigma_{12} \mathcal{E}_1^* \tag{III.2}$$

(where we have just taken the TPR part of the polarisation) Using Eq(III.2) in the Maxwell's Eq(II.15) we get,

$$\frac{\partial \mathcal{E}_1}{\partial z} = -i \frac{\omega N \gamma_{12}}{c \epsilon_0 \hbar} \sigma_{12} \mathcal{E}_1^* \tag{III.3}$$

The two photon vector model of Chapter II shows that the largest possible value of $|\sigma_{12}|$ is 1/2, corresponding to the maximum absorption. Using $\sigma_{12} = -i/2$ in eqn.III.3 we find an upper limit to the beam attenuation.

$$\frac{\partial \mathcal{E}_1}{\partial z} = -\frac{\omega N \gamma_{12}}{2 c \epsilon_0 \hbar} \mathcal{E}_1 \tag{III.4}$$

A two photon characteristic length is defined as:

$$\ell_2 = \frac{\omega N \gamma_{12}}{2 c \epsilon_0 \hbar} \tag{III.5}$$

Using equation (III.5) in (III.4) we get,

$$\mathcal{E}_1(z) = \mathcal{E}_1(0)\, e^{-\ell_2 z}$$

ie. ℓ_2 defines the shortest length in which the field amplitude could drop by a factor of 1/e of its initial value, by two photon absorption. Given sufficient initial energy, most of the input pump pulse energy is depleted at this distance. Two photon absorption as well as THG become negligible after this distance. At 10 torr pressure this distance was 2 cm in case of Li 2S - 4S transition. For a pair of 90° phase shifted pulses, at the end of this distance most of the energy goes from the first pulse to the second and the second pulse can propagate over a longer distance. In this way the generation length is increased.

Lithium 2S - 4S Transition

In this section, third harmonic generation (THG) under the two photon resonant (TPR) transition 2S - 4S in Li vapor will be summarised. A detailed description of the experiment will be found in Ref 2. The resonance wavelength for this trasition is λ = 571.2 nm and the third harmonic is generated at λ = 190.4 nm. In this experiment a pulse pair at λ = 571.2 nm was used as the fundamental pump pulses. The delay and the phase of the pulses were smoothly scanned. The energy required for the two photon transition is 50 mJ/cm^2. For this experiment 6 ps pulses with each an energy of 1 mJ were obtained from the oscillator-amplifier system described in Ref.2 and Ref.3. At operating temperature of 1100 $^{\circ}$K, the vapor pressure of lithium was 10 torr, corresponding to a phase relaxation time T_2 of about 1 ns. The inverse Doppler broadening was 50 ps. 6 ps pulses were short enough for coherent excitation. Nonresonant Mg vapor was added for phase matching. For a given detuning and delay Mg pressure was continuously scanned to get optimum phase matching.[6,2] We did not measure ionisation in these experiments. A theoretical estimate of ionisation was about 6%. A schematic of the experiment is shown in Fig.III.2. Pulses of energy about 1 mJ were sent through a delay line. The description of the delay

SCHEMATIC

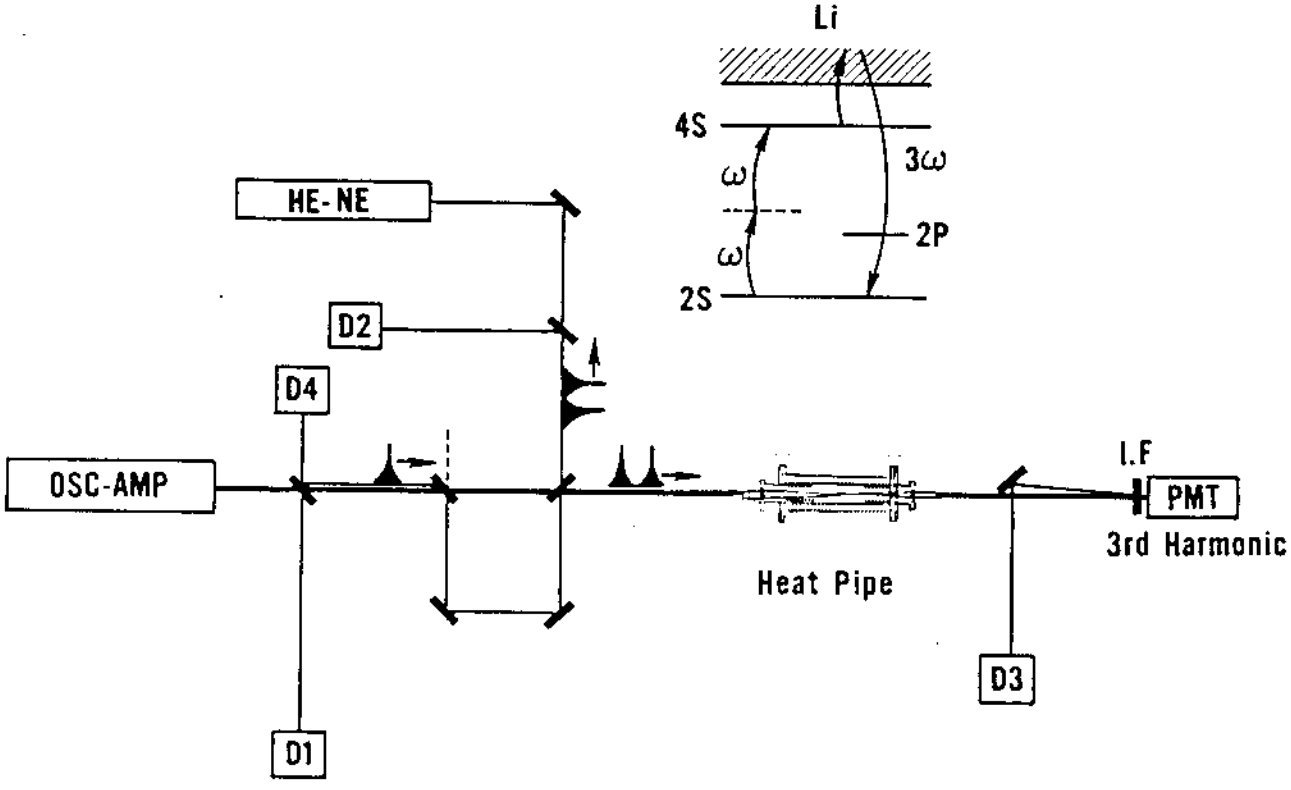

FIG III·2

line can be found in Ref 2. There are two outputs of the delay line. Each output of the delay line consists of two pulses delayed and phase shifted with respect to each other. The delay and phase were determined with an accuracy of 1/20th of a wavelength. One of the outputs of the delay line was sent through a heat pipe[2] containing a mixture of Li and Mg vapors, the other output was used to characterise the incident pulse pair. At the other end of the heat pipe third harmonic signal was detected with a 20 nm bandwidth interference filter. The third harmonic as well as the second harmonic of the incident & transmitted pulse pair were recorded as a function of delay and phase. The second harmonic signals of the incident and transmitted pulse pairs were generated in KDP crystals. Data acquisition was done by a microcomputer ("Smoke Signal Broadcasting"). A detailed description of the data acquisition will be found in Ref 2. Fig. III.3 shows a theoretical simulation of the experiment, done in a thin sample. In each of the graphs the second harmonic of the transmitted pulse pair is drawn as a function of delay (in ps). Each graph was drawn for a different detuning of the incident laser pulse from the zero field TPR frequency. For a different detuning a sharp resonance dip was observed at a different delay. This resonance dip is due to the ac Stark shift.

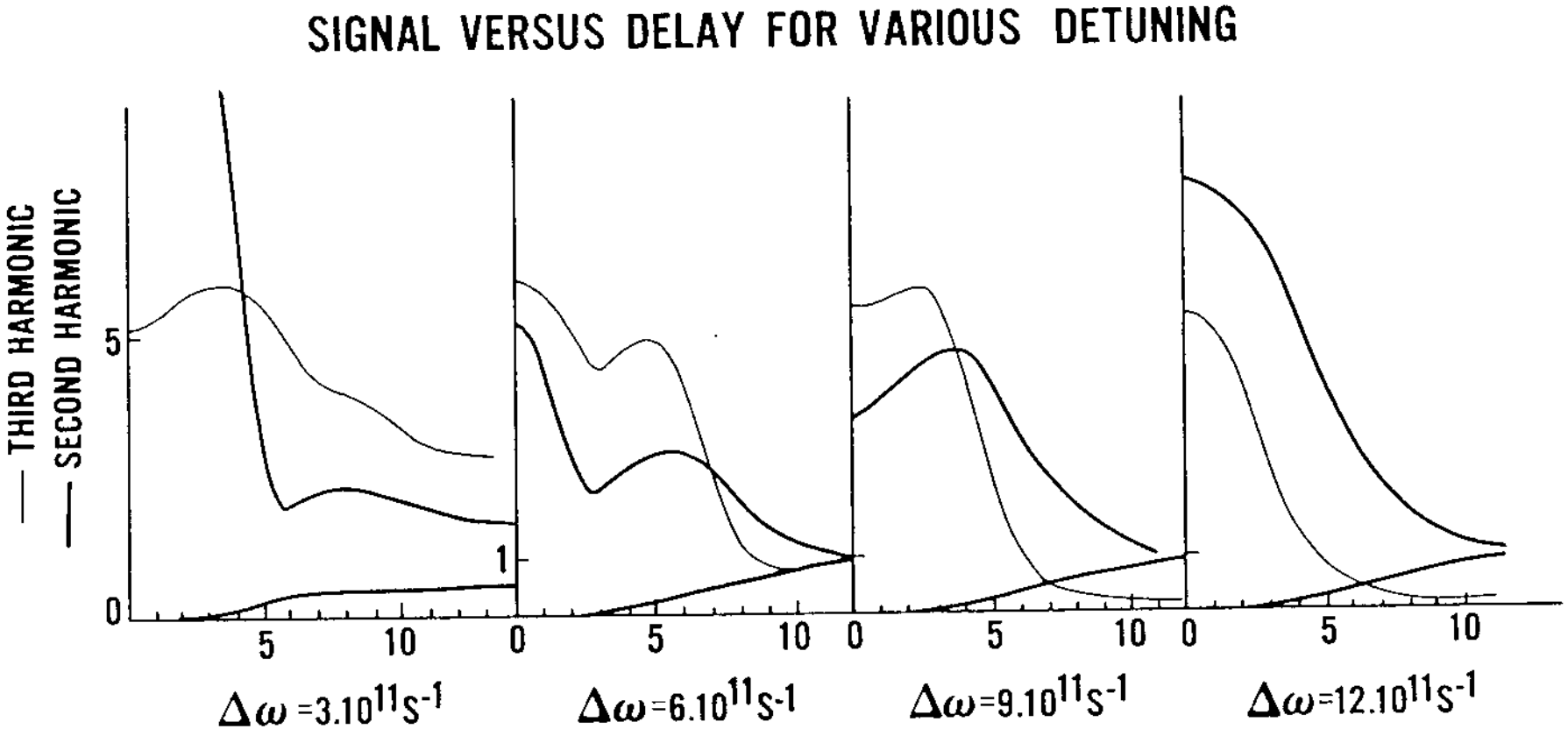
SIGNAL VERSUS DELAY FOR VARIOUS DETUNING
— THIRD HARMONIC
— SECOND HARMONIC
5
1
0
5
10
0
5
10
0
5
10
0
5
10
Δω =3.10^11 S^-1
Δω=6.10^11 S^-1
Δω=9.10^11 S^-1
Δω=12.10^11 S^-1

FIG III·3

From equation (II.4) the net detuning of the TPR interaction is

$$(\Delta\omega)_{21} = 2\omega - \omega_{21} - \delta\omega_{21} \qquad \text{(III.6)}$$

where

$2\omega - \omega_{21}$ = The zero field detuning = $\Delta\omega$

and $\delta\omega_{21}$ is the Stark shift given by equation (II.7).

$$\delta\omega_{21} = \frac{1}{\hbar}\left[\alpha_1'(\omega) - \alpha_2'(\omega)\right]|\mathcal{E}_1|^2 \qquad \text{(III.7)}$$

The Stark shift due to the generated third harmonic field is neglected. This is a good approximation because the polarisabilities are smaller at 3ω.

$$(\Delta\omega)_{21} = \Delta\omega - \delta\omega_{21}$$

We have resonance when $\Delta\omega = \delta\omega_{21}$. A certain amount of zero field detuning " $\Delta\omega$ " is required to be tuned to the Stark shifted resonance frequency " $\omega_{21} + \delta\omega_{21}$".

The Stark shift increases with intensity. With increasing detuning a larger Stark shift (induced by a larger intensity) is needed to bring the atom into resonance. For this transition the Stark shift was negative. The intensity dependent Stark shift is clearly manifested in the second harmonic of the transmitted intensity. As the detuning is increased the resonance dip shifts towards zero delay. With larger detuning it requires larger intensity to bring the atom

into resonance. For very large detuning ($\Delta\omega = -12 \times 10^{11}\ s^{-1}$) there exists no intensity to bring the atom into resonance, resulting in an off resonant excitation. There are several interesting features of the generated third harmonic signal. Maximum third harmonic is not necessarily at the zero delay as we would expect in an incoherent or off resonant interaction. In fact we can see in Fig III.3 (with $-\Delta\omega = 3 \times 10^{11}\ s^{-1}$) that the third harmonic is maximised away from the zero delay. This is due to the two photon coherent effect. Details of the interpretation of experimental results appear in Ref 2.

Fig (III.5) shows a real experimental data of enhanced phase matched third harmonic signal as a function of delay between the pulses. Each point in the upper envelope is a recording of the maximum third harmonic signal for a given delay as the phase between the pulses is scanned from zero to 2π. Each point in the lower envelope represents the corresponding minimum. Third harmonic signal is maximised not at zero delay but at an inter-pulse delay of 1.5 ps. This shows the difference between coherent and incoherent (or off resonant) interaction. In incoherent interaction the third harmonic field $\mathcal{E}_3 \propto \mathcal{E}_1^3$ where $\mathcal{E}_1$ is the fundamental field amplitude. The third harmonic intensity $I_3 \propto \mathcal{E}_1^6$. When I_3 is generated in an incoherent interaction ($I_3 \propto \mathcal{E}_1^6$) by two delayed and phase shifted pump pulses, I_3 would be proportional to third order autocorrelation of the pulses with a 32:1 peak to background

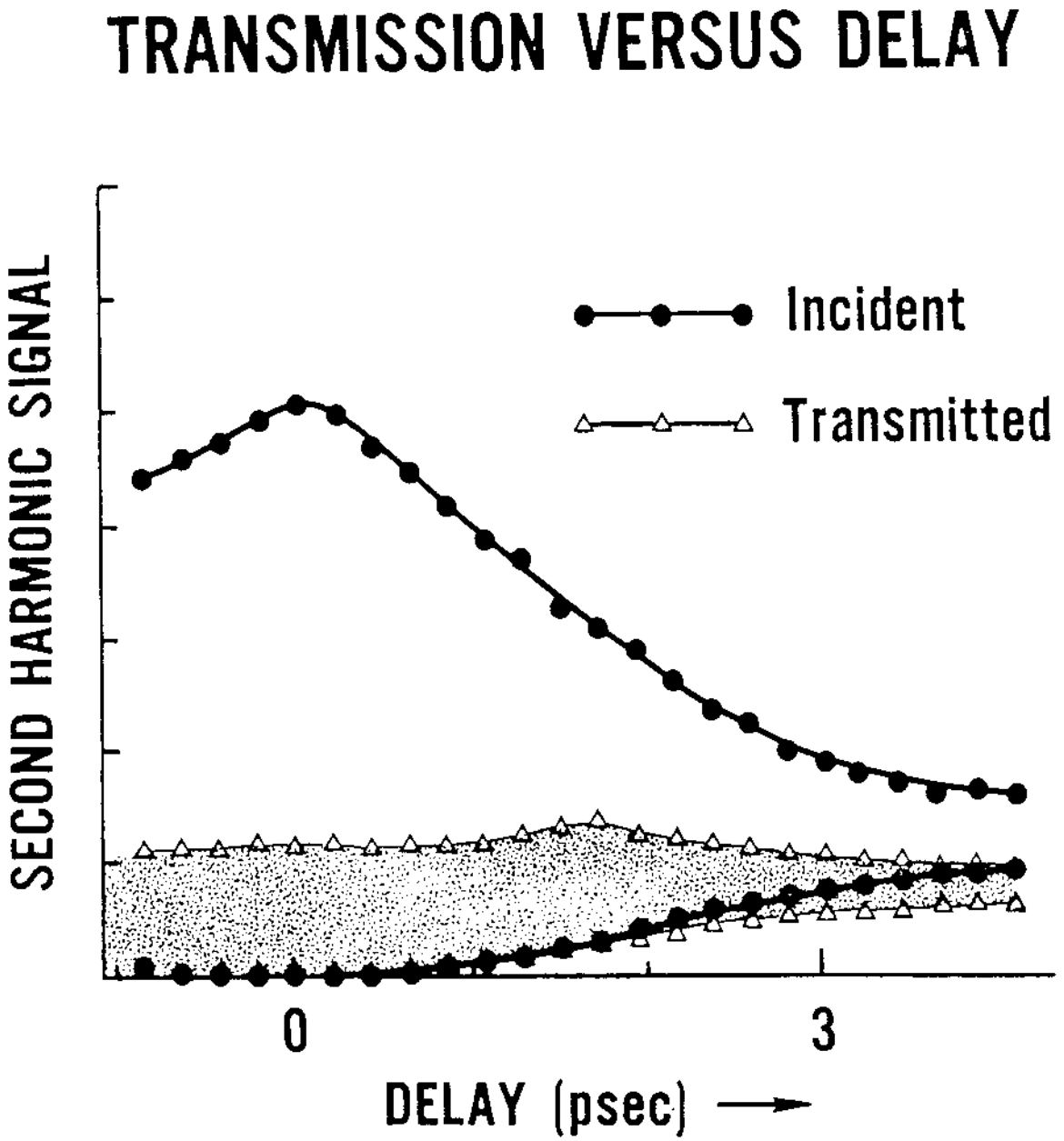
TRANSMISSION VERSUS DELAY
SECOND HARMONIC SIGNAL
Incident
Transmitted
0
3
DELAY (psec) ⟶

FIG III·4

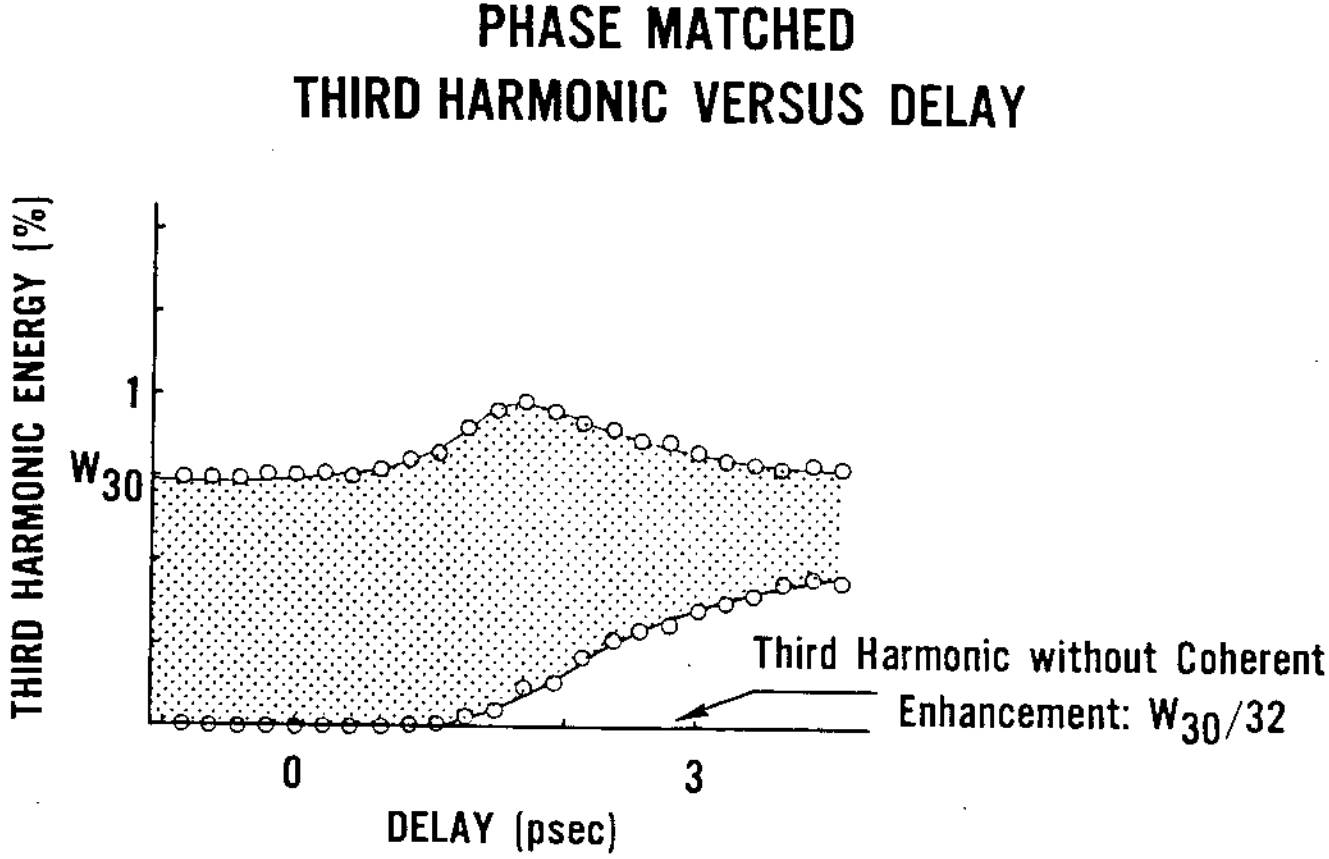
PHASE MATCHED
THIRD HARMONIC VERSUS DELAY
THIRD HARMONIC ENERGY (%)
1
W30
Third Harmonic without Coherent
Enhancement: W30/32
0
3
DELAY (psec)

FIG. III·5

ratio. The enhancement of the third harmonic signal shown in Fig III.5 away from zero delay is clearly a manifestation of two photon coherent effect. The ratio of Mg to Li vapor was 1.5 as opposed to 2 required for linear phase matching. The maximum energy conversion efficiency was 1%. For the same experiment, the second harmonic signal of the incident and the transmitted pulse pair is shown in Fig III.4. Here the upper and lower envelope of the incident and transmitted signals have similar meaning as that for third harmonic. In this experiment a resonance dip appeared at zero delay. Fig III.6 is another recording of the experiment for a different detuning. In this case the unphase-matched third harmonic signal had a similar behaviour as shown in the theoretical simulation (Fig III.3 with $-\Delta\omega = 6 \times 10^{11}\ s^{-1}$) done for a thin sample. In Fig III.6 a very sharp dip has appeared both in the third harmonic as well as in the transmitted signals. Figs III.7 & III.8 are the recordings of the experimental data showing two photon coherent pulse propagation. The anomalous propagation effect is evident from the enhanced modulation of the transmitted signal (as seen from Fig III.7) over an interpulse delay of 3 - 6 ps. This anomalous propagation is due to two photon coherent interaction. The energy lost by the first pulse is coherently recovered by the second pulse. Fig III.8 shows the second harmonic of the transmitted signal as a function of phase at the interpulse delay of 3 ps. The

TRANSMITTED SIGNAL AND THIRD HARMONIC VERSUS DELAY

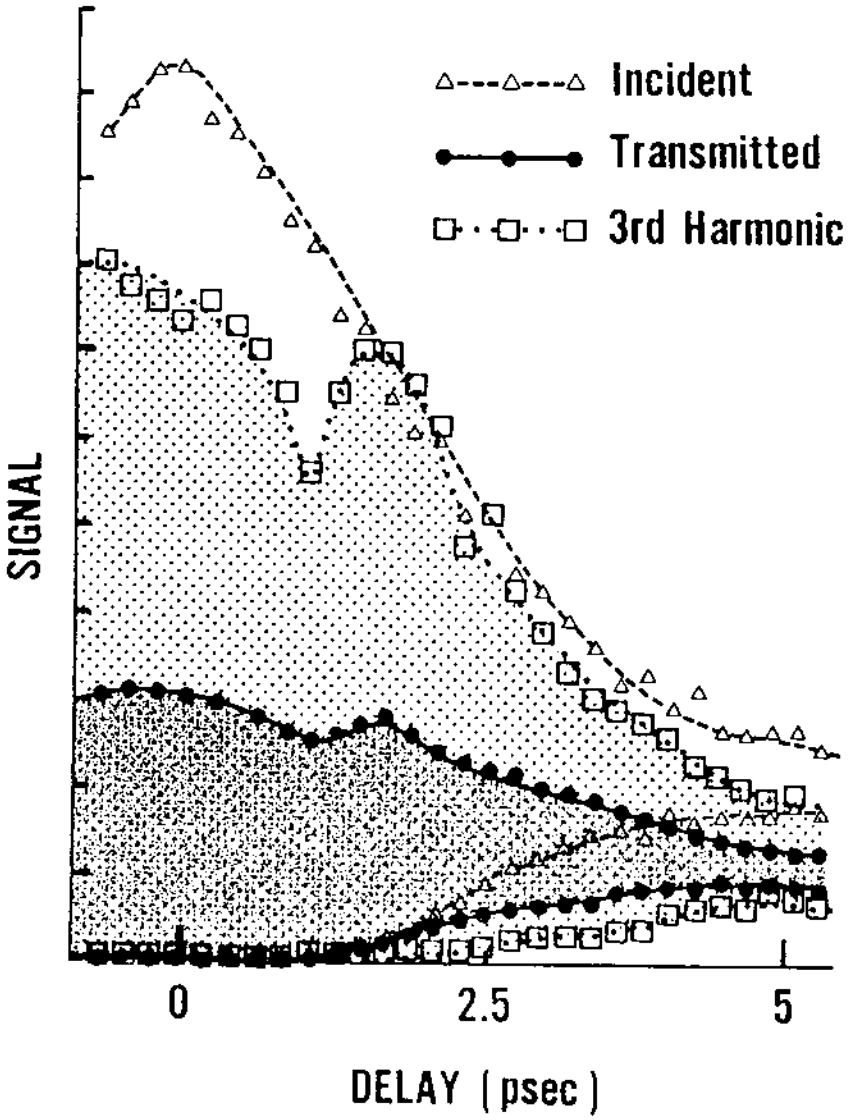

FIG 11·6

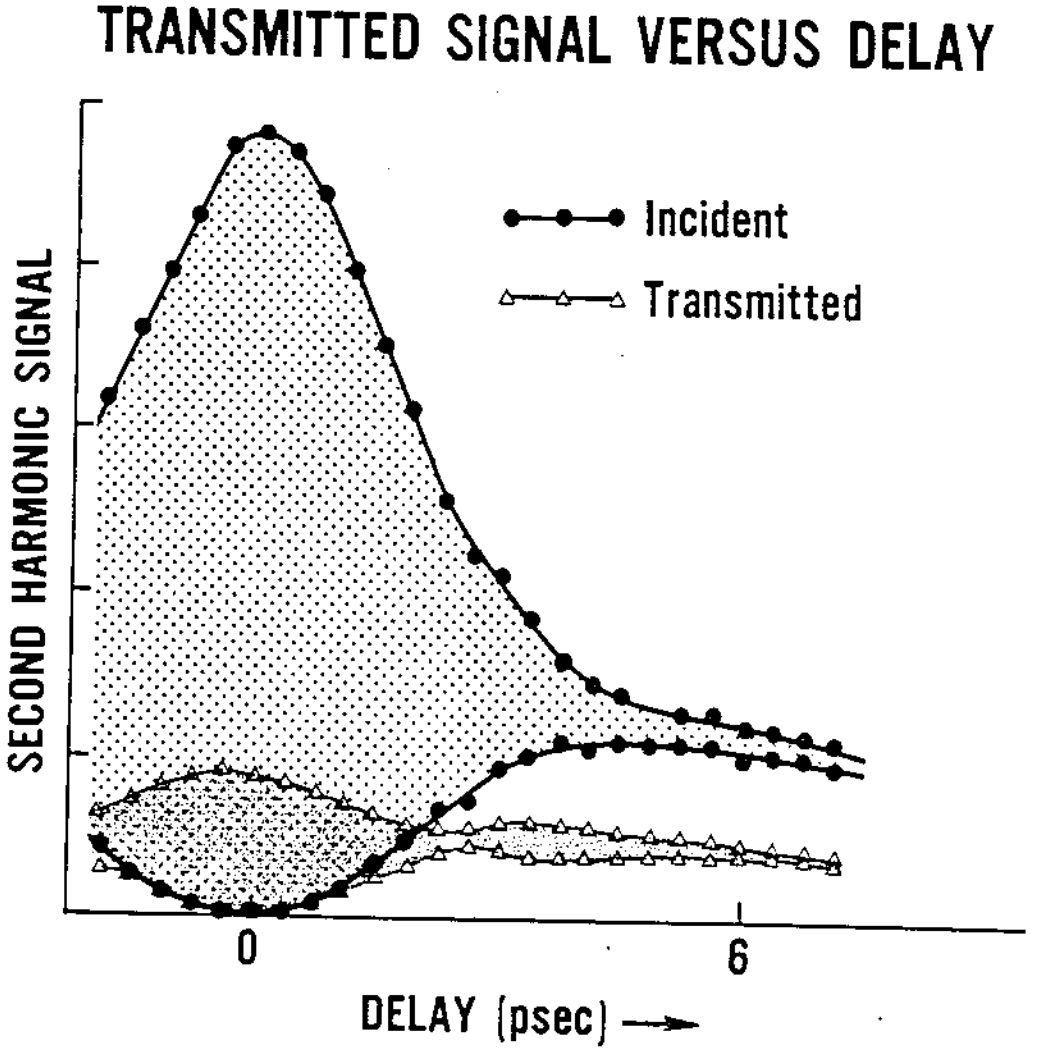
TRANSMITTED SIGNAL VERSUS DELAY
Incident
Transmitted
SECOND HARMONIC SIGNAL
0
6
DELAY (psec) →

FIG III·7

TRANSMITTED SIGNAL VERSUS PHASE

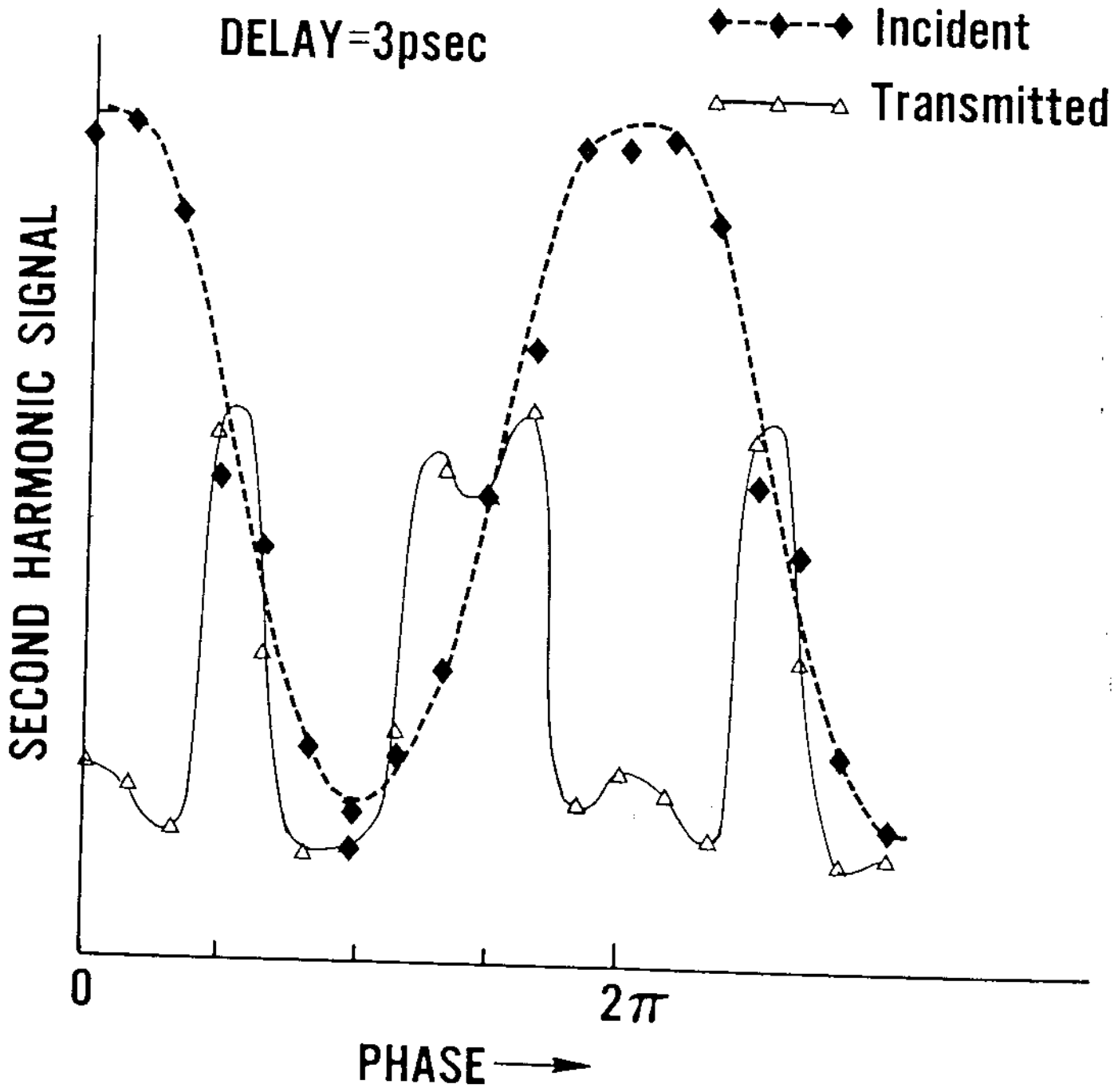

FIG III·8

phase dependent transmitted signal has a periodicity of π rather than 2π . The maximum of the transmitted signal is not at zero phase, but at a relative phase of $\pi/2$ or $3\pi/2$. As expected from theory we see that a 90° phase shifted pulse pair propagate through the resonant medium with less absorption.

From this experiment we can draw the following conclusion:

1. Third harmonic generation is enhanced in presence of two photon resonance.
2. Higher conversion efficiency requires two photon coherent interaction.
3. Tuning in multiphoton resonant interaction is intensity dependent.

Third Harmonic Generation in Li

2S - 3D Transition

In this chapter we study the THG in Li vapor when 2S - 3D transition is in two photon resonance with the incident laser pulse at λ_1 = 639.3 nm. The THG occurs at λ_3 = 213.1 nm. Essentially the same experiment (as in the 2S - 4S transition in Li) was carried out. The generated third harmonic signal and the second harmonic of the incident and the transmitted pulse pair were recorded in the same way as a function of phase and delay of the pump pulses. This time we could not phase match the third harmonic signal with Mg vapor. Fig III.9 shows the second harmonic of the incident pulse pair as a function of their relative delay. Figs III.10, III.11, III.12 and III.13 are the various recordings of the second harmonic signals of the tranmitted pulse pair at various detunings. In each case of the experimental results shown in the Figs III.10 to III.13 we measured the Stark shifts with a newly developed interferometric wavemeter (to be described later) with an accuracy better than 0.5 Å. A positive Stark shift was measured in each case.

TRANSMITTED 2ND HARMONIC SIGNAL VERSUS DELAY

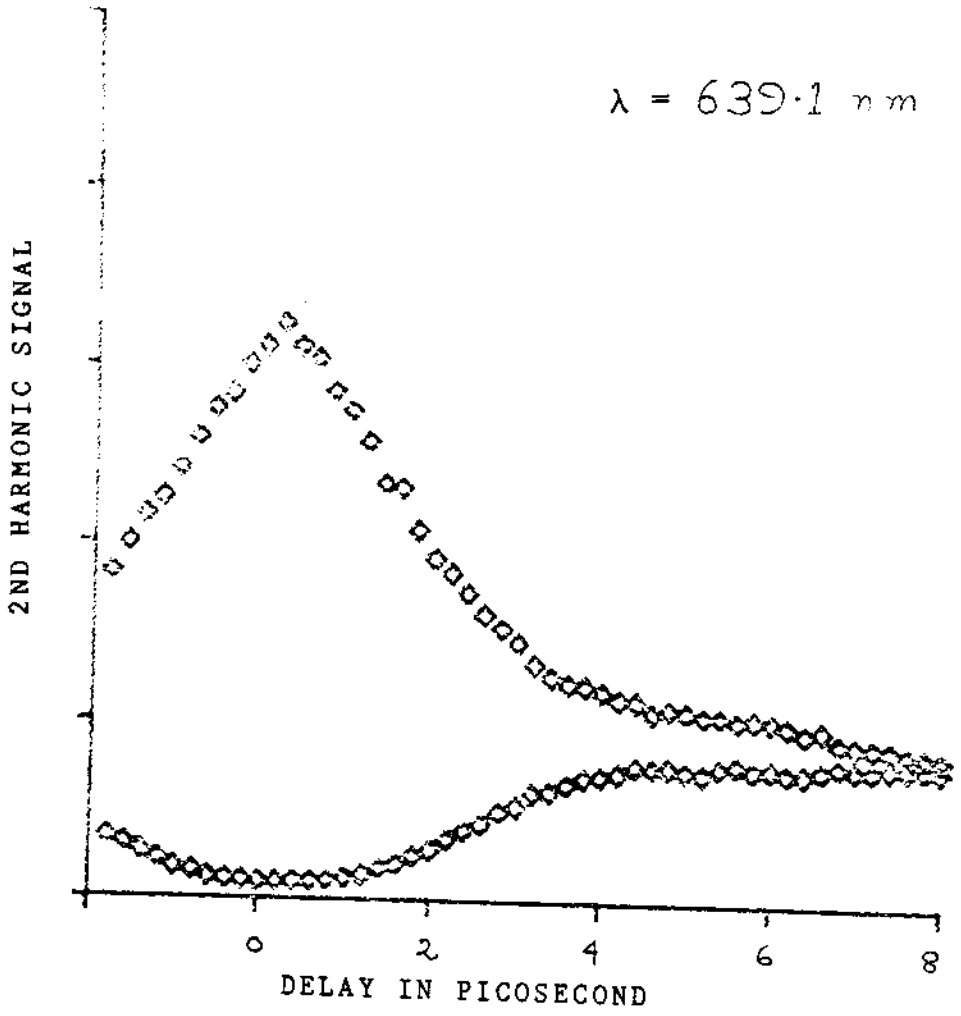

FIG III.9

TRANSMITTED 2ND HARMONIC SIGNAL VERSUS DELAY

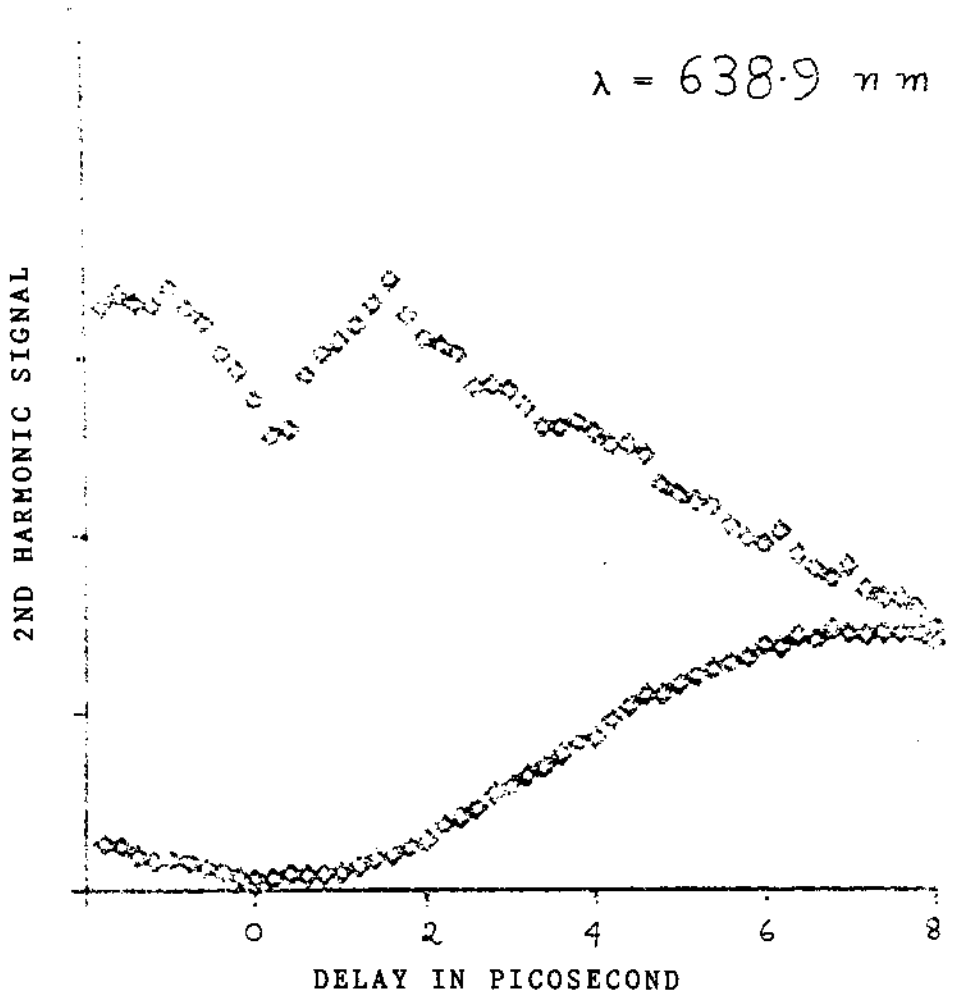

FIG III.10

2ND HARMONIC SIGNAL VERSUS DELAY

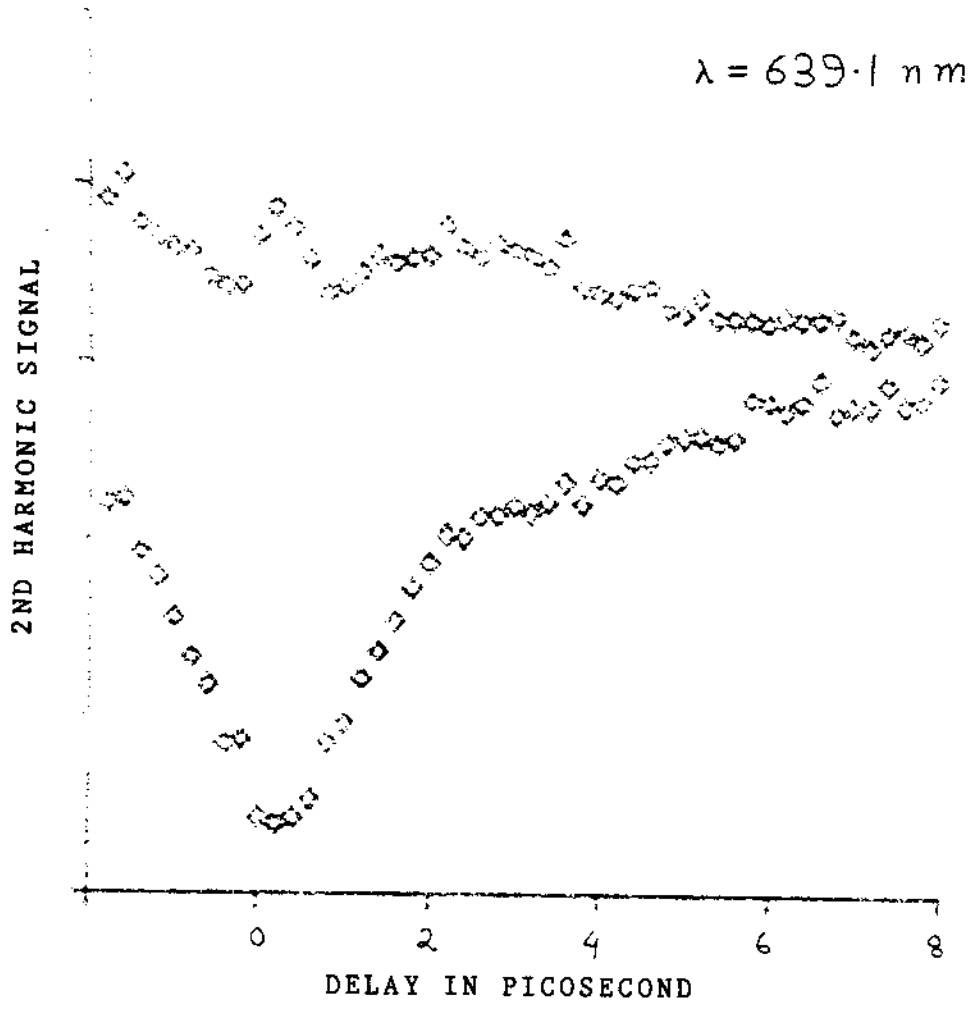

FIG III.11

TRANSMITTED 2ND HARMONIC SIGNAL VERSUS DELAY

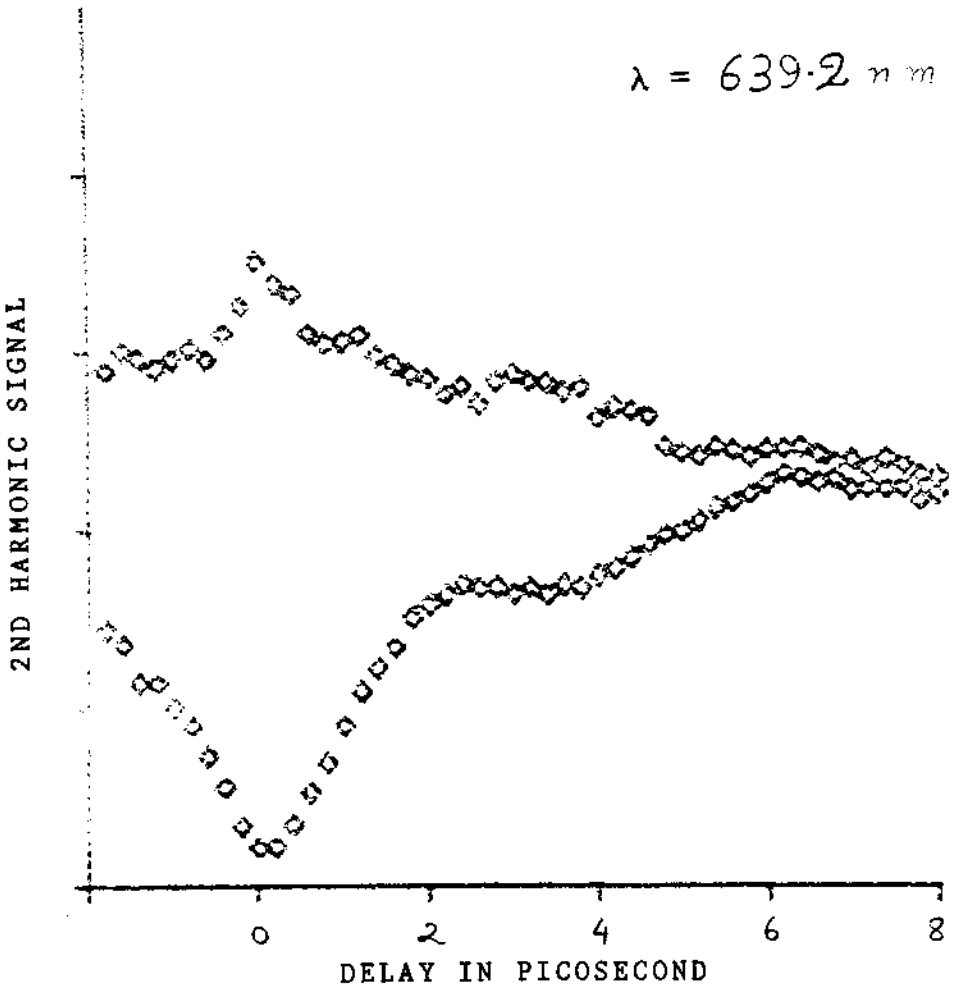

FIG III.12

TRANSMITTED 2ND HARMONIC SIGNAL VERSUS DELAY

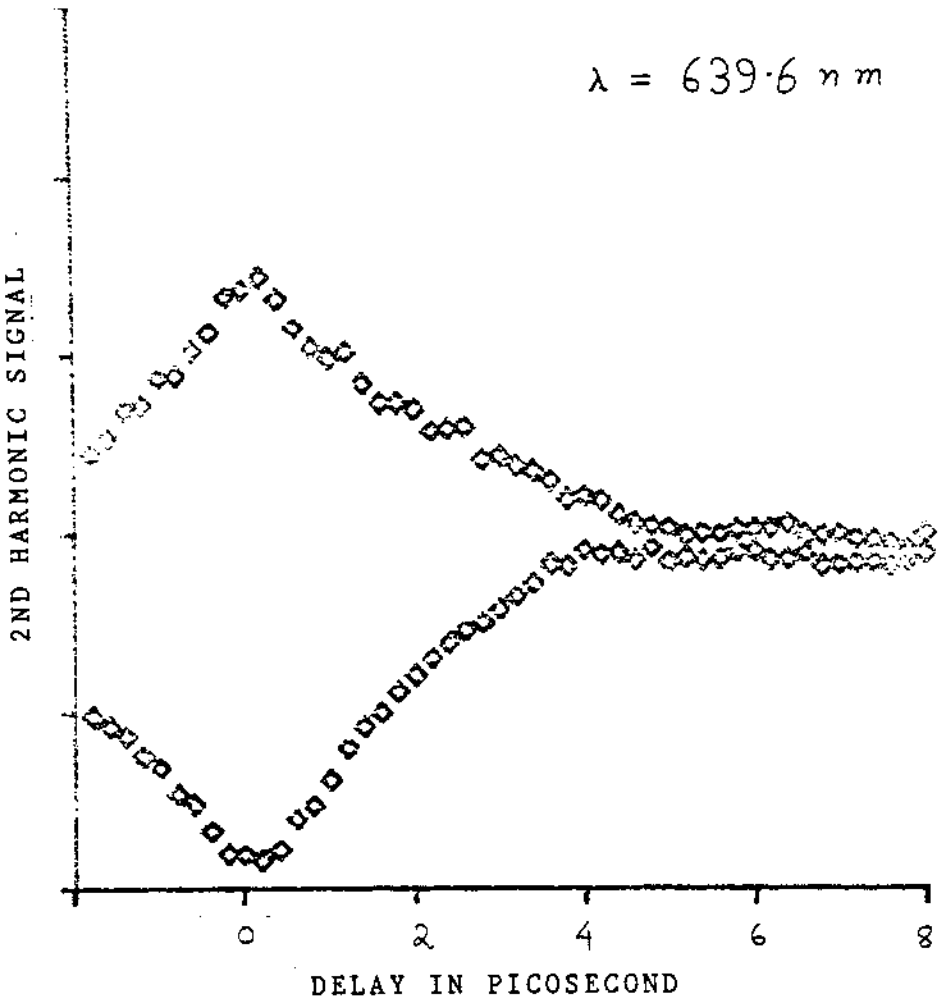

FIG III.13

The various atomic parameters (in MKS units) for 2S - 3D transition are listed below:

Two photon resonance frequency for 2S - 3D transition: ω_o

$$\frac{\omega_{21}}{2} = \omega_o = 2.948 \times 10^{15}\ s^{-1}$$

$$\alpha'_{2S}(\omega_o) = -2.626 \times 10^{-38}$$

$$\alpha''_{2S}(\omega_o) = 0$$

$$\alpha'_{3D}(\omega_o) = -4.203 \times 10^{-38}$$

$$\alpha''_{3D}(\omega_o) = 6.214 \times 10^{-40}$$

$$\gamma_{12} = 2.692 \times 10^{-72}$$

$$\xi_{21} = 0.299\, e^{-i(0.158)} \times 10^{-74}$$

α_i , γ_{12}, ξ_{21} were defined in ChapterII, in eqns. II.10, II.11, II.12 respectively. The transition dipole matrix elements were obtained from oscillator strengths given in Ref 4. The atomic transition frequencies were obtained from the tables of Moore.[5]

From equation (III.7) and from the parameters given

above we find $\delta\omega_{21}$ to be positive in agreement with the experiment. In Fig III.10 the Stark tuned resonance dip appeared at zero delay. The zero field detuning for this experiment as measured by the wavemeter was $\Delta\omega = 36 \times 10^{11}\ s^{-1}$. In this case the input light frequency ω was tuned above the zero field two photon resonance frequency ω_o by an amount $18 \times 10^{11}\ s^{-1}$. It took a very high intensity induced Stark shift to bring the atom into resonance. This very large Stark shift corresponds to a wavelength shift of 0.8 nm, which is four times the bandwidth of the pulse. In other words a completely off resonant interaction was brought into resonance. The third harmonic signal shown in Fig III.14 shows a dip not at zero delay but shifted from it. Such strange nature of third harmonic signal can only be explained in terms of accompaning ionisation. The ionisation near zero delay was estimated to be 60%, which explains the reduction in third harmonic, through the loss of resonant atoms as well as through the atomic coherence loss associated with the high ionisation rate. With decreasing detuning the resonance dip moved towards increasing delay, where the intensity is less. Figs III.11 and III.12 shows resonance dips towards longer delay. The third harmonic signals had similar nature for the two experiments described in Fig (III.11) and (III.12). The third harmonic signal shown in Fig (III.15) did not show any resonance dip. Fig III.13 shows an experimental recrding where the frequency

3RD HARMONIC SIGNAL VERSUS DELAY

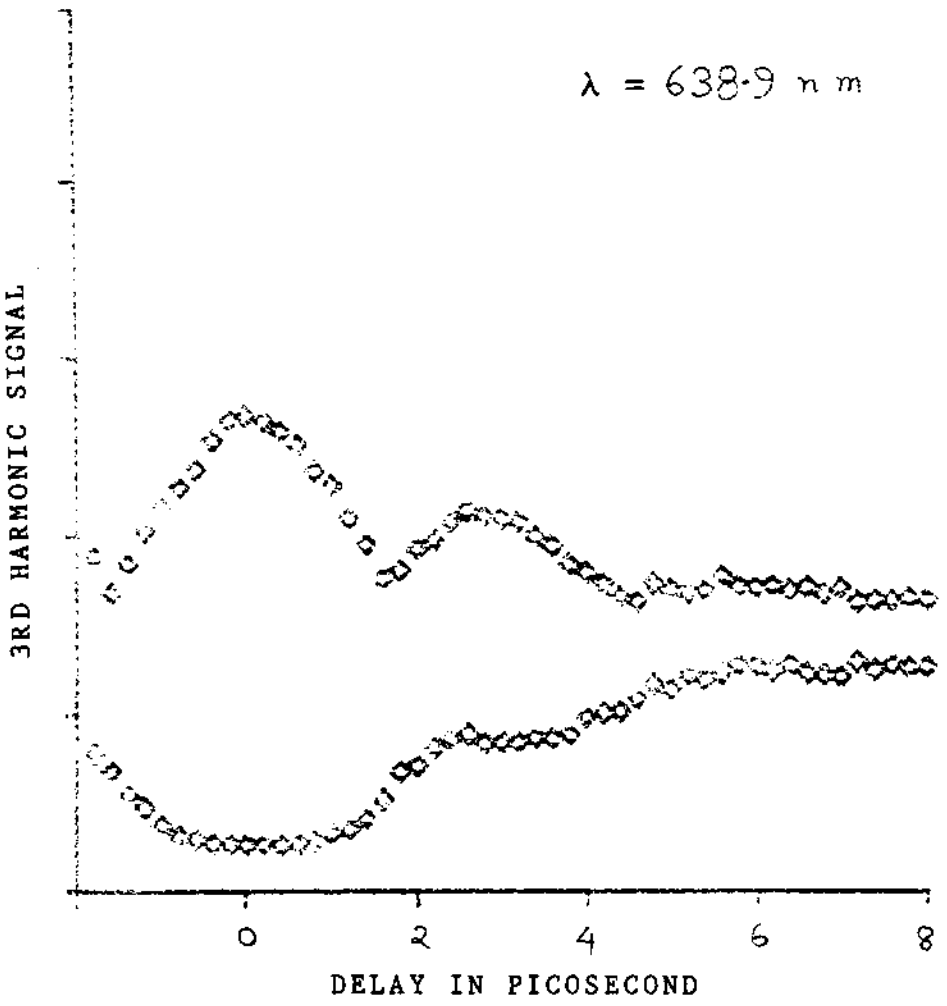

FIG III.14

3RD HARMONIC SIGNAL VERSUS DELAY

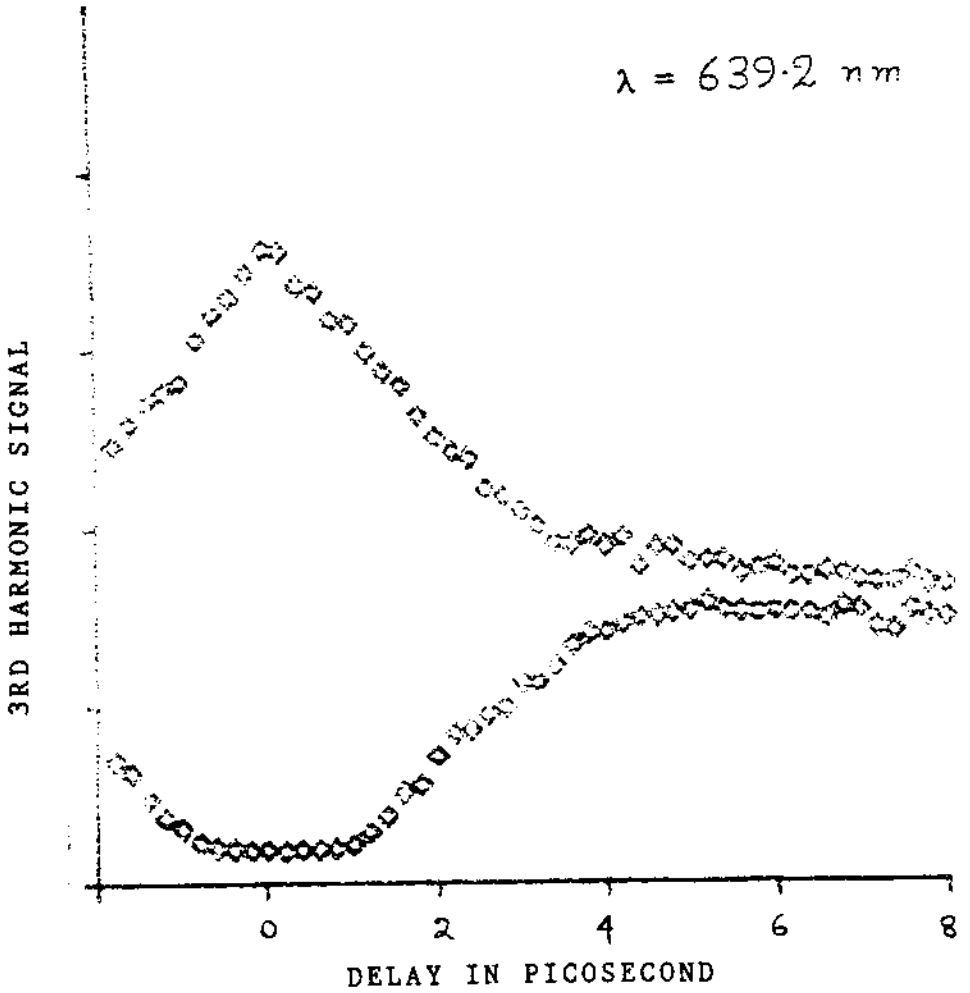

FIG III.15

was tuned below the zero field resonance by 12 X 10^{11} s^{-1}. The net detuning from equation (III.6) is :

$$(\Delta\omega)_{21} = 2\omega - \omega_{21} - \delta\omega_{21}$$

$$\Delta\omega = 2\omega - \omega_{21}$$

$$(\Delta\omega)_{21} = \Delta\omega - \delta\omega_{21}$$

With intensity induced positive Stark shift $\delta\omega_{21}$, we need positive zero field detuning $\Delta\omega$ for resonance tuning. When $\Delta\omega < 0$ (experiment described in Fig III.13) the net detuning $(\Delta\omega)_{21}$, becomes a large negative detuning resulting in an off resonant interaction. No resonance dip was observed in this experiment.

A summary of the experimental results are shown in Table I.

TABLE I

Summary of 2S-3D Experimental Results

2S - 3D zero field two photon resonance wavelength

wavelength λ_o = 639.3 nm

frequency ω_o = 2.9485 X 10^{11} s^{-1}

pulse width τ_p = 6.5 ps

pulse bandwidth = 0.2 nm

Fig No	Tuning Region	λ of Input Light In nm	Detuning per Photon In nm ($\Delta\lambda_o$)	Detuning per Photon In s^{-1} ($\Delta\omega_o$)	Stark Shift In s^{-1} ($\delta\omega_{21}$)
III.10	0-Delay	638.9	-0.4	18×10^{11}	36×10^{11}
III.11	1 ps. Delay	639.1	-0.2	9×10^{11}	18×10^{11}
III.12	2 ps. Delay	639.2	-0.1	4×10^{11}	8×10^{11}
III.13	Off Tuned	639.6	+0.3	-12×10^{11}	

Incident pulse energy density = 14 mJ/cm^2

Two photon area of the pulse = 13

Single pulse absorption = 85%

Fig III.16 shows the second harmonic of the incident and transmitted signal as a function of phase at zero delay corresponding to the experimental recording shown in Fig III.12. From now on, this phase dependent signal will be refered to as the fringe. Fig III.17 shows the third harmonic fringe at zero delay in the same experiment. Fig III.18 and Fig III.19 show similar fringes at a delay of 2.7 ps. There is a phase shift of about 10° between the incident and the third harmonic fringe. The same effect was observed in the case of Li (2S - 4S) experiment.[2] The transmitted fringe also shows a phase shift with respect to the incident one. This could be due to the anomalous propagation where the maximum transmission shifts towards $\pi/2$ rather than toward zero phase. Fig III.20 shows incident and transmitted fringes at 7.8 ps delay. The transmitted fringe shows a clear "double fringe" having an approximate periodicity of π. The maximum of the transmitted signal appeared at a relative phase of 110° instead of 90°. This could be because of the self phase modulation of a large "AREA" pulse resulting in a phase change as a function of distance. As described in Chapter II (see equation II.20), the one photon susceptibility is a function of population (σ_{11} and σ_{22}) which is determined by the intensity of the pulse. As a result the phase of the pulse is also a function of intensity. After propagation the

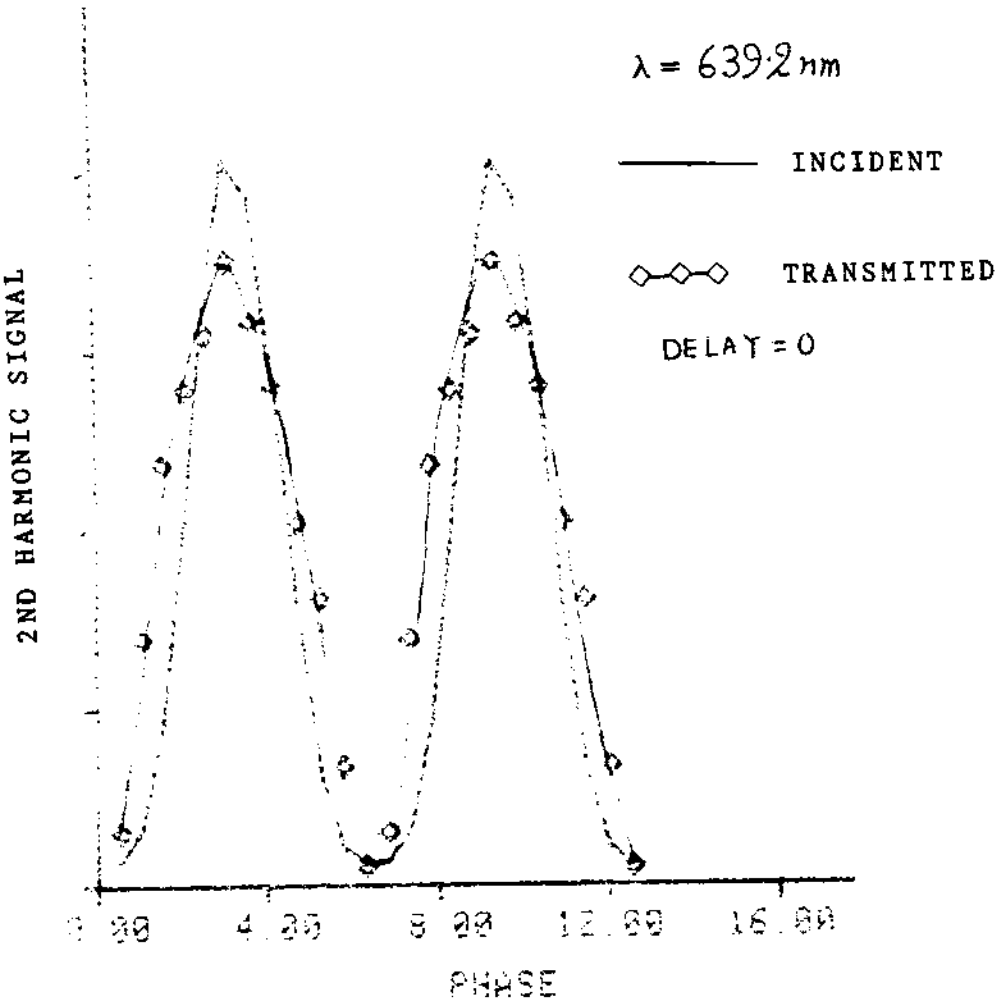
λ = 639.2 nm
INCIDENT
TRANSMITTED
DELAY = 0
2ND HARMONIC SIGNAL
PHASE

FIG III.16

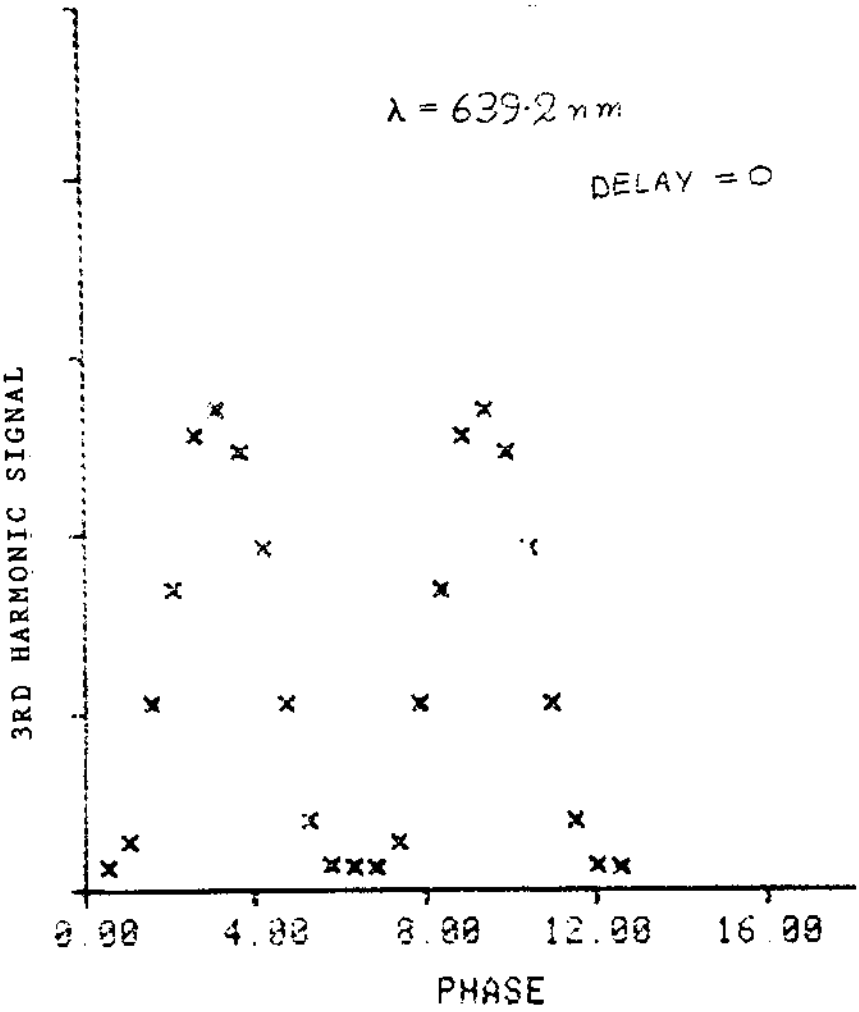
λ = 639·2 nm
DELAY = 0
3RD HARMONIC SIGNAL
0.00
4.00
8.00
12.00
16.00
PHASE

FIG III.17

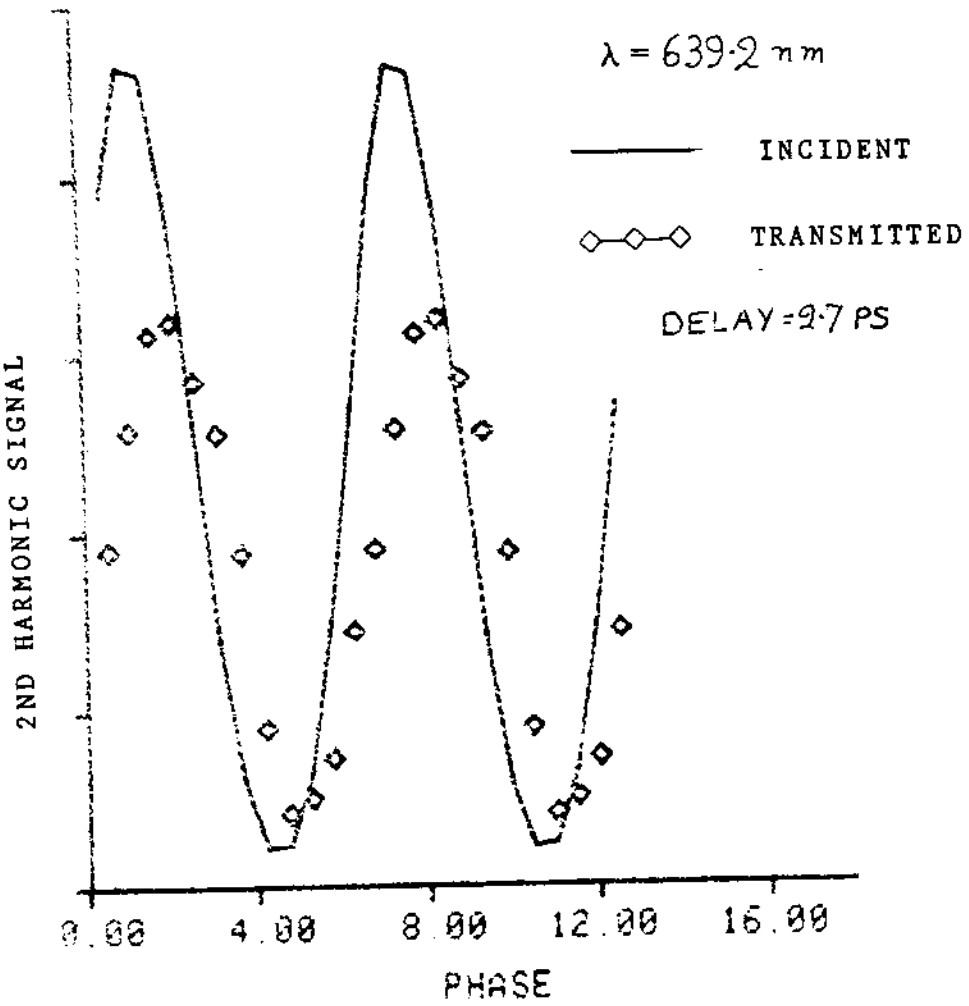
λ = 639·2 nm
INCIDENT
TRANSMITTED
DELAY = 9·7 PS
2ND HARMONIC SIGNAL
0.00
4.00
8.00
12.00
16.00
PHASE

FIG III.18

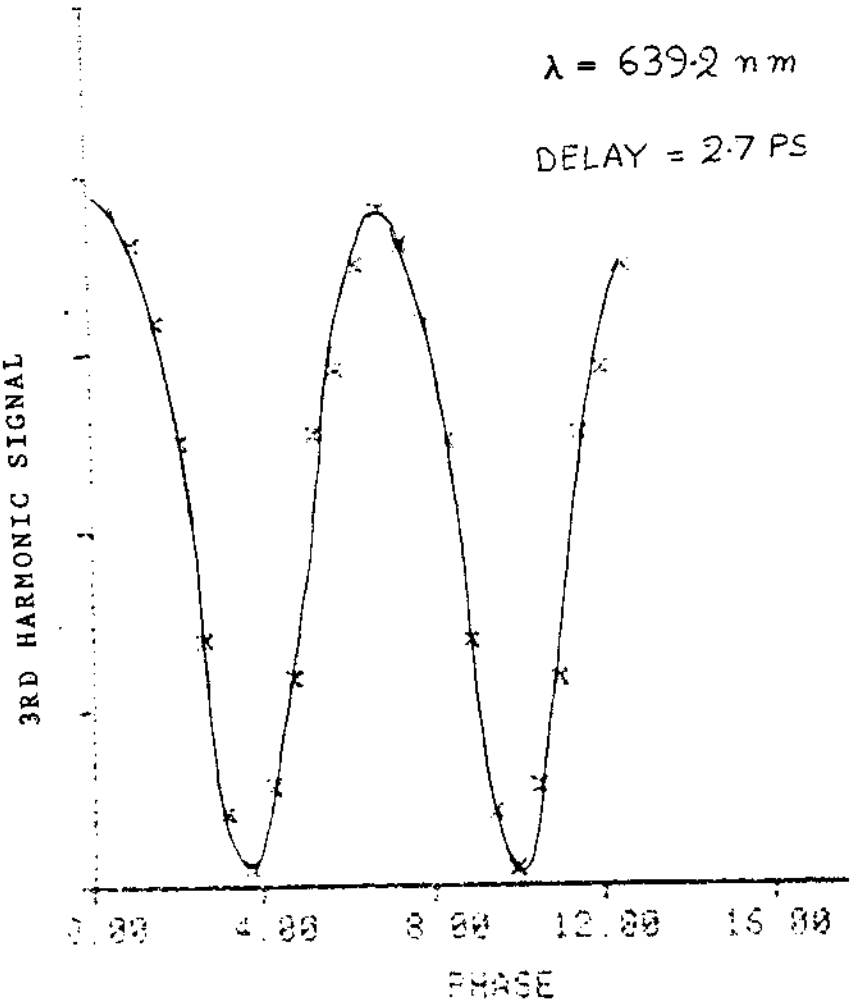
λ = 639·2 nm
DELAY = 2·7 PS
3RD HARMONIC SIGNAL
4.00
8.00
12.00
16.00
PHASE

FIG III.19

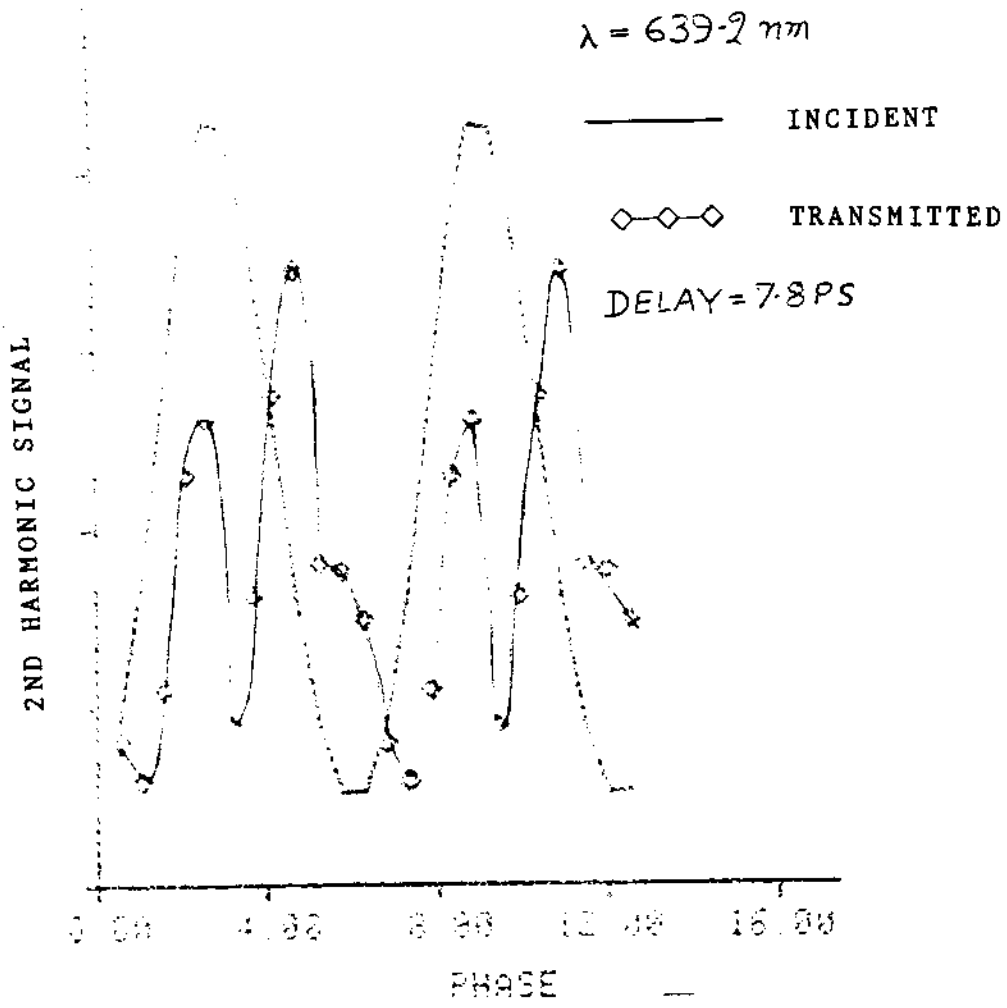
λ = 639·2 nm
INCIDENT
TRANSMITTED
DELAY = 7·8 PS
2ND HARMONIC SIGNAL
PHASE

FIG III.20

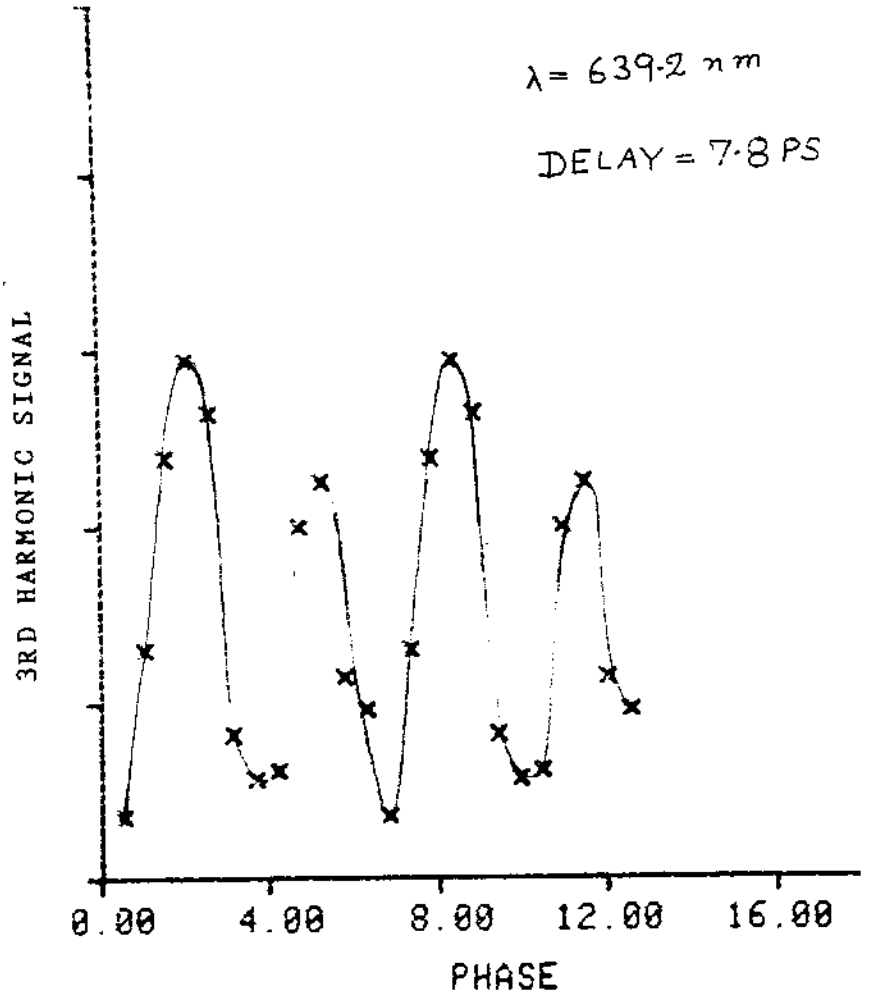
λ = 639·2 nm
DELAY = 7·8 PS
3RD HARMONIC SIGNAL
0.00
4.00
8.00
12.00
16.00
PHASE

FIG III.21

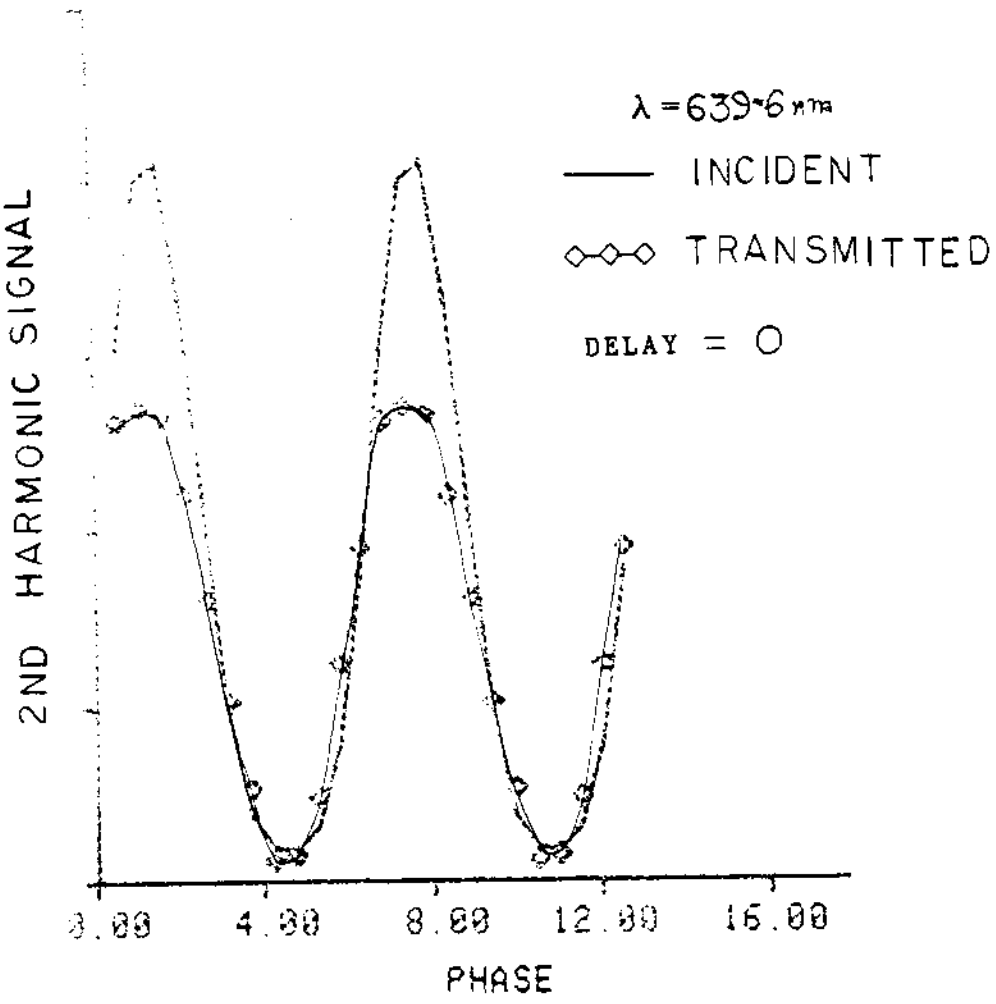
λ = 639·6 nm
INCIDENT
TRANSMITTED
DELAY = O
2ND HARMONIC SIGNAL
4.00
8.00
12.00
16.00
PHASE

FIG Ⅲ.22

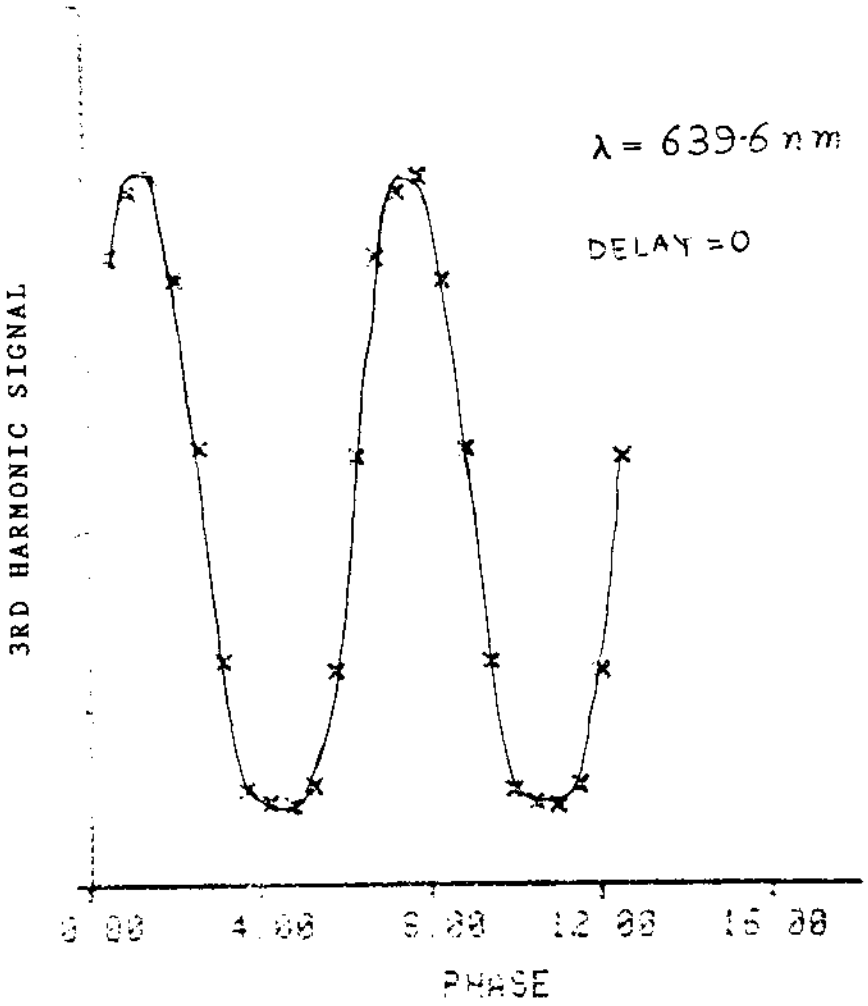
λ = 639·6 nm
DELAY = 0
3RD HARMONIC SIGNAL
0.00
4.00
8.00
12.00
16.00
PHASE

FIG III.23

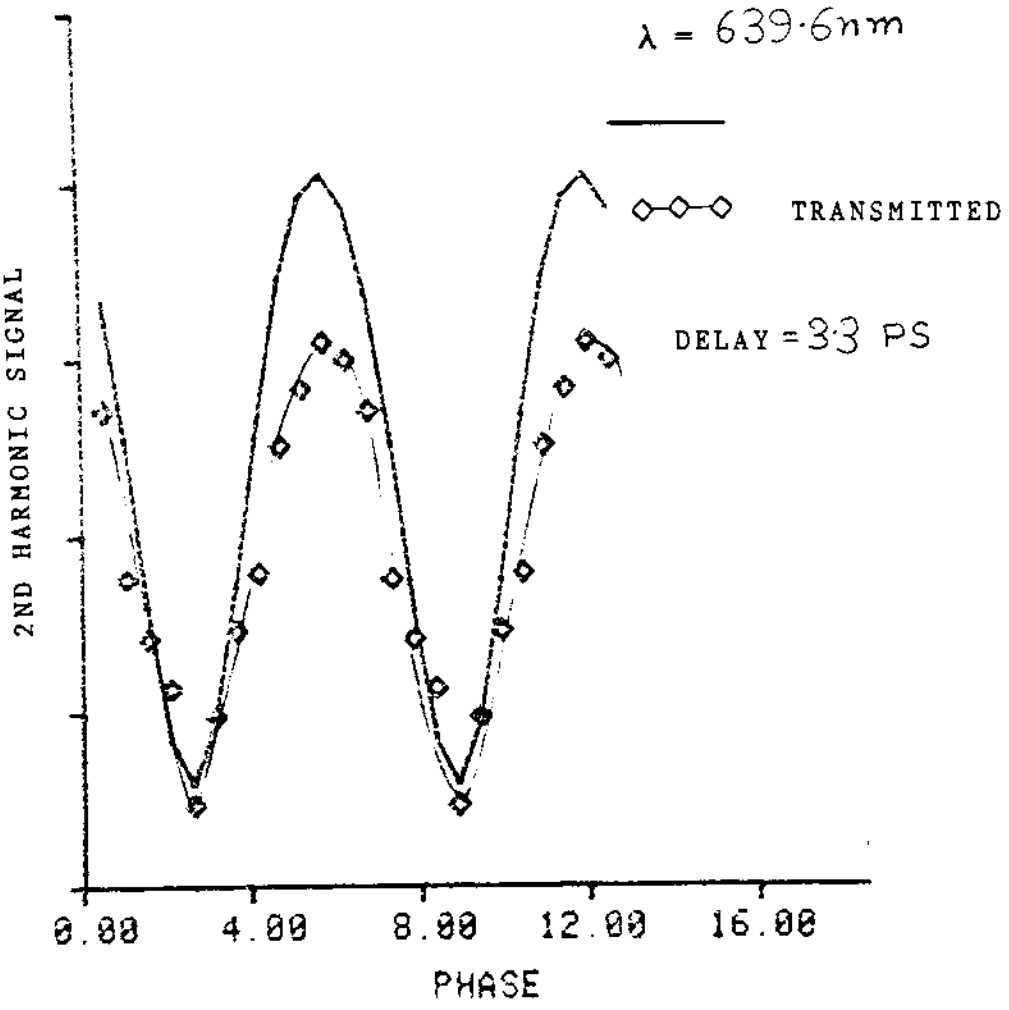
λ = 639·6nm
TRANSMITTED
DELAY = 3·3 PS
2ND HARMONIC SIGNAL
0.00
4.00
8.00
12.00
16.00
PHASE

FIG III.24 (a)

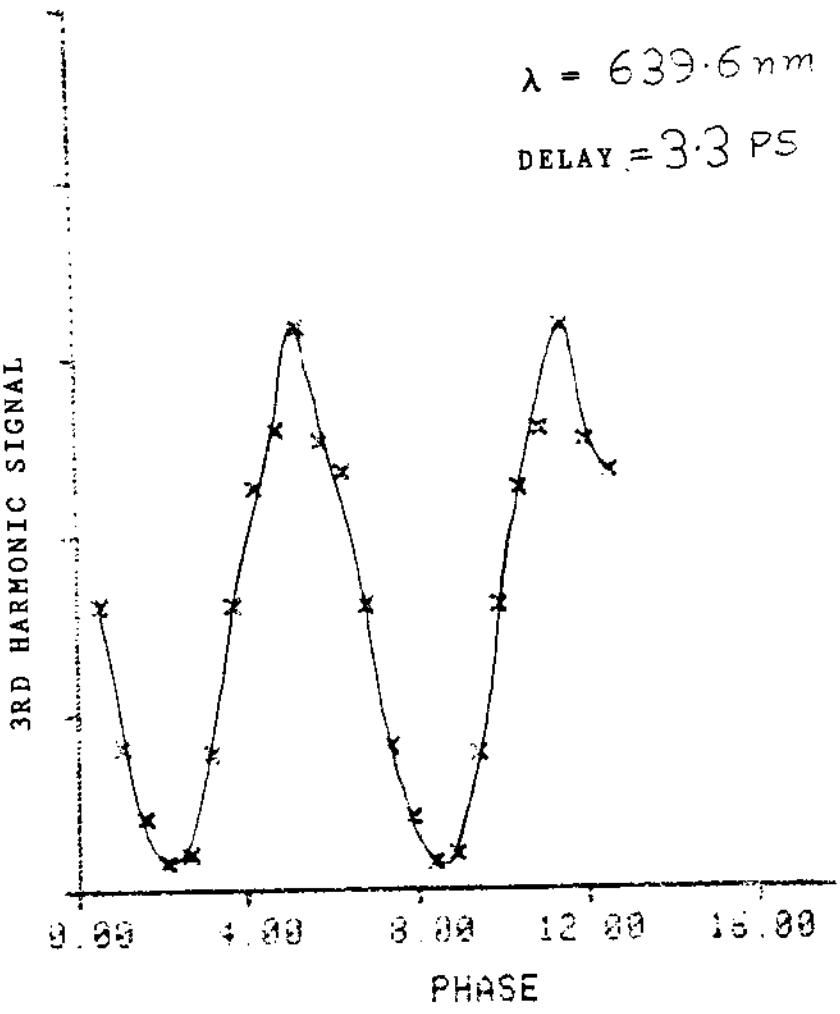
λ = 639·6 nm
DELAY = 3·3 PS
3RD HARMONIC SIGNAL
0.00
4.00
8.00
12.00
16.00
PHASE

FIG III.24 (b)

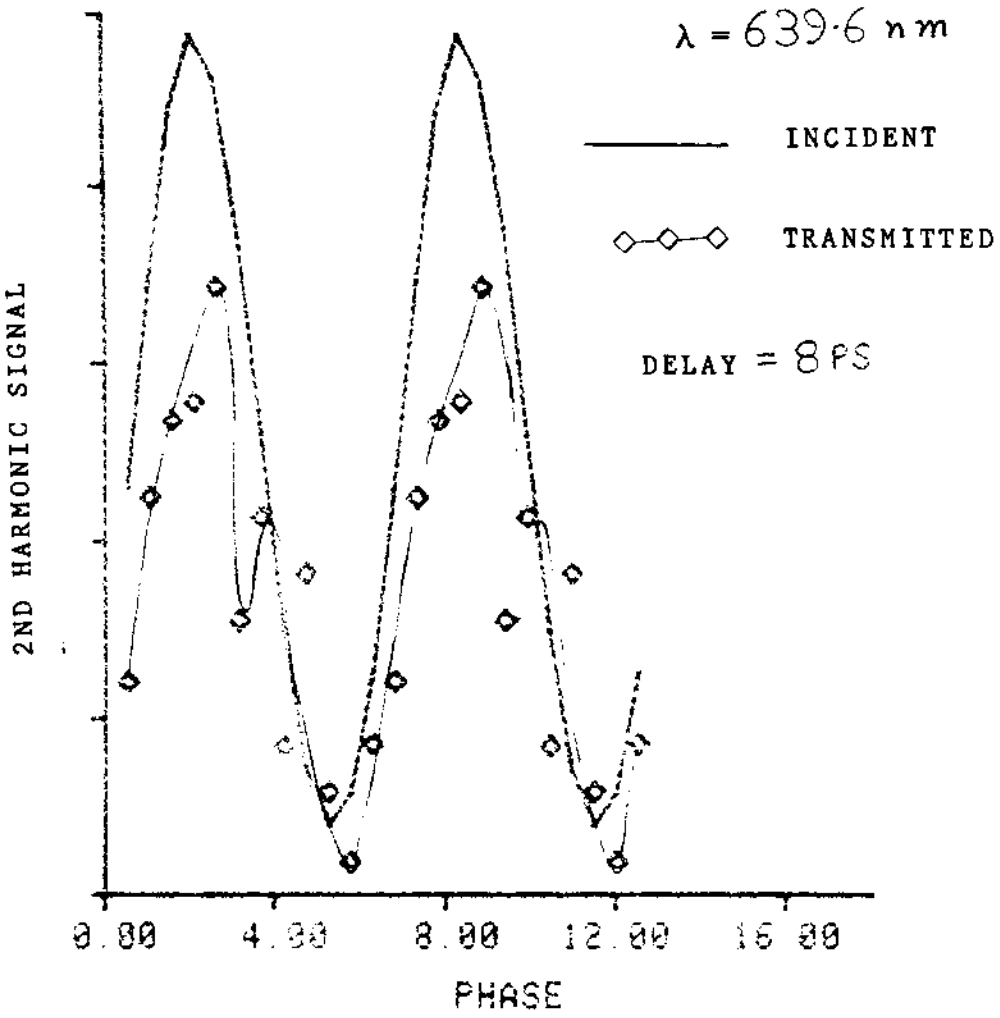
λ = 639·6 nm
INCIDENT
TRANSMITTED
DELAY = 8 PS
2ND HARMONIC SIGNAL
0.00
4.00
8.00
12.00
16.00
PHASE

FIG III.25

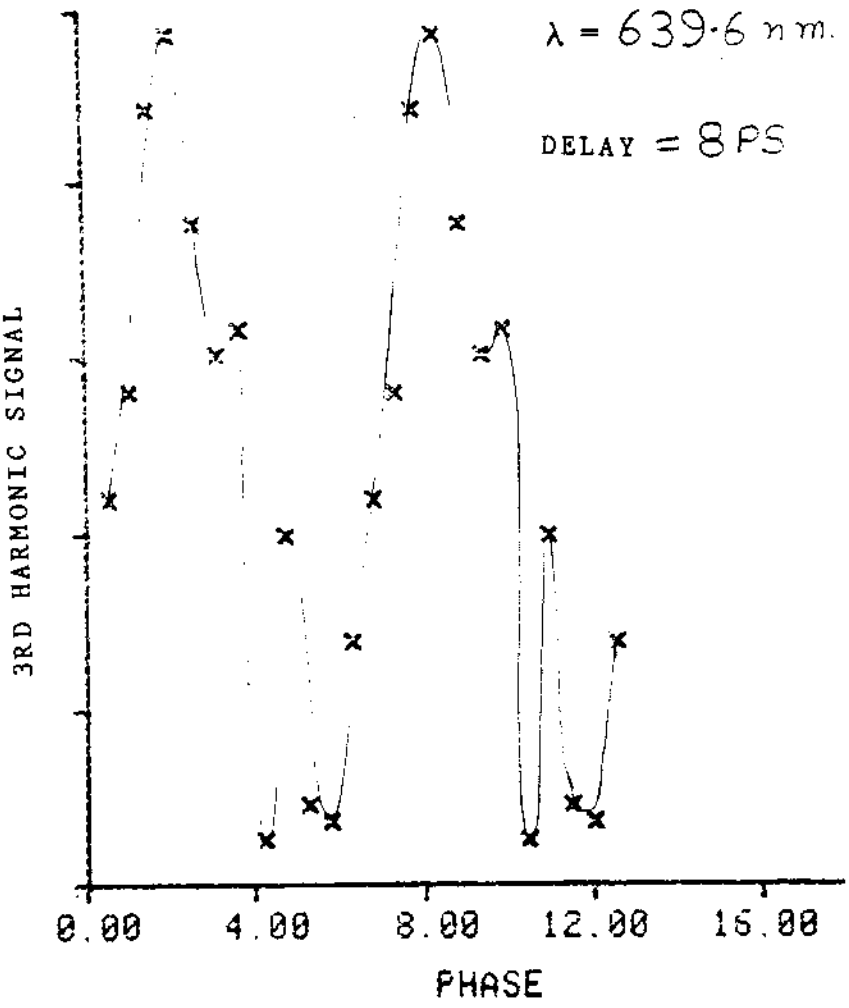
λ = 639·6 nm.
DELAY = 8 PS
3RD HARMONIC SIGNAL
0.00
4.00
8.00
12.00
16.00
PHASE

FIG III.26

different intensities of the two pulses will have different phase modulation and their phase will shift in a different way. Due to this effect, the phase delay required for two photon coherent propagation becomes different from 90°. Fig III.21 shows the third harmonic double double fringe at the same delay as in Fig III.20. Similar fringes were observed for the experiments described in Fig III.11. The group of fringes shown in Figs III.22 to III.26 show incident, transmitted and third harmonic fringes at various delays for the experiment shown in Fig III.13. Due to the off resonant excitation in this experiment we did not observe any double fringe or phase shift effect.

As mentioned earlier, phase matching was not possible by adding Mg vapor. By changing the pressure of the buffer gas in the inner tube of the concentric heat pipe it was possible to change the partial pressure of Mg vapor while the Li vapor pressure was kept constant by the constant temperature bath provided by the outer tube.[2] The middle of the heat pipe contained saturated Li vapor mixed homogeneously with unsaturated Mg vapor. As the delay was kept nearly equal to two pulse widths the Mg pressure was scanned continuously to get optimum third harmonic signal. Fig III.27 shows the third harmonic signal versus the ratio of Mg to Li partial pressures. The starting ratio of Mg to Li vapor density was 0.55. As the pressure of Mg was increased the third harmonic

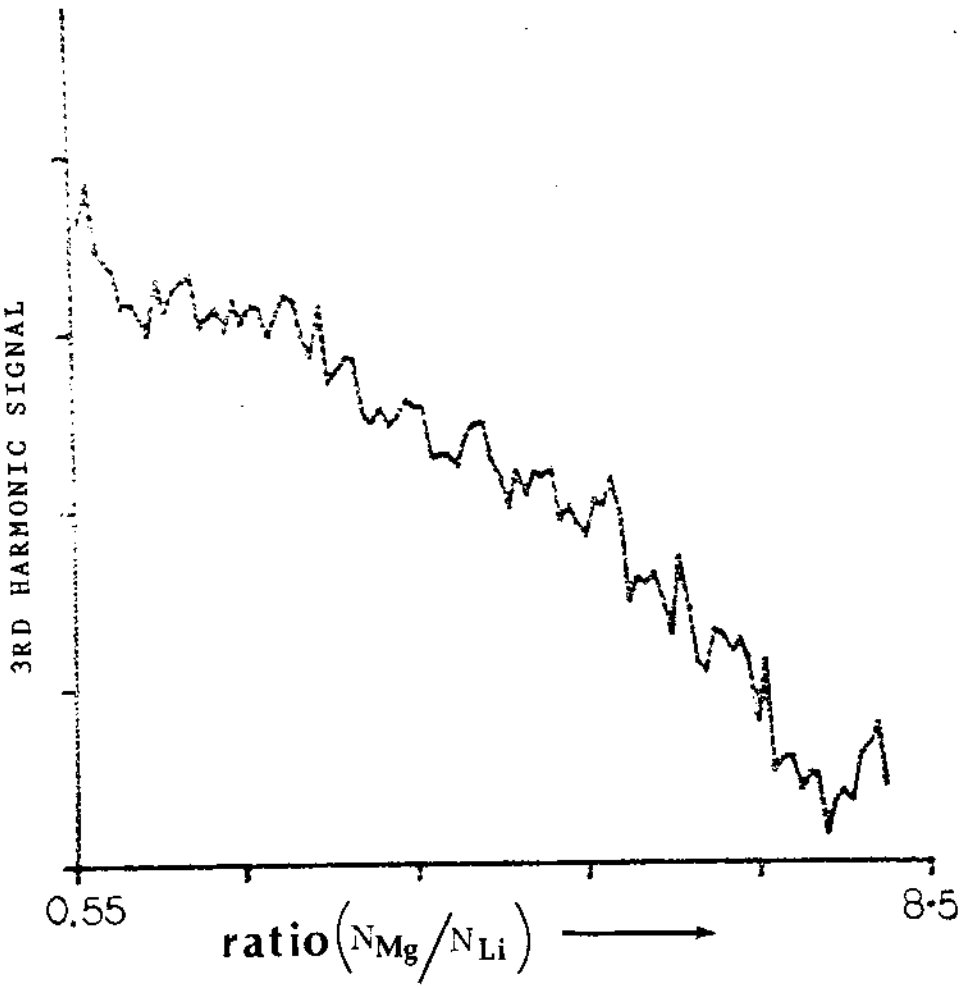

FIG III.27

signal decreased. This should be attributed to the increasing number of dephasing elastic collisions of lithium and magnesium atoms. Indeed at higher partial pressures of Mg, the interaction is no longer coherent. The pressure was scanned up to a ratio (Mg to Li) of 8.5. Third harmonic signal continuously decreased. The maximum conversion was only 10^{-4} %.

2s-4s versus 2s-3d

Although third harmonic generation took place via two photon resonant intermediate step in the same atom there are some characteristic differences between the two transitions which are worth pointing out. In Table II several important atomic parameters for the two transitions are listed. The atomic parameters for 2S - 4S transition were taken from Ref (III.6). The atomic polarisability of the i^{th} resonance level has been defined in Chapter II equation (II.10). r_{12} and ξ_{21} were defined in equations (II.11) and (II.12) respectively. Two photon Bloch equation of Chapter II shows that r_{12} determines the strength of the two photon transition. The two photon "Area" defined in equation (II.19) is given by

$$\Theta = \left(2\gamma_{12}/\hbar^2\right) \int_{-\infty}^{+\infty} \mathcal{E}_1^2 \, dt \qquad \text{(III.8)}$$

TABLE II

Atomic Parameters for 2S-4S and 2S-3D Transitions

Resonance Transition In Li	Two Photon Resonance Wavelength λ_1 (nm)	3rd Harmonic Wavelength λ_3 (nm)	$\alpha_1'(\lambda_1)$ (MKS) $\times 10^{-39}$	$\alpha_2'(\lambda_1)$ (MKS) $\times 10^{-39}$	$\alpha_2''(\lambda_1)$ (MKS) $\times 10^{-40}$	r_{12} (MKS) $\times 10^{-73}$	ξ_{21} (MKS) $\times 10^{-74}$
2S-4S	571.2	190.4	-6.956	-2.74	1.015	1.458	$1.47 \times e^{-i0.481}$
2S-3D	639.3	213.1	-26.26	-42.03	6.214	26.92	$0.299 \times e^{-i0.158}$

From Table II we find that for a given input energy the "area" for 2S - 3D is much larger than 2S - 4S transition. We have,

$$\frac{\theta(2S-3D)}{\theta(2S-4S)} = 18.464 \qquad \text{(III.9)}$$

The 18 times larger "area" of 2S - 3D transition implies a larger angle of rotation of the two photon Bloch vector defined in Chapter II. A larger "area" results in a stronger interaction with larger ionisation, Stark shift etc. In presence of this intensity dependent Stark shift and ionisation, smooth rotation of a pseudo Bloch vector does not take place. The single photon polarisability of the incident pump pulse is given by,

$$\alpha(\omega) = \alpha_1'(\omega)\sigma_{11} + \alpha_2'(\omega)\sigma_{22} \qquad \text{(III.10)}$$

Due to time dependent transfer of population the index of the medium changes sharply with time resulting in a strong self phase modulation of the pulse. A phase modulated pulse looses its self induced transparency effect and gets absorbed. The effect of strong self phase modulation was reflected in the experimental results when the maximum transmission was found at a larger relative phase than 90°. From the above discussion it follows that

2S - 3D trasition with a larger "area" is far more complex than the 2S - 4S transition.

The two photon characteristic length ℓ_2 defined in equation (III.5) for Li 2S - 4S transition at 1 torr vapor pressure was 13.5 cm. At the same pressure ℓ_2 was 0.75 cm for 2S - 3D transition. With stronger two photon absorption the generation length is already reduced.

Using the third harmonic polarisation (equation II.14)

$$P_3 = \frac{\epsilon_{\varphi 21}}{\hbar} \sigma_{12} \mathcal{E}_1 \qquad \text{(III.11)}$$

in Maxwell's equation (II.15) we get

$$\frac{\partial \mathcal{E}_3}{\partial z} = - \frac{i 3\omega N}{2c\epsilon_0} \epsilon_{\varphi 21} \sigma_{12} \mathcal{E}_1$$

By linear integration we find,

$$|\mathcal{E}_3|^2 \propto |\epsilon_{\varphi 21}|^2 \times |\sigma_{12} \mathcal{E}_1|^2 \times (\Delta z)^2$$

(III.12)

From eqn III.12, we find that the third harmonic intensity is proportional to $\epsilon_{\varphi 21}^2$ and $(\Delta z)^2$. Taking Δz to be equal to ℓ_2 and using the parameter values from Table II we can write a ratio of third harmonic intensity produced in the two transitions as follows:

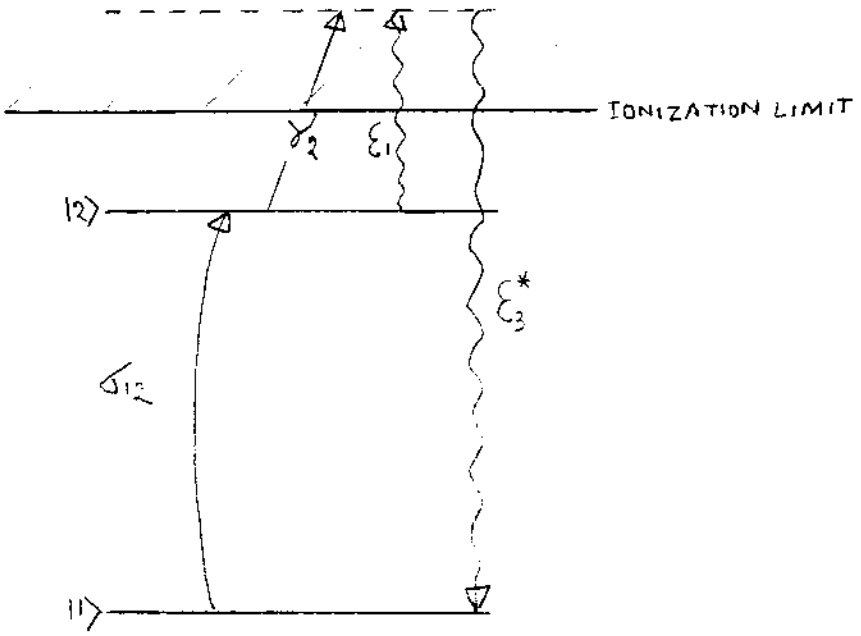
IONIZATION LIMIT
γ_2
ε_1
$|2\rangle$
ε_3^*
σ_{12}
$|1\rangle$

Fig III . 28

$$\frac{|\mathcal{E}_3|^2(2S-4S)}{|\mathcal{E}_3|^2(2S-3D)} = \frac{|\xi_{21}(2S-4S)|^2}{|\xi_{21}(2S-3D)|^2} \times \left(\frac{\ell_2(2S-4S)}{\ell_2(2S-3D)}\right)^2 \qquad \text{(III.13)}$$

$$\simeq 10^{-4}$$

Assuming σ_{12}, $\mathcal{E}_1$ to be the same in both cases and not considering the ionisation or the phase mismatch we can see that 2S-3D transition is less efficient by almost a factor of 10^{-4} than 2S-4S transition. Experimentally the efficiency was found to be 1% for 2S-4S while in 2S-3D it was 10^{-4} %.
To see further differences we have to consider the photoionisation probabilities in the two cases. For 2S - 4S transition, the excited 4S state could only be coupled to a P ($\ell = 1$) state by a single photon dipole allowed transition. In this case the third harmonic level coincides with the same P level in the continuum. The THG competes with the ionisation. From the Bloch equation of Chapter II,

$$\frac{\partial \sigma_{22}}{\partial t} = -\gamma_2 \sigma_{22} - 2\,\mathrm{Im}\left[\left(\frac{r_{12}\mathcal{E}_1^{*2}}{\hbar^2} + \frac{\xi_{21}\mathcal{E}_1\mathcal{E}_3^*}{\hbar^2}\right)\sigma_{12}\right] \qquad \text{(III.14)}$$

We can find that with stronger third harmonic field the two terms $\gamma_2\sigma_{22}$ and $2\,\mathrm{Im}(\xi_{21}\mathcal{E}_1\mathcal{E}_3^*\sigma_{12})$ can compete with each other (see Fig III.28). In case of 2S - 3D transition

the 3D level could be connected either to a P level (ℓ =1) or to a F level (ℓ =3) in the continuum. Since only the P level can be connected to the 2S ground state by allowed dipole transition, the third harmonic level coincides with the P level. While the F level cannot contribute to the third harmonic generation it leads to an independent channel of ionisation. Ionisation takes place via two channels 3D-->F and 3D-->P, whereas third harmonic emission goes via the single channel 3D-->P-->2S. Obviously this results in a lower harmonic generation. Coherence is lost due to the enhanced ionisation rate and σ_{12} remains small. From the definition of ionisation rate, equation (II.9) and from Table II, for the same input pump intensity we get,

$$\frac{\gamma_2^{\omega}(2S-3D)}{\gamma_2^{\omega}(2S-4S)} = 6.12 \qquad \text{(III.15)}$$

The ionisation rate for 2S - 3D transition is at least six times larger than 2S - 4S transition.

In conclusion a two photon resonant S-->S transition is more efficient than an S-->D transition for THG.

Fig. 13

WAVEMETER

In this section we describe a new interferometric technique for measuring wavelength of picosecond pulses with an accuracy better than 0.5 Å. The interferometer is shown in Fig III.29. The incident beam is divided into two equal parts by a beam splitter at the input end of the interferometer. One part goes through a delay arm generated by a 90° prism on a translation stage, while the other part goes through the fixed arm. The two parts are combined by another beam splitter at the output end. There are two outputs for the interferometer shown in Fig III.29. Each output consists of two interfering beams. As the optical path delay between the two beams is changed the output goes from a maxima to a minima at the interval of $\lambda/2$. The output is seen by a photodiode and the signal is stored in the computer as a function of phase and delay. Before we describe the method of measuring λ we must define what we mean by λ of a short pulse of finite bandwidth.

The electric field of an input pulse at a given position in space can be written as

$$E(t) = \xi(t)\, e^{i\omega t + i\varphi(t)} + C.C. \qquad \text{(III.16)}$$

Instantaneous carrier frequency of the pulse

$$= \omega + \frac{\partial \varphi}{\partial t}$$

(III.17)

The average frequency of the pulse

$$\omega_{av} = \omega + \left\langle \frac{\partial \varphi}{\partial t} \right\rangle$$

(III.18)

Angular brackets denote the time averaging. Following Ref III.7 we have,

$$\left\langle \frac{\partial \varphi}{\partial t} \right\rangle = \frac{\int_{-\infty}^{+\infty} \left(\frac{\partial \varphi}{\partial t} \right) \mathcal{E}^2 \, dt}{\int_{-\infty}^{+\infty} \mathcal{E}^2 \, dt} = \frac{\int_{-\infty}^{+\infty} \Omega \, |\tilde{\mathcal{E}}(\Omega)|^2 \, d\Omega}{\int_{-\infty}^{+\infty} |\tilde{\mathcal{E}}(\Omega)|^2 \, d\Omega}$$

(III.19)

where

$$\tilde{\mathcal{E}}(\Omega) = \int_{-\infty}^{+\infty} \mathcal{E}(t) \, e^{i\Omega t + i\varphi(t)} \, dt$$

(III.20)

$\tilde{\mathcal{E}}(\Omega)$ = Fourier Transform of the complex amplitude of the pulse.

The average frequency defined by the equation (III.18 and III.19) defines the average wavelength of the pulse,

$$\lambda_{av} = \frac{2\pi c}{(\omega_{av})} \qquad \text{(III.21)}$$

Relation between average wavelength and interferometric fringe periodicity:

The total electric field of the interfering pulses (at the output of the interferometer) can be written as

$$E(t) = \mathcal{E}(t)\, e^{i\omega t + i\varphi(t)} + \mathcal{E}(t-\mathcal{T})\, e^{i\omega(t-\mathcal{T}) + i\varphi(t-\mathcal{T})} \qquad \text{(III.22)}$$

where $\mathcal{T}$ = time delay corresponding to the optical path delay x.

$$\mathcal{T} = \frac{x}{c} \qquad \text{(III.23)}$$

Assuming $\mathcal{T}$ << the pulse duration $\mathcal{T}_p$ and assuming slowly varying amplitude ($\mathcal{E}(t) \simeq \mathcal{E}(t-\mathcal{T})$) we can write

$$E(t) \simeq \mathcal{E}(t)\, e^{i\omega t + i\varphi(t)} \left[1 + e^{-i\omega\mathcal{T} + i\varphi(t-\mathcal{T}) - i\varphi(t)}\right] \qquad \text{(III.24)}$$

$$\varphi(t-\mathcal{T}) \simeq \varphi(t) - \dot{\varphi}\,\mathcal{T} \qquad \text{(III.25)}$$

$$\dot{\varphi} \equiv \frac{\partial\varphi}{\partial t}$$

[we assume, $\frac{\partial^2\varphi}{\partial t^2} << \dot{\varphi}/\mathcal{T}$]

using equation (III.24) in equation (III.23) we get

$$E(t) \simeq \mathcal{E}(t)\, e^{i\omega t + i\varphi(t)} \left[1 + e^{-i\omega\mathcal{T} - i\dot{\varphi}\mathcal{T}} \right] \tag{III.26}$$

The signal measured by the photodiode is proportional to a quantity S defined by

$$S = \int_{-\infty}^{+\infty} |E(t)|^2 \, dt \tag{III.27}$$

from equation (III.26).

$$|E(t)|^2 = 2\mathcal{E}^2(t) + e^{-i\omega\mathcal{T}}\, \mathcal{E}^2(t)\, e^{-i\dot{\varphi}\mathcal{T}} + e^{i\omega\mathcal{T}}\, \mathcal{E}^2(t)\, e^{i\dot{\varphi}\mathcal{T}} \tag{III.28}$$

Assuming $(\dot{\varphi}\mathcal{T})^2 \ll \dot{\varphi}\mathcal{T}$,

$$e^{-i\dot{\varphi}\mathcal{T}} \simeq 1 - i\dot{\varphi}\mathcal{T} \tag{III.29}$$

$$\int \mathcal{E}^2(t)\, e^{-i\dot{\varphi}\mathcal{T}} dt \simeq \int \mathcal{E}^2(t)\, dt - i\mathcal{T} \int \mathcal{E}^2 \dot{\varphi}\, dt$$

$$= \int \mathcal{E}^2(t)\, dt \left[1 - i\mathcal{T} \frac{\int \mathcal{E}^2 \dot{\varphi}\, dt}{\int \mathcal{E}^2\, dt} \right]$$

using definition (III.19) for $\langle\dot{\varphi}\rangle$,

$$\int_{-\infty}^{+\infty} \mathcal{E}^2(t)\, e^{-i\dot{\varphi}\mathcal{T}} dt \simeq \left[1 - i\mathcal{T}\langle\dot{\varphi}\rangle \right] \int_{-\infty}^{+\infty} \mathcal{E}^2\, dt \tag{III.30}$$

to a first order approximation,

$$1 - i\mathcal{T}\langle\dot{\varphi}\rangle = e^{-i\mathcal{T}\langle\dot{\varphi}\rangle} \tag{III.31}$$

[$(\mathcal{T}\langle\dot{\varphi}\rangle)^2$ and higher order terms are neglected]

using equation (III.31) in equation (III.30),

$$\int_{-\infty}^{+\infty} \mathcal{E}^2(t)\, e^{-i\dot{\varphi}\mathcal{T}}\, dt = e^{-i\mathcal{T}\langle\dot{\varphi}\rangle} \int_{-\infty}^{+\infty} \mathcal{E}^2\, dt$$

(III.32)

and similarly,

$$\int_{-\infty}^{+\infty} \mathcal{E}^2\, e^{i\dot{\varphi}\mathcal{T}}\, dt = e^{i\mathcal{T}\langle\dot{\varphi}\rangle} \int_{-\infty}^{+\infty} \mathcal{E}^2\, dt$$

(III.33)

using equations (III.28),(III.31),(III.33) in equation (III.27) we get,

$$S = 2\int_{-\infty}^{+\infty} \mathcal{E}^2 dt + \int_{-\infty}^{+\infty} \mathcal{E}^2 dt \left(e^{-i\omega\mathcal{T} - i\langle\dot{\varphi}\rangle\mathcal{T}} + e^{i\omega\mathcal{T} + i\langle\dot{\varphi}\rangle\mathcal{T}} \right)$$

(III.34)

let

$$\epsilon = \int_{-\infty}^{+\infty} \mathcal{E}^2 dt$$

$$S = 2\epsilon \left[1 + \cos\left(\omega + \langle\dot{\varphi}\rangle\mathcal{T}\right) \right]$$

(III.35)

using definition (III.18)

$$S = 2\epsilon \left[1 + \cos \omega_{av}\mathcal{T} \right]$$

using $\mathcal{T} = x/c$, and $\lambda_{av} = 2\pi c/\omega_{av}$

$$S = 2\epsilon \left[1 + \cos \frac{2\pi}{\lambda_{av}} x \right]$$

(III.36)

S is called "interference fringe". To a first order approximation the periodicity of the interference fringe determines the average frequency of a pulse. Note that (see equation III.19) for a symmetric pulse spectrum $\langle \dot{\varphi} \rangle = 0$. and we have,

$$\omega_{av} = \omega \quad \text{or} \quad \lambda_{av} = \lambda$$

Method of measuring

A simple way to measure λ_{av} is to count fringes of two different laser beams going through the same path of the interferometer as shown in Fig III.29. One of the laser beams could be a single mode laser of well defined wavelength while the other is the picosecond laser pulse under investigation. Since the optical path delay x is the same for both of them we can write,

$$x = N_1 \lambda_1 = N_2 \lambda_2 \tag{III.37}$$

$$\lambda_2 = \left(\frac{N_1}{N_2}\right) \lambda_1 \tag{III.38}$$

where N_i is the number of fringes at wavelength λ_i. Knowing λ_1, N_1, N_2 we can find λ_2. Counting a large number of fringes the counting error could be minimised. Counting has to be done by a computer. Suppose

λ_1 = wavelength of a standard single mode He-Ne laser

= 6328 A°

$$\lambda_2 = \lambda_{dye} = \left(\frac{N_{He\text{-}Ne}}{N_{dye}}\right)\lambda_{He\text{-}Ne}$$

Assuming an error ΔN in counting we can write

$$\lambda_{dye} \simeq \left(1 + \frac{\Delta N_{He\text{-}Ne}}{N_{He\text{-}Ne}}\right)\mathring{\lambda}_{dye}$$

$\mathring{\lambda}_{dye}$ = the correct dye wavelength.

$\Delta\lambda = \lambda_{dye} - \mathring{\lambda}_{dye}$ = error in measuring the dye wavelength.

$$\Delta\lambda = \left(\frac{\Delta N_{He\text{-}Ne}}{N_{He\text{-}Ne}}\right)\mathring{\lambda}_{dye} \qquad \text{(III.39)}$$

When the delay is determined with an accuracy of $(1/40)^{th}$ of a wavelength (Ref III.2) ΔN is approximately 0.03.

With $N_{He\text{-}Ne} = 1000$ and $\mathring{\lambda}_{dye} = 6400\ \mathring{A}$, $\Delta\lambda = 0.2\ \mathring{A}$ (III.40)

for 6 ps (FWHM) pulses, there are about 3000 fringes within the FWHM. Counting of 1000 fringes can be quite accurately done by a computer.

In the above method the error increases with less number of periods (for shorter pulses) and cannot be applied when there is appreciable pulse to pulse intensity fluctuation.

The following method (of finding λ_{av}) is based upon the construction of a single average fringe. Experimental setup is the same as before. The delay accurate to $(1/40)^{th}$ of a wavelength is determined from the fringe of a single mode He-Ne laser. A single period of dye fringe is divided into several phase channels and the data of dye fringe is stored in respective phase channels (see Ref III.2).

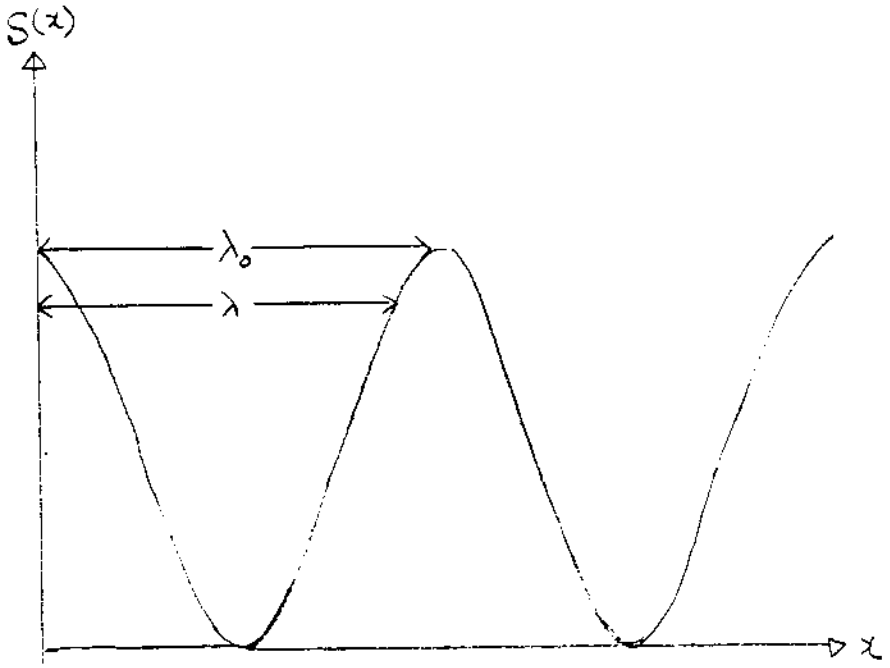

Fig III · 30

Phase delay

$$\varphi = 2\pi x/\lambda - 2\pi n \qquad \text{(III.41)}$$

where n is an integer, $\lambda \equiv \lambda_{av}$.

φ is determined from zero to 2π, x is the absolute distance determined from the He-Ne fringe. λ is the approximate dye laser wavelength measured for example by a fairly crude monochromator with 5 Å resolution. Maximum distance $x_{max} = N\lambda$ where N = number of periods for averaging.

For example, if zero to 2π phase is divided into 25 phase intervals the data of N periods will be distributed in 25 phase channels and an average fringe can be constructed.[2] The accuracy of averaging is determined by the accuracy of the determination of λ . An average fringe calculated with a wrong wavelength will deviate from the pure cosine function shown in equation (III.36). From the deviation and "trial and error" fitting, λ can be determined with an accuracy up to 0.2 Å.

Error Estimate

Following Fig III.30 an average fringe fringe can be written as

$$F(x) = \frac{1}{(N+1)} \sum_{j=0}^{N} \cos\left(x + j\lambda\right) \frac{2\pi}{\lambda_0} \qquad \text{(III.42)}$$

where N+1 = the total periods for averaging

λ_0 = the correct wavelength

λ = the trial wavelength

If $\lambda = \lambda_o$ $\quad F(x) = \cos(2\pi x/\lambda_o)$

If $\lambda \neq \lambda_o$ $\quad F(x)$ will deviate from the cosine function and from the deviation $(\lambda - \lambda_o)$ can be measured.

Suppose $\lambda = \lambda_o + \delta\lambda$

$$F(x) = \frac{1}{(N+1)} \sum_{j=0}^{N} \cos\left(\frac{2\pi x}{\lambda_o} + j\,\frac{\delta\lambda}{\lambda_o}\,2\pi\right) \qquad \text{(III.43)}$$

Suppose $x' = 2\pi x/\lambda_o$ and $a = 2\pi\,\frac{\delta\lambda}{\lambda_o}$

$$F(x) = \frac{1}{(N+1)} \sum_{j=0}^{N} \cos(x' + ja) \qquad \text{(III.44)}$$

Deviation error ERR (x ,N,a) is given by,

$$ERR(x', N, a) = F(x') - \cos(x') \qquad \text{(III.45)}$$

ERR (x ,N,a) is a nonlinear function of x ,N and a.

From equation (III.44) and (III.45),

$$ERR(x', N, a) = \frac{-N}{(N+1)} \cos x' + \frac{1}{(N+1)} \left\{ \cos x' \left(\sum_{j=1}^{N} \cos ja \right) - \sin x' \left(\sum_{j=1}^{N} \sin ja \right) \right\} \qquad \text{(III.46)}$$

with $Na \ll 1$, $\cos(ja) \cong 1$ and $\sin(ja) \cong ja$

we have,

$$ERR(x, N, a) = -(aN/2) \sin(x') \qquad \text{(III.47)}$$

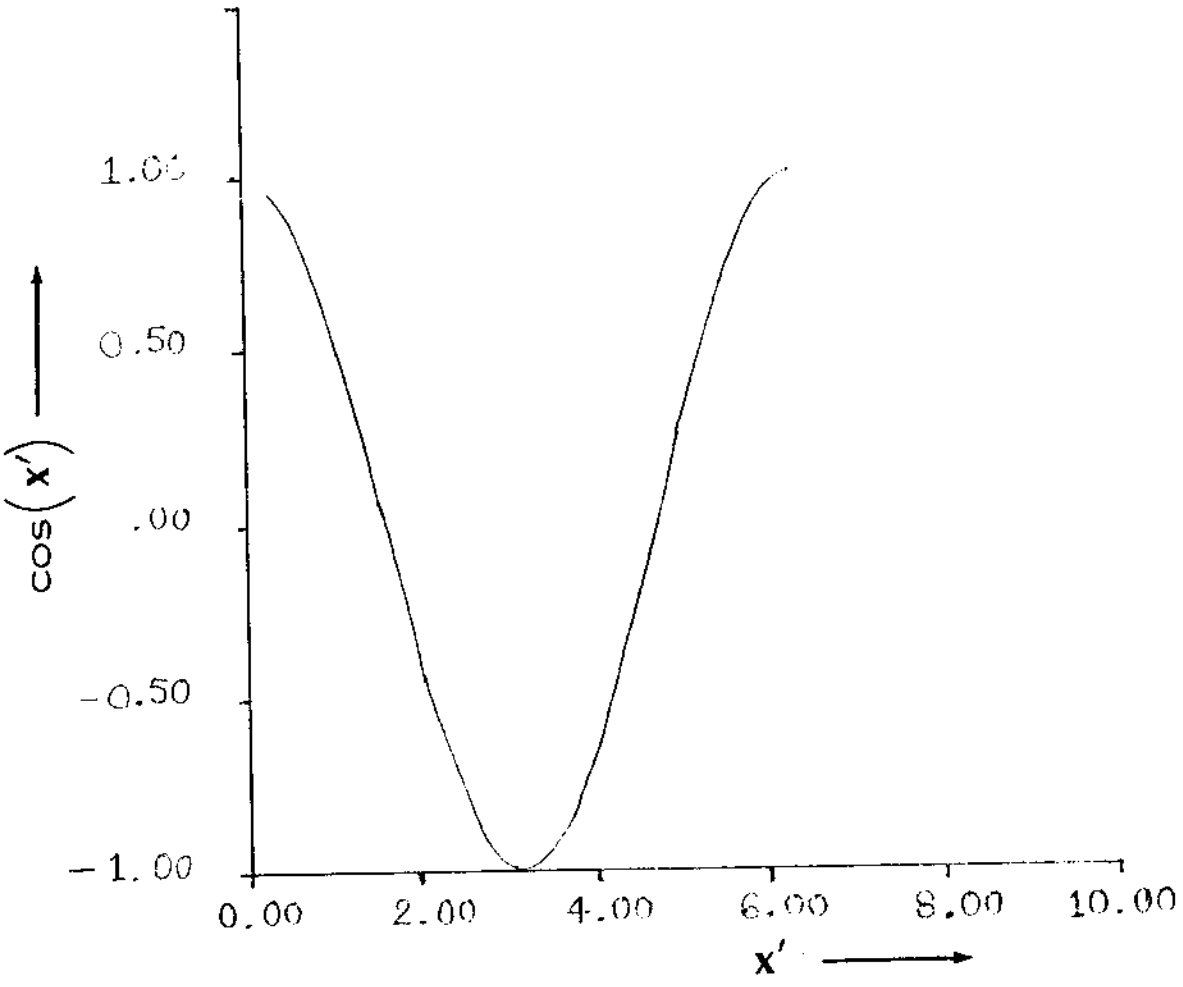

FIG III.31

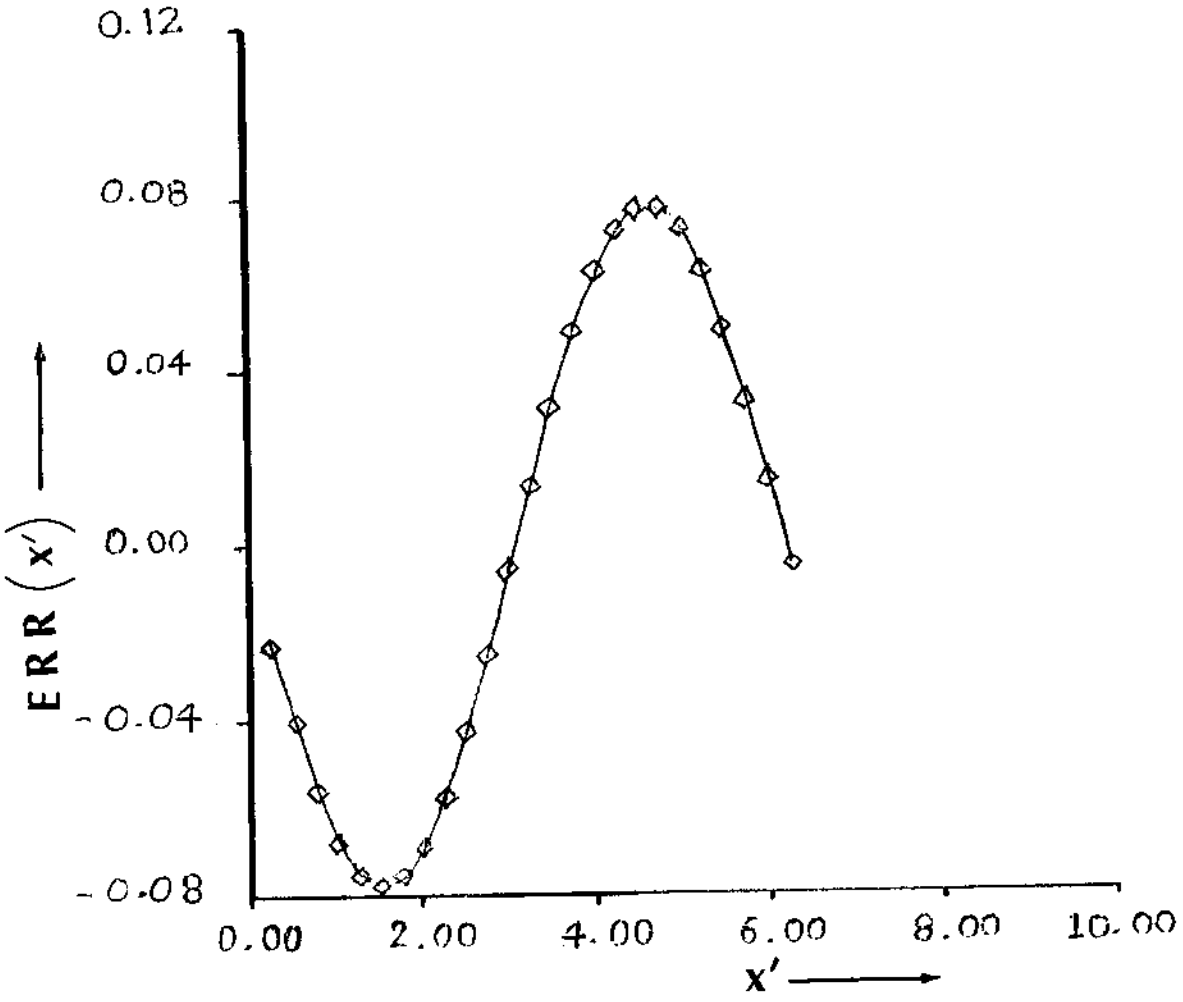

FIG III. 32.

for $\delta\lambda = 0.2$ Å, $\lambda = 6700$ Å and $N = 501$

$a = 1.87 \times 10^{-4}$ and $aN = 0.09$, with all these the above approximation ($Na << 1$) is valid.

If $\delta\lambda$ is replaced by $-\delta\lambda$, ERR(x ,N,a) shifts its phase by π . From the sign of the error we know whether we are above or below the correct wavelength. Fig III.31 shows a pure cosine function. Fig III.32 shows that the error function ERR(x ,N,a) is a sine function. In this case, we have assumed $\delta\lambda/\lambda = 0.5 \times 10^{-4}$ and $N = 500$. This corresponds to an error of about 0.35 Å in $\lambda = 6700$ Å. As we approach the correct wavelength ($\delta\lambda \rightarrow 0$) the error function becomes a straight line. The amplitude of the error function gives the magnitude of $\delta\lambda$ and phase of the error fuction gives the sign of $\delta\lambda$.

Second harmonic fringe S2 is given by,

$$S_2 \propto \int_{-\infty}^{+\infty} |E^2(t)|^2 \, dt \qquad \text{(III.48)}$$

where E(t) is defined in equation (III.24). Near zero delay we have (Ref III.8)

$$S2 = \cos x' + 0.25 \cos(2x') \qquad \text{(III.49)}$$

Fig III.33 shows a pure second harmonic fringe given by

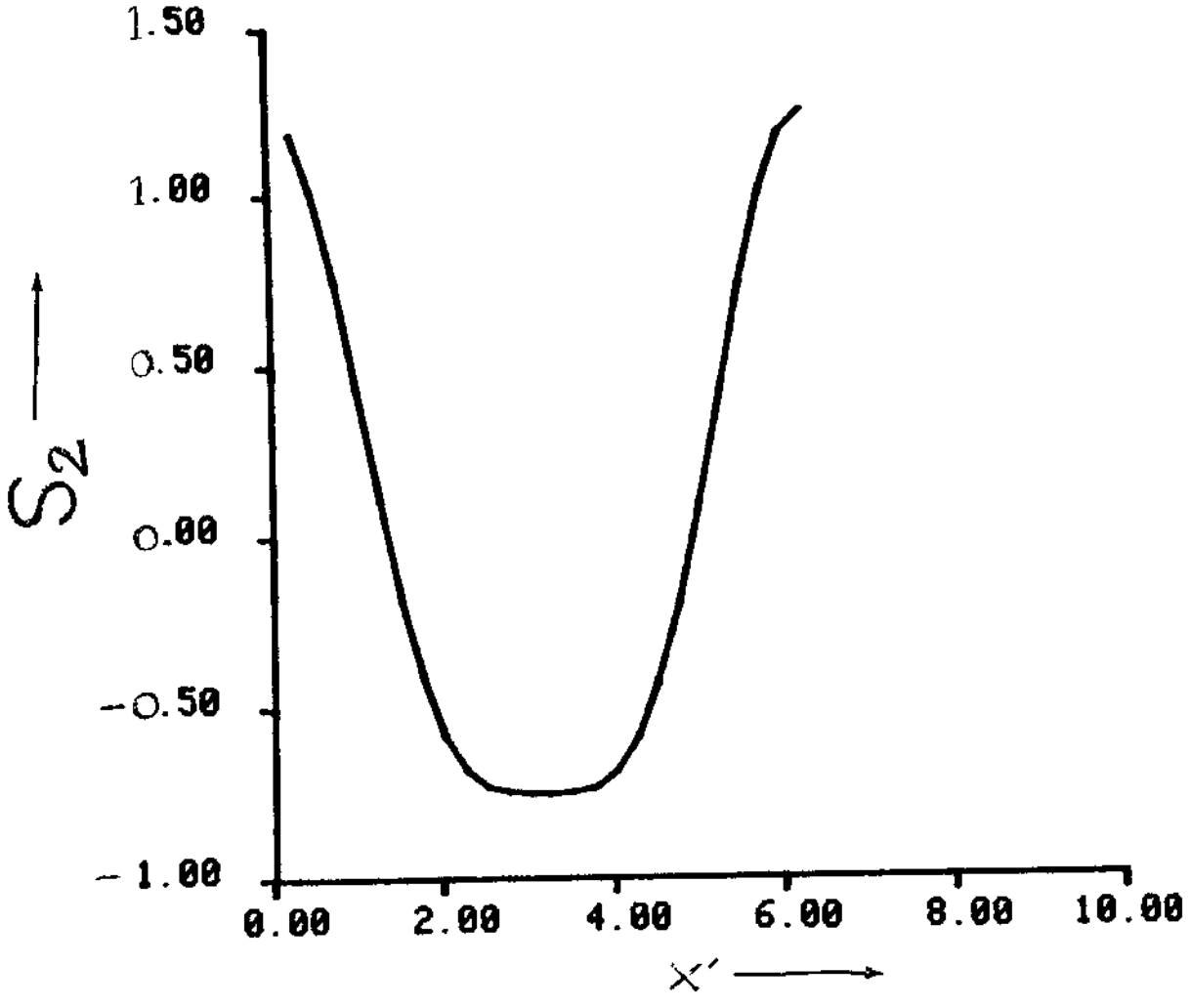

FIG III.33

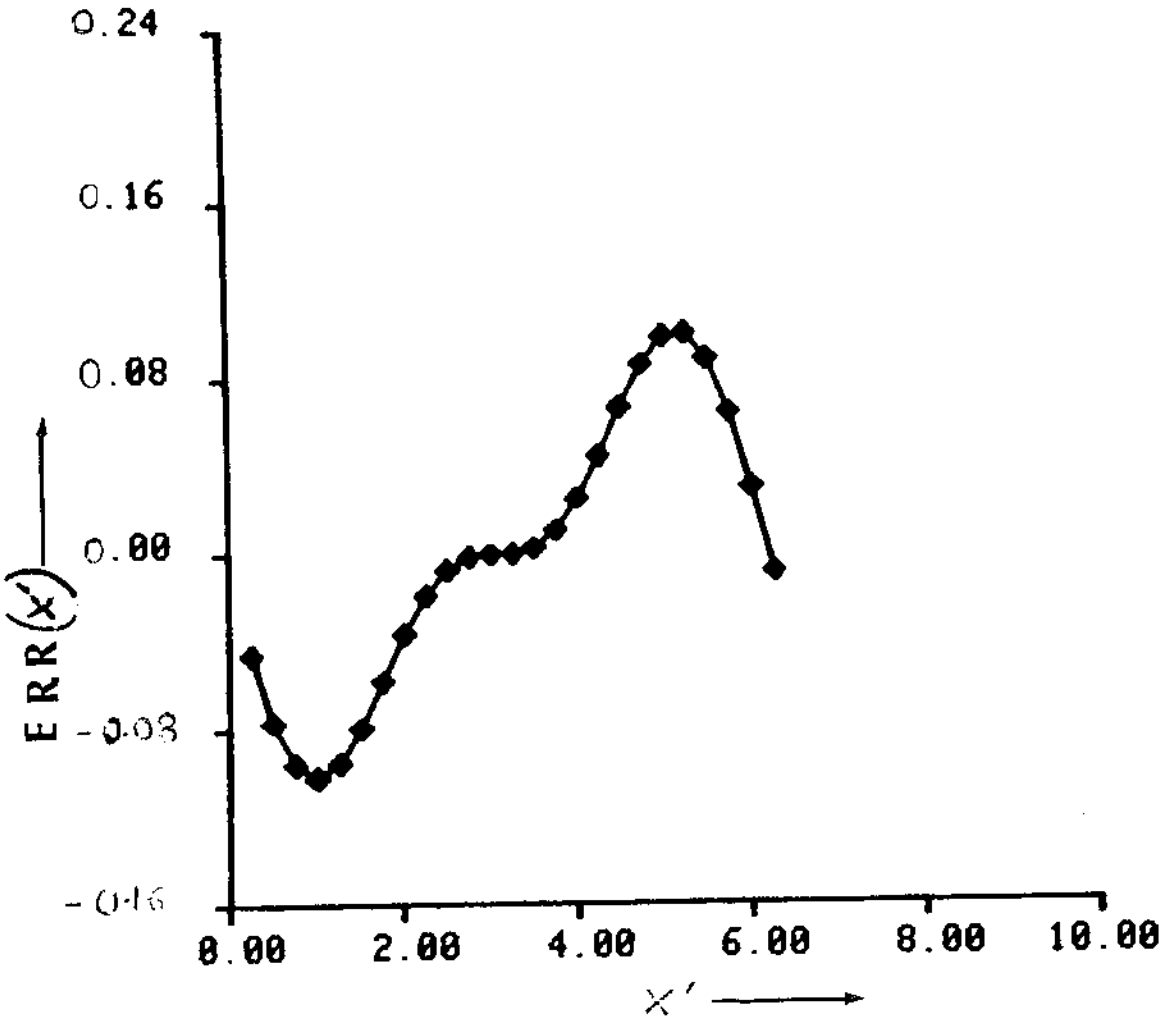

FIG III-34

equation III.49. Fig III.34 shows the error function for $\frac{\delta\lambda}{\lambda} = 0.5 \times 10^{-4}$ and N = 500 periods. The error is more pronounced in the case of second harmonic fringe. This implies a better determination of $\delta\lambda$.

For a picosecond pulse Fabry-Perot interferometer would require mirror spacing as close as 1 to 2 mm which results in broad transmission peaks. A very high finesse (mirrors with high reflectivity $\simeq$ .99) is required for good resolution (1 Å). For a weak intensity pulse this is not particularly suitable. On the other hand the interferometric method used here is based on averaging and it can be applied to moderately fluctuating pulse trains.

CHAPTER BIBLIOGRAPHY

1. Kuhn.H.G.,"Atomic Spectra",Academic press,NY 1969.

2. Mukherjee. A.,Ph.D Thesis ,NTSU (1987).

3. Vanherzeele et al., "Spatial and Temporal Properties of a tunable picosecond dye-laser oscillator-amplifier system", Applied Optics, Vol.23, No.13, (1 July, 1984), 2056-2061.

4. Miles et al.,"Optical third harmonic generation in alkali metal vapors", IEEE J.Qn.Elec. QE-9, 470(1973).

5. C.E.Moore ,"Atomic energy levels",National Bureau of Standards.(GPO,Washington,D.C.,1971.)

6. Diels J-C. & Georges A. T., "Coherent two-photon resonant third- and fifth-harmonic vacuum- ultraviolet generation in metal vapors", Physical Review A, Vol 19, No.4, (April, 1979), 1589-1606.

7. Diels J-C. & Hahn E. L.,"Carrier-frequency distance dependence ...." Physical Review A, Vol.8, No.2, 1084 (August,1973).

8. Diels *et al.*,"Control and measurement of ultrashort pulse shapes ...." Applied Optics, *24*, 1270 (1985).

CHAPTER IV

HARMONIC GENERATION IN FOUR-PHOTON RESONANT COHERENT INTERACTION

In this chapter we present a theory of harmonic generation in a four photon resonant coherent interaction. We have already seen examples where third harmonic generation is enhanced due to an intermediate two photon resonance. Higher harmonics are generated through higher order processes. Higher order susceptibility can be enhanced whenever there is an intermediate resonance. We will be dicussing the nonlinear interaction in atomic vapor,where due to inversion symmetry only odd harmonics are generated. Two photon resonant fifth harmonic generation of dye laser radiation in Na vapor has been reported by Dinev et al.,1980.[1] A ten fold enhancement of the fifth harmonic signal was observed as the laser was tuned through the 3s-3s5s two photon resonance in Na. Saturation of the conversion was observed for pump intensities higher than 10^{8} Watt/cm^{2}. For higher harmonic generation a higher order resonance should be preferred over the lower order one. A higher order resonance will have less multiphoton absorption loss for pump wave. The saturation can be avoided by coherent (as opposed to incoherent)interaction. Third harmonic

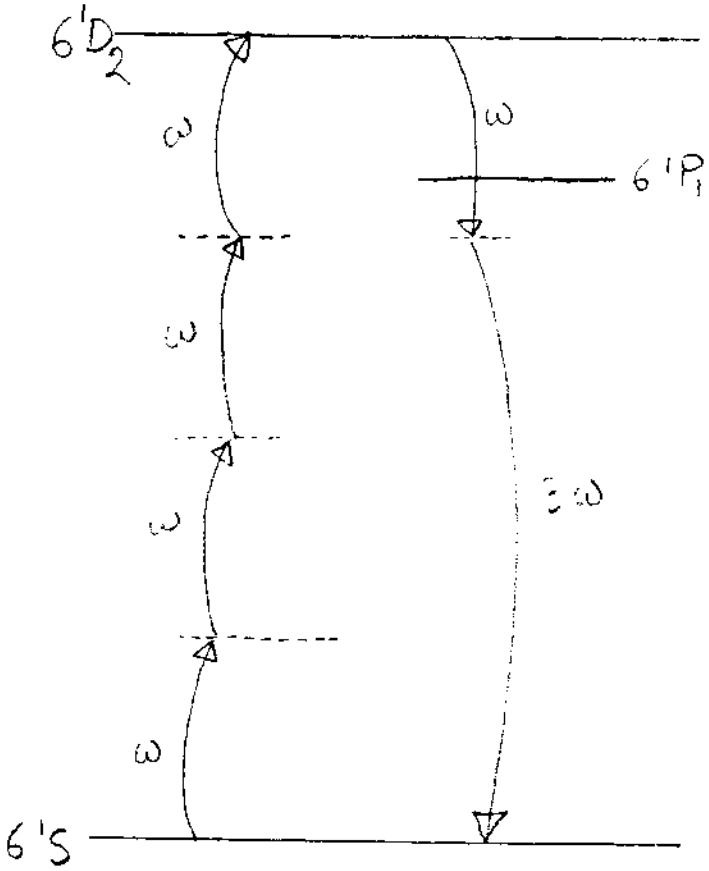

Fig IV.1

generation in four photon resonant Hg atom has been observed by Arlee V.Smith,1985;[2] and by Normand et al.,1983.[3] Third harmonic signal was peaked as the input laser wavelength was tuned through 6^1S_0-6^1D_2 resonance of Hg vapor. Although there was not any real level at the third harmonic frequency of the incident laser,the genereated third harmonic wavelength was exactly one third the wavelength of the input pump wave. In this case the VUV emission is due to four photon resonant six wave mixing as shown in FigIV.1. A red shift of the singlet 6^1D_2 level was observed in the experiment mentioned above. This red shift increased with intensity. This intensity dependent Stark shift is a very special effect in multiphoton interaction. Besides the dynamic Stark shift there will be resonant multiphoton ionisation - the most important limiting factor in higher harmonic generation. In the experiments of four photon resonant (FPR) third harmonic generation (THG) in Hg vapor the ionisation rate was found to be rather low. A steady state situation prevailed since nanosecond (ns) pulses were used in all the experiments mentioned above.

Here we are interested in studying the resonant wave mixing processes with pulses much shorter than the atomic relaxation times. In presence of coherent interaction a definite phase relationship exists between the induced polarisation and the inducing field. This allows control over absorption, phase matching etc. for optimum harmonic

generation as we have seen in the examples of Chapter III. The higher harmonic susceptibility diverges in the presence of intermediate resonance and accurate expression of third harmonic polarisation can only be found by a complete solution of Schroedinger equation. From the solution of Schroedinger equation space-time dependent expression of induced polarisations at various harmonics (of the incident field frequency) can be obtained. These polarisations will be the source terms in Maxwell's equation generating fields at various harmonics. Simultaneous solutions of Schroedinger and Maxwell's equations describe the harmonic generation processes. In this chapter a complete theory is developed to describe the harmonic generation process in a FPR medium using Schroedinger and Maxwell's equations.

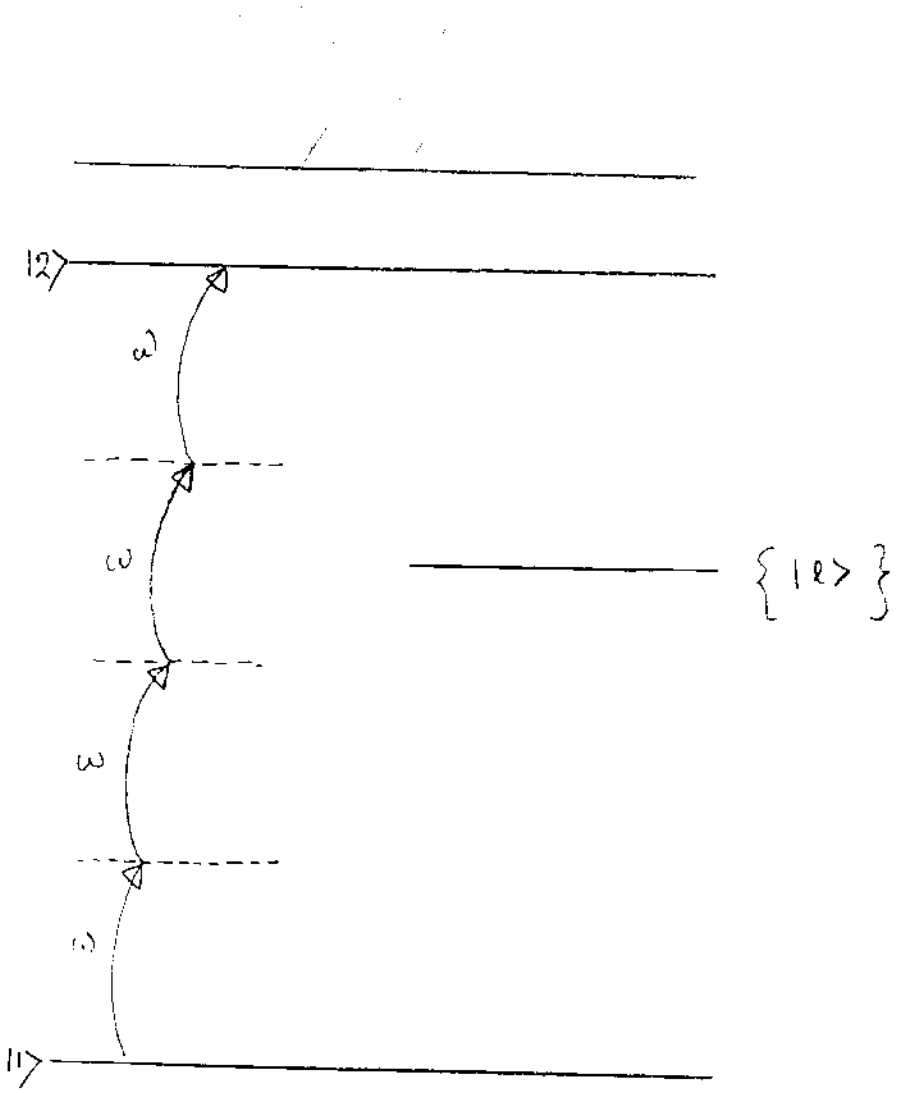

Fig IV·2

Derivation of Four Photon Resonant Equations

An incident laser pulse is assumed to be FPR between the ground state and an upper excited state of a multilevel atom. Transitions involving all other levels are assumed to be off- resonant with the incident light. In Fig.IV.2 all off-resonant levels including ionisation continuum are represented by $\{\ell\}$. I1> is the ground state. I2> is the excited state coupled to the ground state with four photons from the incident laser pulse. For coherent interaction the pulse duration has to be much less than the population and phase relaxation times, as well as the inverse detunings. Doppler broadening can be neglected in most cases when we deal with pulses of few picosecond (or less) duration. Doppler broadening can be handled by proper doppler averaging whenever it is needed.

Suppose:

$\tau_p \equiv$ input pulse width

$T_1 \equiv$ population relaxation time

T_2 ≡ Pressure induced phase relaxation time

T_2^* ≡ Inverse doppler width

we assume,

$$\tau_p < T_2^*, T_2, T_1 \qquad -(IV.1)$$

The linewidth of a resonant coherent excitation is determined only by the pulse bandwidth. The detuning and the pulse bandwidth determines the resonance condition.

Suppose:

$\Delta\omega_p$ ≡ input pulse bandwidth

$\Delta_\ell^{(n)} = \omega_{\ell 1} - n\omega$ ≡ n-photon detuning of the ℓ^{th} level.

where,

$\omega_{\ell 1}$ is the resonance frequency of the ℓ^{th} excited state from the ground state.

We assume:

$$|(\omega_{21} - 4\omega)| \lesssim 4(\Delta\omega_p) \qquad -(IV.2)$$

$$\text{and} \quad \frac{|(\omega_{\ell 1} - n\omega)|}{n(\Delta\omega_c)} \gg 1 \quad \text{for } \ell \neq 1,2 \qquad -(IV.3)$$

$$n = 1, 2, 3, \ldots\ldots$$

When equation (IV.3) is satisfied we can apply the "Adiabatic Following" approximation to all off-resonant levels to convert the problem of many level atom into a problem of an equivalent two level atom. In this way we derive the four photon "Bloch Equation".[4] For the "free" levels in the continuum there seems to be a problem with the condition of equation (IV.3). But as explained by Georges A.T. in his Ph.D. thesis,[5] the effect of the coupling with the continuum can be treated as a weak perturbation since bound-free dipole matrix elements are much smaller than bound-bound matrix elements. In this derivation the electromagnetic field of the laser is treated classically by the Maxweel's equation while the atom is treated quantum mechanically by the density matrix equations. The density matrix operator ρ describes the state of the atom. The relaxation terms involving T_1 and T_2 can be incorporated phenomenologically into the density matrix equations. When equation (IV.1) is satisfied, the phase-coherent density matrix operator ρ (of a single atom) satisfies the following equation:

$$\frac{\partial \rho}{\partial t} = \frac{i}{\hbar}\left[\rho, H\right] \qquad -(IV.4)$$

Where

H is the total Hamiltonian of a single atom.

Under dipole approximation we have

$$H = H_o - \vec{\mu} \cdot \vec{E} \qquad -(IV.5)$$

Where

H_o is the Hamiltonian of a single unperturbed atom.

$\vec{\mu} = e\vec{r} \equiv$ The dipole moment operator of the atom.

$e \equiv$ Electronic charge ($e = -1.6 \times 10^{-19}$ Coul.)

Due to FPR between levels I1> and I2> we have:

$$\mu_{12} = 0 \qquad -(IV.6)$$

$E(z,t)$ is the total electric field of the incident and generated wave.

$$E = E(z,t) = \mathcal{E}_1(z,t)\, e^{i\omega t - ikz} + \mathcal{E}_3(z,t)\, e^{i3(\omega t - kz)} + \mathcal{E}_5(z,t)\, e^{i5(\omega t - kz)} + C.C. \qquad -(IV.7)$$

$E(z,t)$ is assumed to be a plane wave propagating along $\hat{z}$.

$$\mathcal{E}_i(z,t) = |\mathcal{E}_i(z,t)|\, e^{i\varphi_i(z,t)} \qquad -(IV.8)$$

$i = 1,3,5.$

Where

$\varphi_i(z,t)$ = space-time dependent phase function of the i^{th} harmonic field.

$i = 1$ corresponds to the first harmonic

field and so on.

From equation (IV.4) we get the equation of motion for the elements of the density matrix:

$$\frac{\partial \rho_{12}}{\partial t} = i\omega_{21}\rho_{12} - \frac{iE}{\hbar}\left[\sum_j \left(\mu_{j2}\rho_{1j} - \mu_{1j}\rho_{j2}\right)\right] \qquad -(IV.9)$$

$$\frac{\partial \rho_{22}}{\partial t} = -\frac{iE}{\hbar}\left[\sum_j \left(\mu_{j2}\rho_{2j} - \mu_{2j}\rho_{j2}\right)\right] \qquad -(IV.10)$$

$$\frac{\partial \rho_{11}}{\partial t} = -\frac{iE}{\hbar}\left[\sum_j \left(\mu_{j1}\rho_{1j} - \mu_{1j}\rho_{j1}\right)\right] \qquad -(IV.11)$$

and in general,

$$\frac{\partial \rho_{kl}}{\partial t} = i\omega_{lk}\rho_{kl} - \frac{iE}{\hbar}\left[\sum_j \left(\mu_{jl}\rho_{kj} - \mu_{kj}\rho_{jl}\right)\right] \qquad -(IV.12)$$

"$\sum_{\downarrow}$" signifies the summation over the discrete states and integration over the continuum.

Adiabatic Approximation for the off-resonant density matrix elements

For the off-resonant density matrix we may write

$$\rho_{kl} = \sum_{n=-\infty}^{+\infty} \sigma_{kl}(n\omega, t)\, e^{in\omega t} \qquad -(IV.13)$$

$\sigma_{kl}(n\omega, t)$ is the slowly varying Fourier amplitude of ρ_{kl}.

To demonstrate the idea of adiabatic approximation we consider the contribution only from the first harmonic field. A generalisation to include the effect of all the harmonic fields is straightforward.

The electric field at the position of the atom (neglecting the higher harmonic fields) is given by,

$$E(t) = \mathcal{E}_1(t)\, e^{i\omega t} + \text{C.C.} \qquad -(\text{IV.14})$$

Using equation (IV.13) and (IV.14) in equation (IV.12) we get ,

$$\frac{\partial \sigma_{kl}(n)}{\partial t} + i\,(n\omega - \omega_{lk})\,\sigma_{kl}(n)$$

$$= -i\left[\sum_j \left(\frac{\mu_{jl}\mathcal{E}_1}{\hbar}\,\sigma_{kj}(n-1) + \frac{\mu_{jl}\mathcal{E}_1^*}{\hbar}\,\sigma_{kj}(n+1)\right)\right.$$

$$\left. - \sum_j \left(\frac{\mu_{kj}\mathcal{E}_1}{\hbar}\,\sigma_{jl}(n-1) + \frac{\mu_{kj}\mathcal{E}_1^*}{\hbar}\,\sigma_{jl}(n+1)\right)\right] \qquad -(\text{IV.15})$$

where

$$\sigma_{kl}(n) \equiv \sigma_{kl}(n\omega, t)$$

We define,

$$\Omega_{jl} = \frac{\mu_{jl} |E_1|}{\hbar} \qquad -(IV\cdot 16)$$

$$\frac{\partial \sigma_{kl}(n)}{\partial t} + i(n\omega - \omega_{lk})\,\sigma_{kl}(n)$$

$$= (-i) \sum_{\substack{p=n-1 \\ n+1}} \left[\Omega_{jl}\,\sigma_{kj}(p) - \Omega_{kj}\,\sigma_{jl}(p) \right] e^{i(n-p)\varphi_1} \qquad -(IV\cdot 17)$$

where Einstein's summation convention is implied over the repeated indices.

Multiplying both sides of Eqn(IV.17) by $e^{i(n\omega - \omega_{lk})t}$ we get,

$$\frac{\partial}{\partial t}\left[\sigma_{kl}(n)\, e^{i(n\omega - \omega_{lk})t} \right]$$

$$= (-i) \sum_{\substack{p=n-1, \\ n+1}} \left[\Omega_{jl}\,\sigma_{kj}(p) - \Omega_{kj}\,\sigma_{jl}(p) \right] \times e^{i(n-p)\varphi_1} \times e^{i(n\omega - \omega_{lk})t}$$

intregating both sides and using the initial conditions

$$\sigma_{11}(t=0) = 1.$$

and $\sigma_{kl}(n\omega, 0) = 0$ for $k, l \neq 1$

we get,

$$\sigma_{kl}(n) = (-i)\, e^{-i\Delta_{lk}(n)t} \sum_{\substack{p=n-1 \\ n+1}} \int_0^t \left\{ \left(\Omega_{jl}\sigma_{kj}(p) - \Omega_{kj}\sigma_{jl}(p) \right) \times e^{i(n-p)\varphi_1} \times e^{i\Delta_{lk}(n)t'} \right\} dt'$$

$$\Delta_{lk}(n) = n\omega - \omega_{lk} \qquad -(IV.18)$$

Integration by parts gives -

$$\sigma_{kl}(n) = (-i) \left(\frac{e^{-i\Delta_{lk}(n)t}}{i\,\Delta_{lk}(n)} \right) \sum_{p=n-1,n+1} \left[\Omega_{jl}\sigma_{kj}(p) - \Omega_{kj}\sigma_{jl}(p) \right] \times e^{i(n-p)\varphi_1 + i\Delta_{lk}(n)t} + i \left(\frac{e^{-i\Delta_{lk}(n)t}}{i\,\Delta_{lk}(n)} \right) \sum_{p=n-1,n+1} \int_0^t \frac{\partial S(p)}{\partial t'} e^{i\Delta_{lk}(n)t'} dt'$$

$$-(IV.19)$$

in equation (IV.19)

$$S(p) = \left[\Omega_{jl}\, \sigma_{kj}(p) - \Omega_{kj}\, \sigma_{jl}(p) \right] e^{i(n-p)\varphi_1}$$

$$\sigma_{kj}(p) \sim \xi_1^p$$

S(p) goes like ξ_1^n for p=n-1, n+1

$$\frac{\partial \xi_1}{\partial t} \sim \frac{\xi_1}{\tau_p}$$ where τ_p = pulse duration

$$\frac{\partial S}{\partial t} \sim n\, \xi_1^{n-1} \frac{\partial \xi_1}{\partial t}$$

or $$\frac{\partial S}{\partial t} \sim \frac{n S}{\tau_p} \qquad - (IV.20)$$

If $$\Delta_{lk}(n) >> \frac{n}{\tau_p} \qquad - (IV.21)$$

then $e^{i\Delta_{lk}(n)t'}$ in $\int \frac{\partial S}{\partial t'} e^{i\Delta_{lk}(n)t'} dt'$ will oscillate many times

before $\frac{\partial S}{\partial t}$ changes significantly. Under this situation the

integral will average to zero.

Using $\frac{1}{\tau_p} = \Delta\omega_p$ from eqns (IV.21) we get,

$$\Delta_{\ell k}(n) >> n\,\Delta\omega_p$$

or,
$$\frac{\Delta_{\ell k}^{(n)}}{r_1\,\Delta\omega_p} >> 1 \qquad -(IV.22)$$

Eqn(IV.22) says that the n-photon detuning of the transition between $\ell \leftrightarrow k$ is much larger than the line-width of n-photon resonance between the levels. Under this off-resonant condition expressed by eqn(IV.22) ,the integral in the left hand side of Eqn(IV.19) can be neglected ,and we get,

$$\sigma_{k\ell}^{(n)} = \frac{(-1)}{(n\omega - \omega_{\ell k})} \sum_{p=n-1,n+1} \left[\Omega_{j\ell}\,\sigma_{kj}^{(p)} - \Omega_{kj}\,\sigma_{j\ell}^{(p)} \right] e^{i(n-p)\varphi_1}$$

$$-(IV.23)$$

Eqn (IV.23) gives the adiabetically approximated n^{th} fourier component of the off resonant density matrix element $\rho_{k\ell}$.

Under similar off-resonant approximation with the third and fifth harmonic field a straightforward generalisation of Eqn(IV.23) will give,

$$\sigma_{kl}(n)$$

$$= -\alpha_{lk}(n) \sum_{p_1 = n-1, n+1}' \left[\sigma_{kj}(p_1)\,\Omega_{jl} - \Omega_{kj}\,\sigma_{jl}(p_1) \right] e^{i\frac{(n-p_1)}{|n-p_1|}\varphi_1}$$

$$- \alpha_{lk}(n) \sum_{p_3 = n-3, n+3} \left[\sigma_{kj}(p_3)\,\beta_{jl} - \beta_{kj}\,\sigma_{jl}(p_3) \right] e^{i\frac{(n-p_3)}{|n-p_3|}\varphi_3}$$

$$- \alpha_{lk}(n) \sum_{p_5 = n-5, n+5} \left[\sigma_{kj}(p_5)\,\delta_{jl} - \delta_{kj}\,\sigma_{jl}(p_5) \right] e^{i\frac{(n-p_5)}{|n-p_5|}\varphi_5}$$

$$-(IV.24)$$

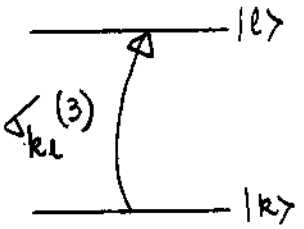
|ℓ⟩
$\sigma_{k\ell}^{(3)}$
|k⟩

(a)

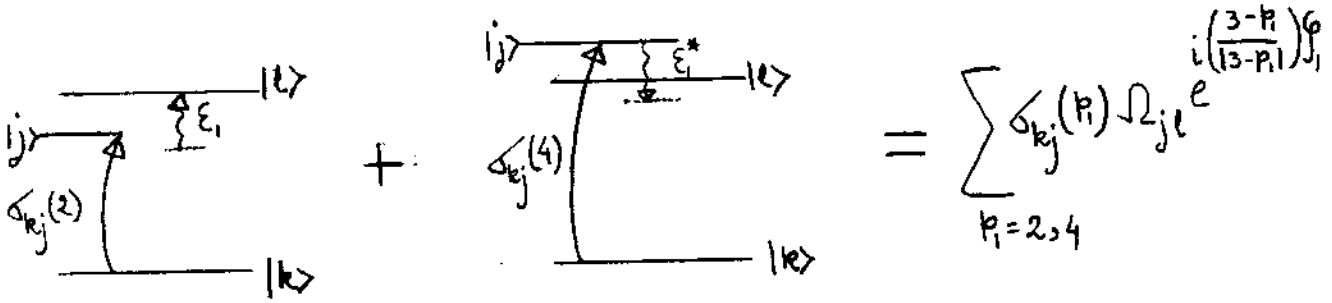
|ℓ⟩
|j⟩
$\mathcal{E}_1$
$\sigma_{kj}^{(2)}$
|k⟩
+
|j⟩
$\mathcal{E}_1^*$
|ℓ⟩
$\sigma_{kj}^{(4)}$
|k⟩
=
$\sum_{p_1=2,4} \sigma_{kj}(p_1)\,\Omega_{j\ell}\, e^{i\left(\frac{3-p_1}{|3-p_1|}\right)\varphi_1}$

(b)

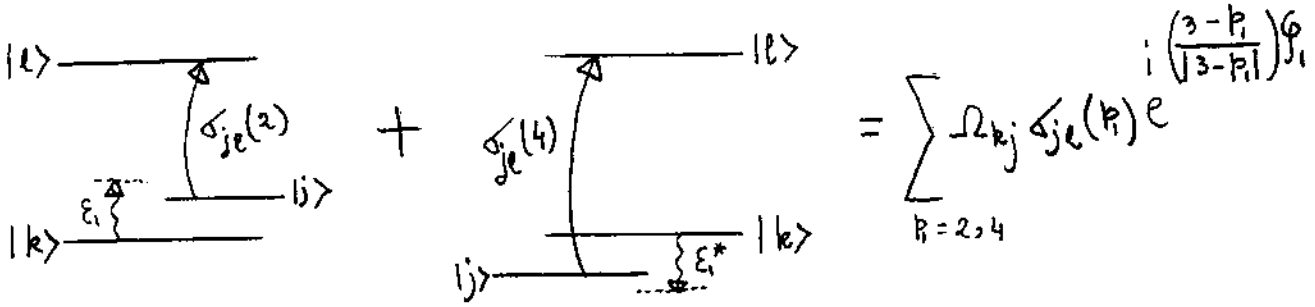
|ℓ⟩
$\sigma_{j\ell}^{(2)}$
|j⟩
$\mathcal{E}_1$
|k⟩
+
|ℓ⟩
$\sigma_{j\ell}^{(4)}$
|k⟩
|j⟩
$\mathcal{E}_1^*$
=
$\sum_{p_1=2,4} \Omega_{kj}\,\sigma_{j\ell}(p_1)\, e^{i\left(\frac{3-p_1}{|3-p_1|}\right)\varphi_1}$

(c)

Fig IV·3

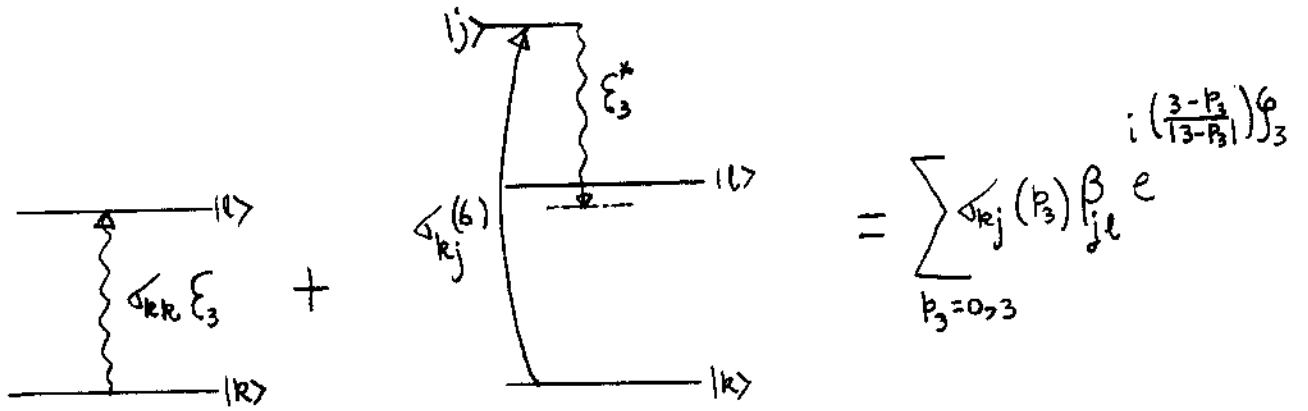

(d)

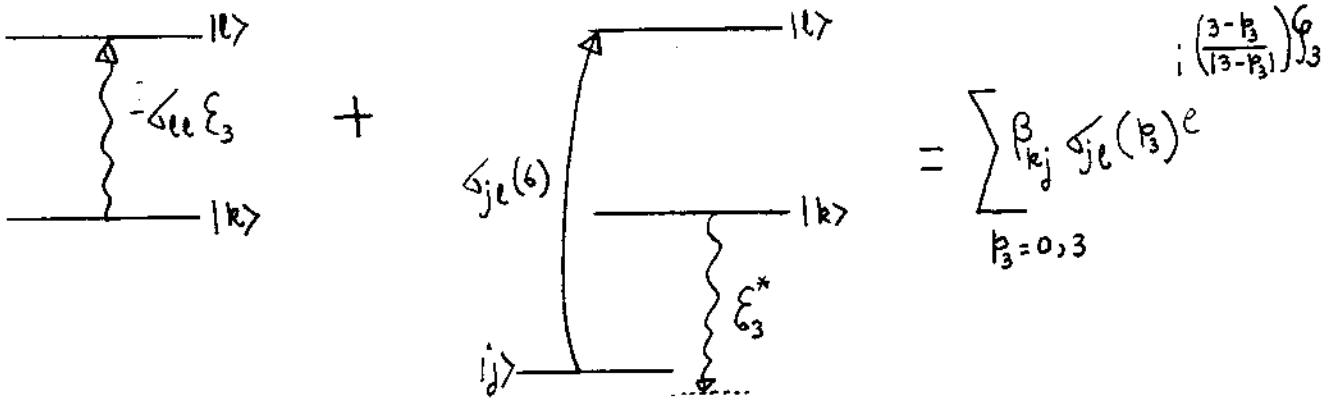

(e)

Fig IV·3 (CONTD.)

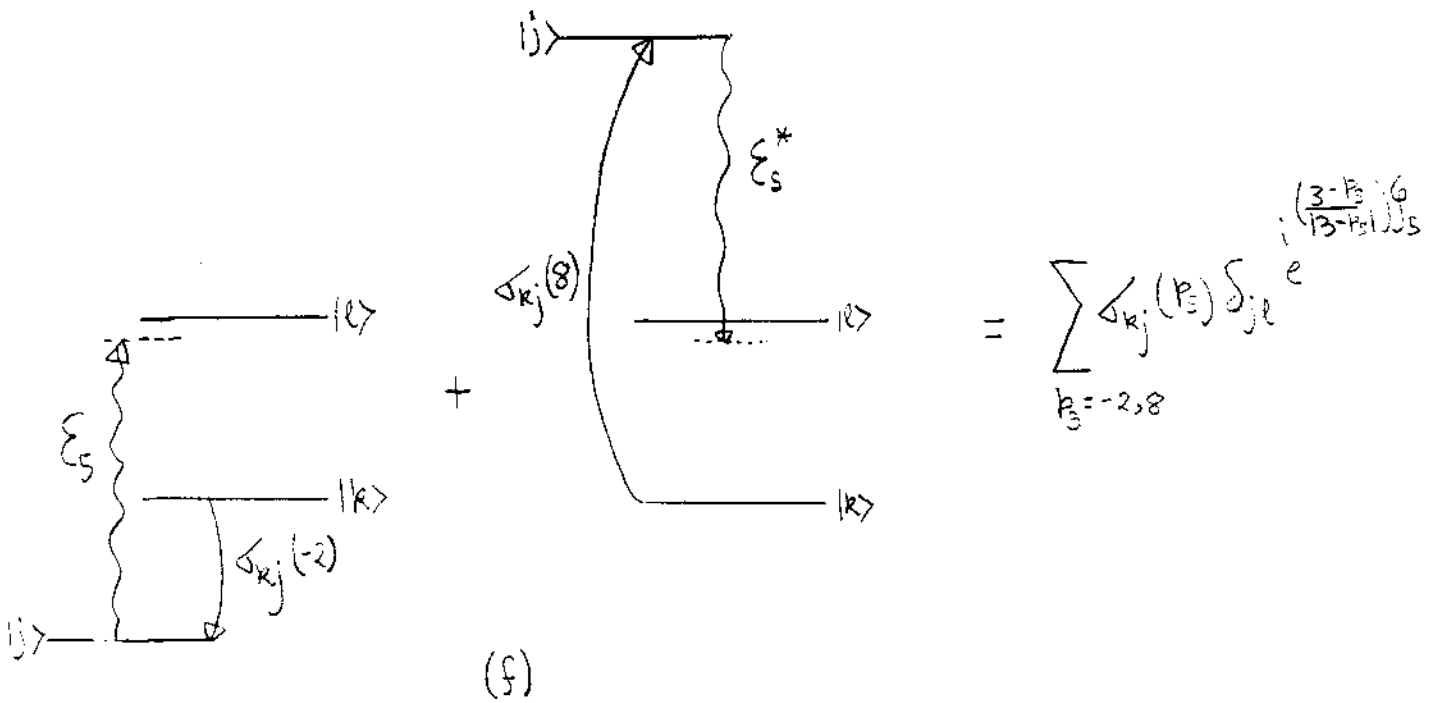

(f)

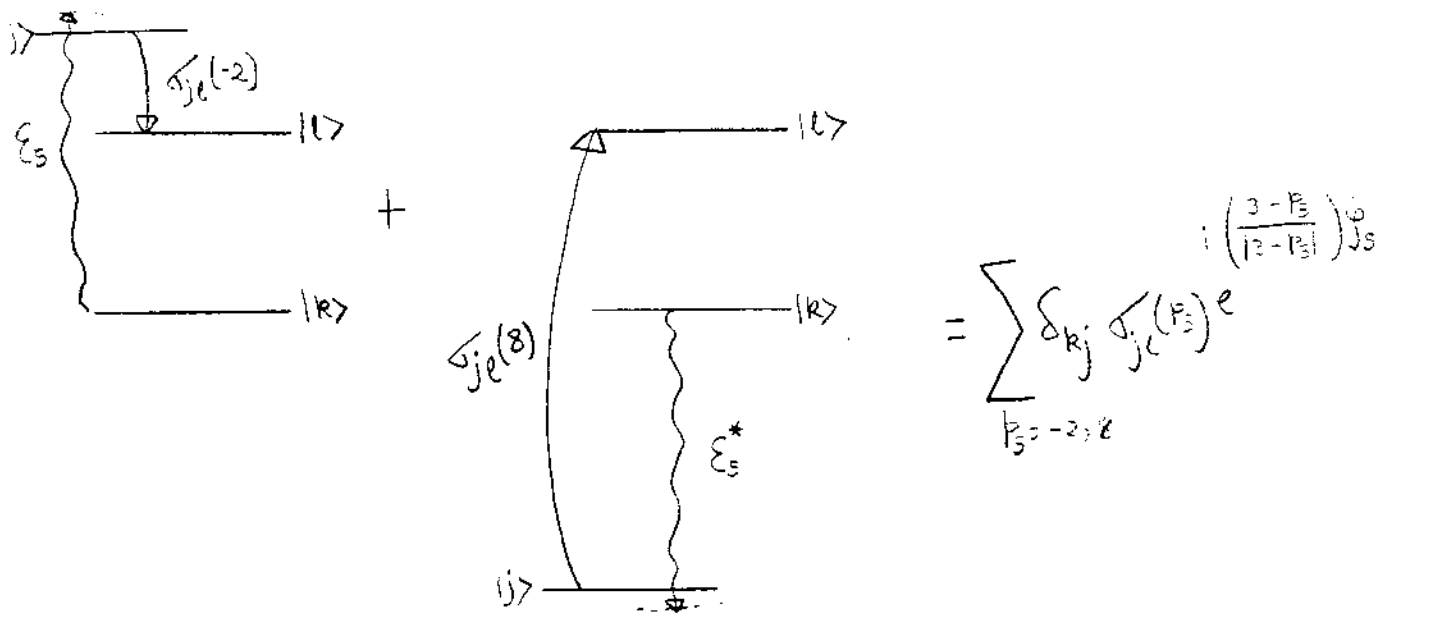

(g)

Fig IV·3 (CONTD.)

where,

$$\Omega_{jl} = \frac{\mu_{jl}|E_1|}{\hbar}$$

$$\beta_{jl} = \frac{\mu_{jl}|E_3|}{\hbar}$$

$$\delta_{jl} = \frac{\mu_{jl}|E_5|}{\hbar}$$

-(IV.25)

$$\alpha_{lk}^{(n)} = \frac{1}{(n\omega - \omega_{lk})}$$

-(IV.26)

Fig(IV.3) shows the various terms of Eqn(IV.24) for n=3 . Fig(IV.3a) shows the density matrix element $\sigma_{kl}^{(3)}$ for the transition between levels l and k . Fig (IV.3b) to Fig(IV.3g) show the generation of $\sigma_{kl}^{(3)}$ through second order scaterring proecesses assisted by the 1st ,third and fifth harmonic

fields. Each of the generated terms can be further expanded in the same ways either through similar diagrams or analytically using Eqn(IV.24). A demonstration of analytical expansion is given in appendix A. It will be shown in later sections that in order to generate equations containing fourth power of E_1 in a FPR system an expansion up to third power of the electric field will be needed for all off-resonant matrix elements. This expansion is equivalent to a perturbation expansion of the off-resonant density matrix elements. In the derivation of the atomic Eqns and polarisations shown in later sections both the analytical and diagramatical methods were used.

Derivation of Four-photon resonant Bloch-Eqn using Adiabatic Approximation

Under four-photon resonance between levels I1> and I2>,

$$\omega_{21} \simeq 4\omega$$

the resonant density matrix can be written as:

$$\rho_{12} = \sigma_{12}(t)\, e^{i4\omega t} \qquad -(IV.27)$$

Using Eqn(IV.13) in Eqn(IV.9) we get:

$$\frac{\partial \sigma_{12}}{\partial t} + i(4\omega - \omega_{21})\sigma_{12}$$

$$= (-i) \sum_{P_1 = 3,5} \left[\Omega_{\ell 2}\, \sigma_{1\ell}(P_1) - \Omega_{1\ell}\, \sigma_{\ell 2}(P_1) \right] e^{i \frac{(4-P_1)\varphi_1}{|4-P_1|}}$$

$$+ (-i) \sum'_{P_3 = 1,7} \left[\beta_{\ell 2}\, \sigma_{1\ell}(P_3) - \beta_{1\ell}\, \sigma_{\ell 2}(P_3) \right] e^{i \frac{(4-P_3)\varphi_3}{|4-P_3|}}$$

$$+ (-i) \sum'_{P_5 = -1,9} \left[\delta_{\ell 2}\, \sigma_{1\ell}(P_5) - \delta_{1\ell}\, \sigma_{\ell 2}(P_5) \right] e^{i \frac{(4-P_5)\varphi_5}{|4-P_5|}} \qquad -(IV.28)$$

where $\Omega_{\ell 2}$, $\beta_{\ell 2}$, $\delta_{\ell 2}$ are defined in Eqn(IV.25).

$\sigma_{1\ell}$ and $\sigma_{\ell 2}$ in Eqn(IV.28) can be eliminated by using adiabatic approxition Eqn(IV.24). Expansion of $\sigma_{1\ell}$ and $\sigma_{\ell 2}$ up to third power of the field will generate an equation of σ_{12} containing fourth power in the field. At the final step of the expansion all off-resonant scattering has been expressed through the FPR interaction. The final form of Equation of motion of σ_{12} :

$$\frac{\partial \sigma_{12}}{\partial t} + i(4\omega - \omega_{21} - \delta\omega)\sigma_{12} + \left(\frac{\gamma_1 + \gamma_2}{2}\right)\sigma_{12}$$

$$= i(\sigma_{22} - \sigma_{11})\left[\frac{r_{12}\mathcal{E}_1^4}{\hbar^4} + \left\{\xi_{21} + \frac{a_3|\mathcal{E}_1|^2}{\hbar^2}\right\}\frac{\mathcal{E}_1\mathcal{E}_3}{\hbar^2}\right.$$

$$\left. + \left\{\xi_{21}^* + \frac{c_5^*|\mathcal{E}_1|^2}{\hbar^2}\right\}\frac{\mathcal{E}_1^*\mathcal{E}_5}{\hbar^2} + \frac{d_5^*\mathcal{E}_1^2\mathcal{E}_5\mathcal{E}_3^*}{\hbar^4}\right]$$

-(IV.29)

Definition of various terms in equation of motion

ω_{21} =zero-field resonance frequency of $|1\rangle \leftrightarrow |2\rangle$ transition.

$\delta\omega$ = laser induced Stark shift of $|1\rangle \leftrightarrow |2\rangle$ transition.

The Stark shift is determined by the the real part of polarizability of the resonant levels and intensity of the incident and generated fields.

$$\delta\omega = \frac{1}{\hbar}\left[\alpha_1'(\omega) - \alpha_2'(\omega)\right]|\mathcal{E}_1|^2$$

$$+ \frac{1}{\hbar}\left[\alpha_1'(3\omega) - \alpha_2'(3\omega)\right]|\mathcal{E}_3|^2$$

$$+ \frac{1}{\hbar}\left[\alpha_1'(5\omega) - \alpha_2'(5\omega)\right]|\mathcal{E}_5|^2$$

-(IV.30)

where, $\alpha_j'(n\omega) \equiv$ Polarisability of j^{th} level at frequency $n\omega$ is,

$$\alpha_j(n\omega) = \alpha_j'(n\omega) - i\alpha_j''(n\omega) \qquad -(IV.31)$$

$$\alpha_j(\omega) = \alpha_j^{(0)}(\omega) + \alpha_j^{(1)}(\omega) \qquad -(IV.32)$$

$$j=1,2$$

$$\alpha_j^{(0)}(\omega) = \frac{1}{\hbar}\sum_{\ell}\left[\frac{|\mu_{\ell j}|^2}{(\omega_{\ell j}-\omega)} + \frac{|\mu_{\ell j}|^2}{(\omega_{\ell j}+\omega)}\right] \qquad -(IV.33)$$

$$j=1,2$$

$$\alpha_j^{(1)}(\omega) = \frac{1}{\hbar}\left[\frac{\mu_{jf}\mu_{fk}\mu_{k\ell}\mu_{\ell j}}{(\omega_{\ell j}-\omega)(\omega_{kj}-2\omega)(\omega_{fj}-\omega)} + \frac{\mu_{jf}\mu_{fk}\mu_{k\ell}\mu_{\ell j}}{(\omega_{\ell j}+\omega)(\omega_{kj}+2\omega)(\omega_{fj}+\omega)}\right]\frac{|\mathcal{E}_1|^2}{\hbar^2} \qquad -(IV.34)$$

$$j=1,2$$

$\alpha_j^{(1)}(\omega) \equiv$ Intensity dependent polarisability of level I1> and I2> at the first harmonic frequency ω. From equations (IV.30),(IV.32),(IV.33),(IV.34) it follows that $\alpha_j^{(0)}(\omega)$

gives the intensity dependent quadratic Stark shift where as $\alpha_j^{(1)}(\omega)$ gives the intensity square dependent quartic Stark shift.

$$\alpha_j(n\omega) = \frac{1}{\hbar}\sum_{\ell}\left[\frac{|\mu_{\ell j}|^2}{(\omega_{\ell j}-n\omega)} + \frac{|\mu_{\ell j}|^2}{(\omega_{\ell j}+n\omega)}\right] \qquad -(IV.35)$$

$n=3,5 \qquad j=1,2$

We have neglected the intensity dependent polarisability for the third and fifth harmonic field, because, to a good approximation the peak field intensity of the higher harmonic fields are much smaller. The intensity dependent Stark shift changes as the intensity of the interacting field changes across the pulse. As a result, the detuning of the four photon interaction changes dynamically across the pulse.

$4\omega - \omega_{21} - \delta\omega_{21}$ = The net time dependent detuning.

$4\omega - \omega_{21}$ ≡ The zero field detuning.

For a given zero field detuning, an atom will come in and out of resonance as the pulse passes by. As we have seen in the two-photon resonance case, Stark shift could be as big as several pulse bandwidth. In this way laser induced Stark shift broadens the width of multiphoton resonance.

$\gamma_1 = \gamma_1^{5\omega}$ = Single photon ionisation rate from the ground state by the fifth harmonic field.

$$\gamma_1^{5\omega} = \frac{2\alpha_1''(5\omega)}{\hbar} |\mathcal{E}_5|^2 \qquad -(IV.36)$$

γ_2 = Total ionisation rate from level I2>

$$\gamma_2 = \gamma_2^{\omega} + \gamma_2^{2\omega} + \gamma_2^{3\omega} + \gamma_2^{5\omega} \qquad -(IV.37)$$

γ_2^{ω} = Single photon ionisation rate from level I2>, by the first harmonic field.

$$\gamma_2^{\omega} = \frac{2}{\hbar} \alpha_2^{(0)''}(\omega) |\mathcal{E}_1|^2 \qquad -(IV.38)$$

$\gamma_2^{2\omega}$ = Two photon ionisation rate from level I2> by the first harmonic field.

$$\gamma_2^{2\omega} = \frac{2}{\hbar} \alpha_2^{(1)''}(\omega) |\mathcal{E}_1|^2 \qquad -(IV.39)$$

$\gamma_2^{3\omega}$ = Single photon ionization rate from level I2> by third harmonic field.

$$\gamma_2^{3\omega} = \frac{2}{\hbar} \alpha_2''(3\omega) |\mathcal{E}_3|^2 \qquad -(IV.40)$$

$\gamma_2^{5\omega}$ = Single photon ionization rate from level I2> by the fifth harmonic field.

$$\gamma_2^{5\omega} = \frac{2}{\hbar} \alpha_2''(5\omega) |\mathcal{E}_5|^2 \qquad -(IV.41)$$

Ionization is an incoherent loss mechanism, leading to a shrinkage of the "pseudo polarisation vector" through a reduction of σ_{12}.

The four photon transition matrix element γ_{12} is given by

$$\gamma_{12} = \frac{\mu_{1f}\,\mu_{fk}\,\mu_{ke}\,\mu_{e2}}{(\omega_{e1}-3\omega)(\omega_{k1}-2\omega)(\omega_{f1}-\omega)} \qquad -(IV.42)$$

where Einstein's summation convention is implied.

$\gamma_{i2}\left(\frac{\mathcal{E}_1}{\hbar}\right)^4$ is the Rabi rate for FPR transition.

$$\xi_{21} = \frac{\mu_{2\ell}\,\mu_{\ell 1}}{(\omega_{\ell 1} - 3\omega)} + \frac{\mu_{2\ell}\,\mu_{\ell 1}}{(\omega_{\ell 2} + 3\omega)} \qquad -(IV.43)$$

ξ_{21} is the coefficient of the resonant Raman pumping term in presence of the third harmonic field. Later on we will see that ξ_{21} is the coefficient of FPR third harmonic generation.

$$a_3 = -\mu_{2f}\,\mu_{fk}\,\mu_{k\ell}\,\mu_{\ell 1} \times$$

$$\left[\frac{1}{(3\omega - \omega_{\ell 1})(2\omega - \omega_{k1})(3\omega - \omega_{f1})} \right.$$

$$+ \frac{1}{(\omega - \omega_{f1})(2\omega - \omega_{k1})(\omega - \omega_{\ell 1})}$$

$$\left. + \frac{1}{(5\omega - \omega_{f1})(2\omega - \omega_{k1})(\omega - \omega_{\ell 1})} \right]$$

$-(IV.44)$

a_3 is the coefficient of a higher order Raman scattering produced by the first and third harmonic fields.

$$\mathcal{S}_{21} = \frac{\mu_{2\ell}\,\mu_{\ell 1}}{(\omega_{\ell 1} - 5\omega)} + \frac{\mu_{2\ell}\,\mu_{\ell 1}}{(\omega_{\ell 2} + 5\omega)} \qquad -(IV.45)$$

$$C_5 = -\,\mu_{2f}\,\mu_{fk}\,\mu_{k\ell}\,\mu_{\ell 1} \times \left[\frac{1}{(\omega - \omega_{\ell 1})(5\omega - \omega_{f1})(6\omega - \omega_{k1})} + \frac{1}{(5\omega - \omega_{\ell 1})(6\omega - \omega_{k1})(5\omega - \omega_{f1})} \right] \qquad -(IV.46)$$

$\mathcal{S}_{21}$ = The coefficient of Raman scattering with the first and fifth harmonic field. Later on we will see that $\mathcal{S}_{21}$ is the coupling coefficient of the FPR fifth harmonic generation.

C_5 = The coefficient of a higher order scattering for first and fifth harmonic fields.

$$d_5 = -\mu_{2f}\mu_{fk}\mu_{kl}\mu_{l1} \times$$

$$\left[\frac{1}{(\omega-\omega_{l1})(7\omega-\omega_{f1})(6\omega-\omega_{k1})} + \frac{1}{(\omega-\omega_{l1})(7\omega-\omega_{f1})(2\omega-\omega_{k1})}\right.$$

$$+ \frac{1}{(5\omega-\omega_{l1})(7\omega-\omega_{f1})(6\omega-\omega_{k1})} + \frac{1}{(5\omega-\omega_{l1})(3\omega-\omega_{f1})(6\omega-\omega_{k1})}$$

$$\left. + \frac{1}{(\omega-\omega_{l1})(3\omega-\omega_{f1})(6\omega-\omega_{k1})}\right] \qquad -(IV.47)$$

d_5 = Coefficient of the multiwave scattering term.

Note that in the equation of σ_{12} we have kept the term up to fourth power in E_1, where as only up to first power of E_3 and E_5 are kept. This is a good approximation when E_3 and E_5 are the generated fields having intensities much weaker than the fundamental field E_1. The meaning of the various terms becomes clear when we draw pictures for each processes. Fig.(IV.4) shows the various terms. From Fig.(IV.4) we can see that drawing pictures for each scattering process and using the resonant denominators we can generate each of the terms of equation of σ_{12}. In a similar way equation of motion

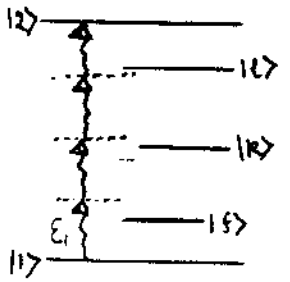

$$= \gamma_{12} \left(\frac{\mathcal{E}_1}{\hbar}\right)^4$$

(a)

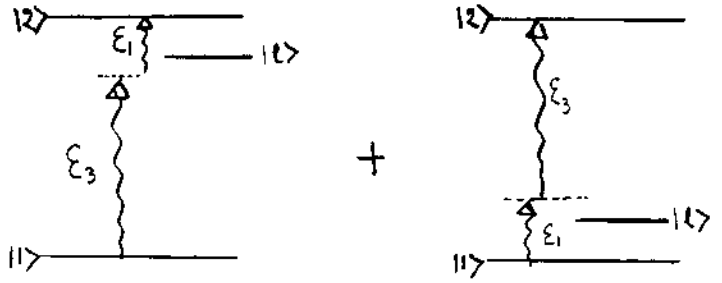

$$= \frac{\mathcal{E}_{2,1}}{\hbar^2} \mathcal{E}_1 \mathcal{E}_3$$

(b)

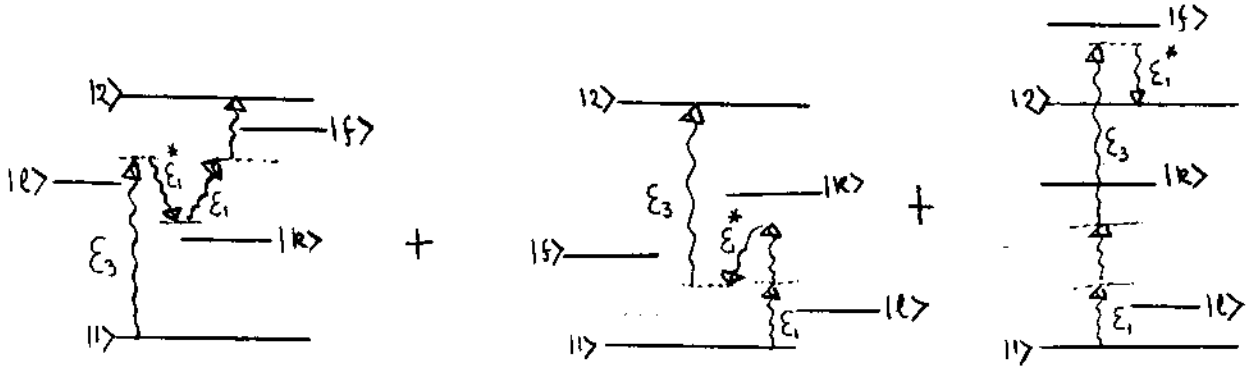

$$= \frac{a_3 |\mathcal{E}_1|^2}{\hbar^2} \left(\frac{\mathcal{E}_1 \mathcal{E}_3}{\hbar^2}\right)$$

(c)

Fig IV · 4

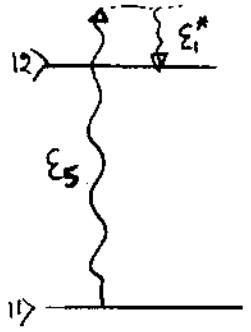

$$= \frac{\mathcal{S}_{21}^*}{\hbar^2}\,\mathcal{E}_5\,\mathcal{E}_1^*$$

(d)

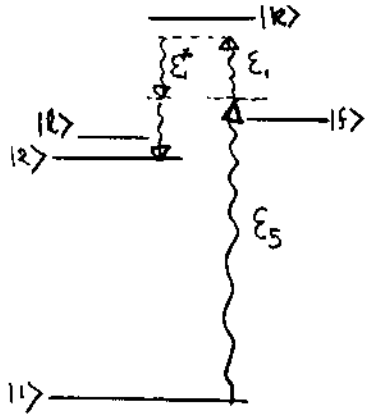

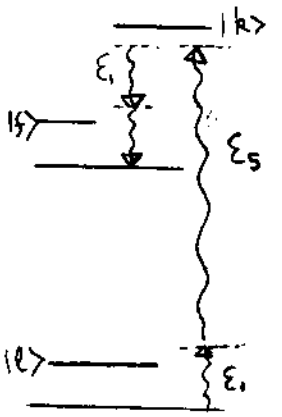

$$= \frac{C_5^*\,|\mathcal{E}_1|^2}{\hbar^2}\;\frac{\mathcal{E}_1^*\,\mathcal{E}_5}{\hbar^2}$$

(e)

Fig IV·4 (CONTD.)

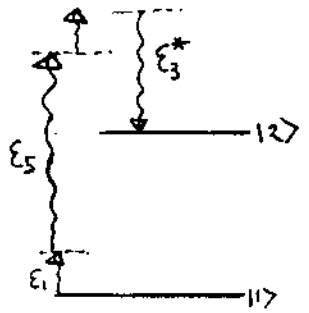

+

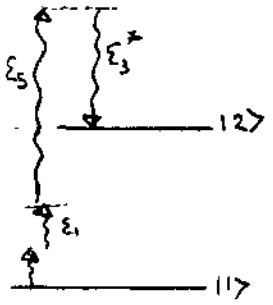

+

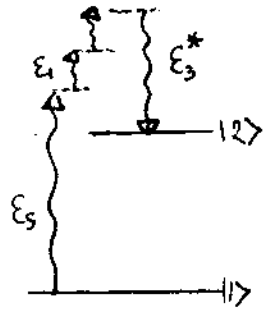

+

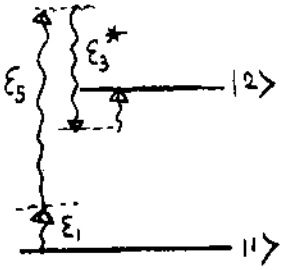

+

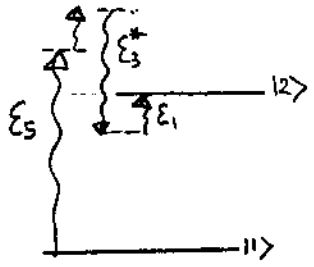

$$= \frac{d_5^* \mathcal{E}_1^2 \mathcal{E}_5 \mathcal{E}_3^*}{\hbar^4}$$

(f)

Fig IV.4 (CONTD.)

of ρ_{22} and ρ_{11} were found. With,

$$\sigma_{22} = \rho_{22} \qquad \text{and} \qquad \sigma_{11} = \rho_{11} \qquad -(IV.48)$$

where σ_{22} and σ_{11} are the probabilities of population of level I2> and I1> respectively. We have,

$$\frac{\partial \sigma_{22}}{\partial t} + \gamma_2 \sigma_{22} = -2\, Im \left[\left\{ r_{12} \left(\frac{\mathcal{E}_1^*}{\hbar}\right)^4 + \left(\xi_{21} + \frac{a_3 |\mathcal{E}_1|^2}{\hbar^2}\right) \frac{\mathcal{E}_1^* \mathcal{E}_3^*}{\hbar^2} + \left(\xi_{21} + \frac{c_5 |\mathcal{E}_1|^2}{\hbar^2}\right) \frac{\mathcal{E}_1 \mathcal{E}_5^*}{\hbar^2} + \frac{d_5}{\hbar^4} \mathcal{E}_1^{*2} \mathcal{E}_3 \mathcal{E}_5^* \right\} \sigma_{12} \right] \qquad -(IV.49)$$

$$\frac{\partial}{\partial t}(\sigma_{11} + \sigma_{22}) = -\gamma_2 \sigma_{22} - \gamma_1 \sigma_{11} \qquad -(IV.50)$$

equation (IV.50) is the conservation equation for population.

Four Photon Bloch Equation

By eliminating all the off resonant density matrix elements using the adiabatic following approximation we have already converted the many level atom into a two level atom represented by a 2 X 2 density matrix containing only the resonant terms.

The 2 X 2 density matrix is given by,

$$\rho = \begin{pmatrix} \sigma_{11} & \sigma_{12} e^{i4\omega t} \\ \sigma_{21} e^{-i4\omega t} & \sigma_{22} \end{pmatrix} \qquad - (IV.51)$$

$$\rho = \rho^{\dagger} \quad \text{implies} \quad \rho_{12} = \rho_{21}^{*}$$

$$\text{or} \quad \sigma_{12} = \sigma_{21}^{*} \qquad - (IV.52)$$

Introducing the relaxation terms T_1 , T_2 phenomenologically, in the equation for σ_{12}, σ_{22}, σ_{11} , we get ,

$$\frac{\partial \sigma_{12}}{\partial t} + i(4\omega - \omega_{21} - \delta\omega)\sigma_{12} + \left(\frac{\gamma_1 + \gamma_2}{2} + \frac{1}{T_2}\right)\sigma_{12}$$

$$= i(\sigma_{22} - \sigma_{11}) \left[\gamma_{12} \left(\frac{\mathcal{E}_1}{\hbar}\right)^4 + \left\{ \xi_{21} + \frac{a_3 |\mathcal{E}_1|^2}{\hbar^2} \right\} \frac{\mathcal{E}_1 \mathcal{E}_3}{\hbar^2} \right.$$

$$\left. + \left\{ \xi_{21}^{*} + \frac{c_5^{*} |\mathcal{E}_1|^2}{\hbar^2} \right\} \frac{\mathcal{E}_1^{*} \mathcal{E}_5}{\hbar^2} + \frac{d_5^{*}}{\hbar^4} \mathcal{E}_1^2 \mathcal{E}_5 \mathcal{E}_3^{*} \right]$$

$$- (IV.53)$$

$$\frac{\partial \sigma_{22}}{\partial t} + \gamma_2 \sigma_{22} + \frac{\sigma_{22}}{T_1}$$

$$= -2\, \mathrm{Im} \left[\left\{ r_{12} \left(\frac{\mathcal{E}_1^*}{\hbar} \right)^4 + \left(\xi_{21} + \frac{a_3 |\mathcal{E}_1|^2}{\hbar^2} \right) \frac{\mathcal{E}_1^* \mathcal{E}_3^*}{\hbar^2} \right.\right.$$

$$\left.\left. + \left(\xi_{21} + \frac{c_5 |\mathcal{E}_1|^2}{\hbar^2} \right) \frac{\mathcal{E}_1 \mathcal{E}_5^*}{\hbar^2} + \frac{d_5}{\hbar^4} \mathcal{E}_1^{*2} \mathcal{E}_3 \mathcal{E}_5^* \right\} \sigma_{12} \right]$$

— (IV.54)

$$\frac{\partial (\sigma_{11} + \sigma_{22})}{\partial t} = -\gamma_2 \sigma_{22} - \gamma_1 \sigma_{11} \qquad \text{— (IV.55)}$$

The system of equations (IV.53) to (IV.55) are the four photon Bloch Equations (in analogy with the Bloch Equations in magnetic spin resonance). The two states of the equivalent two level system are connected resonantly by four photons of the incident pulse. The effect of all other levels come through the generation of higher harmonics, through various scattering processes, ionisation and level shifts. Solution of the above four photon Bloch equations will give the density matrix ρ as a function of the electric fields.

Calculation of Polarisation in the Four Photon Resonant Medium

The calculation of the induced polarisations at various harmonics, up to third power in the applied (fundamental) electric field will be given below.

The dipole moment induced in the atom is given by,

$$\vec{P} = Tr(\rho\vec{\mu}) \qquad -(IV.56)$$

or,

$$\vec{P} = \sum_{lk} \rho_{lk}\,\vec{\mu}_{kl} \qquad -(IV.57)$$

using $$\rho_{lk} = \sum_{n} \sigma_{lk}(n)\, e^{inwt}$$

$$\vec{P} = \sum_{l,k,n=-\infty}^{n=+\infty} \sigma_{lk}(n)\,\vec{\mu}_{kl}\, e^{inwt} \qquad -(IV.58)$$

or,

$$\vec{P} = \sum_{l,k,n=-\infty}^{n=1}{}' \sigma_{lk}(n)\,\vec{\mu}_{kl}\, e^{inwt} + \sum_{l,k,n=1}^{n=+\infty} \sigma_{lk}(n)\,\vec{\mu}_{lk}\, e^{inwt}$$

or,

$$\vec{P} = \sum_{\ell,k,n=1}^{n=\infty} \sigma_{\ell k}(-n)\,\vec{\mu}_{k\ell}\, e^{-in\omega t} + \sum_{\ell,k,n=1}^{n=+\infty} \sigma_{\ell k}(n)\,\vec{\mu}_{k\ell}\, e^{in\omega t} \qquad -(IV.59)$$

using,

$$\rho^{+} = \rho \qquad \text{and} \qquad \mu^{+} = \mu$$

we have,

$$\sigma^{*}_{\ell k}(-n) = \sigma_{k\ell}(n) \qquad -(IV.60)$$

and

$$\mu^{*}_{\ell k} = \mu_{k\ell} \qquad -(IV.61)$$

$$\vec{P} = \sum_{\ell,k,n=1}^{\infty} \left[\sigma^{*}_{\ell k}(n)\,\vec{\mu}^{*}_{k\ell}\, e^{-in\omega t} + \sigma_{\ell k}(n)\,\vec{\mu}_{k\ell}\, e^{in\omega t} \right]$$

The dummy summation index ℓ and k are interchanged in the first term.

$$\vec{P} = \sum_{\ell,k,n=1}^{\infty} \left[\sigma_{\ell k}(n)\, \vec{\mu}_{k\ell}\, e^{inwt} + c.c. \right] \qquad -(IV.62)$$

we can also write,

$$\vec{P} = \sum_{n} \left[\vec{\rho}_n\, e^{inwt} + c.c \right] \qquad -(IV.63)$$

from equations (IV.62) and (IV.63) we can write,

$$\vec{\rho}_n = \sum_{\ell,k} \sigma_{\ell k}(n)\, \vec{\mu}_{k\ell} \qquad -(IV.64)$$

using $\mu_{12} = \mu_{21} = 0$ we arrive at the following expression

$$\rho_n = \sum_{\ell \neq 1,2} \left[\sigma_{1\ell}(n)\mu_{\ell 1} + \sigma_{2\ell}(n)\mu_{\ell 2} + \sigma_{\ell 1}(n)\mu_{1\ell} + \sigma_{\ell 2}(n)\mu_{2\ell} \right] + \sum_{\substack{\ell \neq 1,2 \\ k \neq 1,2}} \sigma_{\ell k}(n)\mu_{k\ell} \qquad -(IV.65)$$

with n=1,3,5 we get the amplitude of the first, third and fifth harmonic dipole moment amplitude. $\sigma_{1\ell}(n)$ etc. are to be expanded by adiabatic approximation up to the third power of the fundamental field $\mathcal{E}_1$. Using repeated adiabatic approximation (equation (IV.24)), we get expressions for $\mathcal{P}_1$, $\mathcal{P}_3$, $\mathcal{P}_5$. The procedure is the same as that used to derive the equations of motion for σ_{12} and σ_{22}.

The polarisation $\mathcal{P}_1$ is,

$$\mathcal{P}_1 = \left\{\left(\alpha_1^{(0)}(\omega) + 2\alpha_1^{(1)}(\omega)\right)\sigma_{11} + \left(\alpha_2^{(0)}(\omega) + 2\alpha_2^{(1)}(\omega)\right)\sigma_{22}\right\}\mathcal{E}_1$$

$$+ 4\gamma_{12}\left(\frac{\mathcal{E}_1^*}{\hbar}\right)^3\sigma_{12} + \left(\xi_{21} + \frac{a_3}{\hbar^2}|\mathcal{E}_1|^2\right)\frac{\sigma_{12}\mathcal{E}_3^*}{\hbar}$$

$$+\left(\xi_{21}^* + \frac{c_5^*|\mathcal{E}_1|^2}{\hbar^2}\right)\frac{\mathcal{E}_5\sigma_{21}}{\hbar} + \frac{3\alpha_3}{\hbar^3}\mathcal{E}_3\mathcal{E}_1^{*2}\sigma_{11} + 2\frac{d_5}{\hbar^3}\mathcal{E}_1^*\mathcal{E}_3\mathcal{E}_5^*\sigma_{12} \qquad \text{(IV.66)}$$

The intensity dependent polarisabilities $\alpha_1^{(1)}(\omega)$ and $\alpha_2^{(1)}(\omega)$ will give rise to a strong phase modulation in the pulse.

$4\gamma_{12}\left(\frac{\mathcal{E}_1^*}{\hbar}\right)^3\sigma_{12}$ is the first harmonic dipole moment created by the FPR transition. The four terms are generated

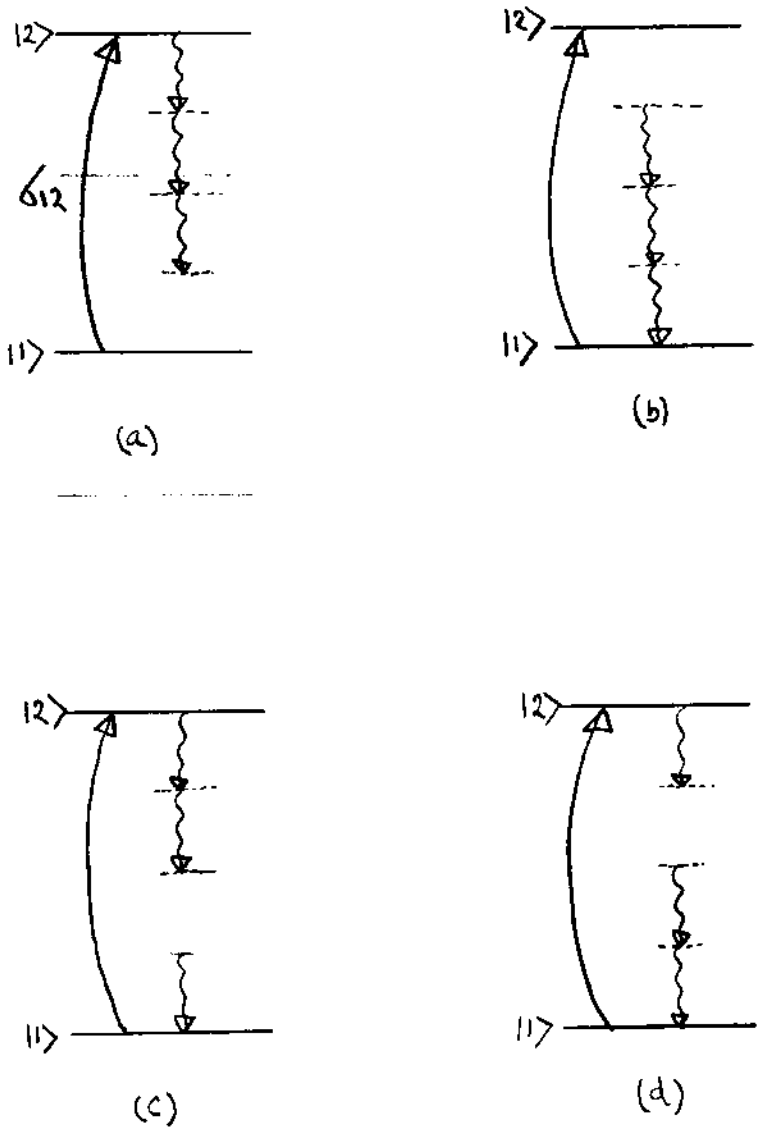

Fig IV · 5

by proper permutations of the emission process as illustratraed in Fig(IV.5).

$\left(\xi_{21} + \frac{a_3 |\mathcal{E}_1|^2}{\hbar^2}\right) \frac{\sigma_{12}}{\hbar} \mathcal{E}_3^*$ are terms showing flow of energy from the fundamental to the third harmonic frequency.

$\left(\xi_{21}^* + \frac{c_5^* |\mathcal{E}_1|^2}{\hbar^2}\right) \frac{\mathcal{E}_5 \sigma_{12}}{\hbar}$ are terms showing flow of energy from the fundamental to the fifth harmonic frequency.

$$\alpha_3 = \frac{\mu_{1f}\mu_{fk}\mu_{ke}\mu_{e1}}{(\omega_{f1} - \omega)(\omega_{k1} - 2\omega)(\omega_{e1} - 3\omega)} \qquad -(IV \cdot 67)$$

α_3 gives the off resonant third harmonic susceptibility .

$2\frac{d_5}{\hbar^3} \mathcal{E}_1^* \mathcal{E}_3 \mathcal{E}_5 \sigma_{12}$ is a term representing the FPR wave-mixing process.

Similarly we write the amplitude of the third harmonic polarisation,

$$P_3 = \left[\alpha_1(3\omega)\sigma_{11} + \alpha_2(3\omega)\sigma_{22}\right]\mathcal{E}_3$$

$$+ \left[\mathcal{E}_{321} + \frac{a_3|\mathcal{E}_1|^2}{\hbar^2}\right]\frac{\mathcal{E}_1^*\sigma_{12}}{\hbar} + \frac{\alpha_3\mathcal{E}_1^3}{\hbar^3}\sigma_{11}$$

$$+ \frac{d_5^*\mathcal{E}_1^2\mathcal{E}_5}{\hbar^3}\sigma_{21} \qquad \text{-(IV.68)}$$

The third harmonic generation takes places through the FPR harmonic generation, stimulated Raman process, wave mixing and the off-resonant processes.

$\frac{\mathcal{E}_{321}}{\hbar}\mathcal{E}_1^*\sigma_{12}$ is the dominant FPR third harmonic generation term

$\frac{\alpha_3}{\hbar^3}\mathcal{E}_1^3\sigma_{11}$ is the off resonant third harmonic generation term. These two competing processes are illustrated in Fig(IV.6).

We will see later how the off resonant and on resonant terms compete with each other and add to P_3 with different phases. One important difference between the two terms lie in different absorption losses. The off resonant generation process does not have any multiphoton absorption loss.

Fig(IV.7) describes the higher order resonant mixing term given by $\left(\frac{a_3|\mathcal{E}_1|^2}{\hbar^2}\right)\frac{\mathcal{E}_1^*\sigma_{12}}{\hbar}$.

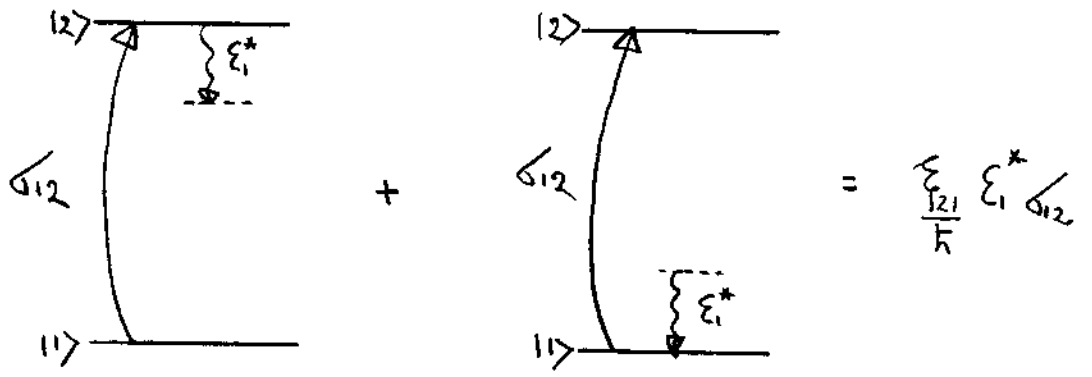
|2⟩
$\mathcal{E}_1^*$
σ_{12}
|1⟩
+
|2⟩
σ_{12}
$\mathcal{E}_1^*$
|1⟩
$= \frac{\alpha_{21}}{\hbar} \mathcal{E}_1^* \sigma_{12}$

(a)

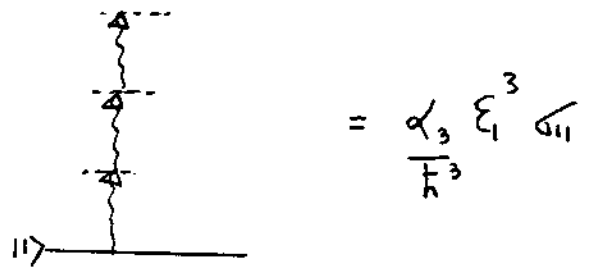
|1⟩
$= \frac{\alpha_3}{\hbar^3} \mathcal{E}_1^3 \sigma_{11}$

(b)

Fig IV · 6

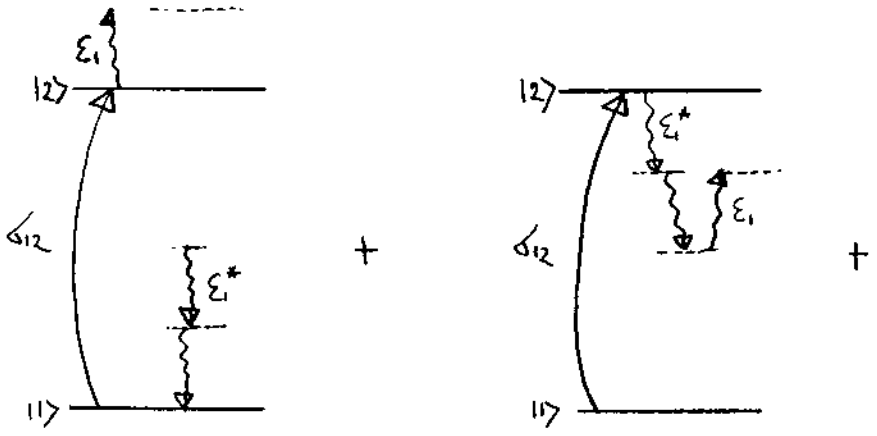

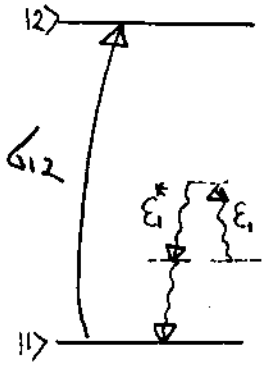

$$= \frac{a_3 |\varepsilon_1|^2}{\hbar^2} \frac{\varepsilon_1^* \sigma_{12}}{\hbar}$$

Fig IV · 7

The last term in $\mathcal{P}_3$ describes the resonant mixing process with fifth harmonic field.

Similarly the amplitude of the fifth harmonic polarisation is given by,

$$\mathcal{P}_5 = \left[\alpha_1(5\omega)\,\sigma_{11} + \alpha_2(5\omega)\,\sigma_{22}\right]\mathcal{E}_5$$

$$+ \left[S_{21} + \frac{c_5 |\mathcal{E}_1|^2}{\hbar^2}\right]\frac{\sigma_{12}\,\mathcal{E}_1}{\hbar} + \frac{d_5}{\hbar^3}\mathcal{E}_1^{*2}\mathcal{E}_3\,\sigma_{12} \,. \qquad -(IV.69)$$

Finally the polarisation at the first, third and fifth harmonic fields are given by,

$$\vec{P}_1 = N\vec{\mathcal{P}}_1(z,t)\, e^{i\omega t - ikz} + c.c$$

$$\vec{P}_3 = N\vec{\mathcal{P}}_3(z,t)\, e^{i3(\omega t - kz)} + c.c$$

$$\vec{P}_5 = N\vec{\mathcal{P}}_5(z,t)\, e^{i5(\omega t - kz)} + c.c. \qquad -(IV.70)$$

where P_1 , P_3 , P_5 are given in equations (IV.63),(IV.65) and (IV.66).

Maxwell-Bloch Equation for Four Photon Resonant System

From equation (II.15) in Chapter II we have Maxwell's equation in SVEA and written in reduced time frame,

$$\frac{\partial \mathcal{E}_m}{\partial z} = -i \frac{\omega_m N P_m}{2c\epsilon_0} \qquad -(IV.71)$$

$m=1,3,5$

From the solution of four photon Bloch equations (described by equations (IV.53) to (IV.55)) with given incident fields, we get the density matrix at a certain point in space as a function of time. From the density matrix we calculate the induced polarisations using equations (IV.65) to (IV.69). These polarisations become the source term in the Maxwell's equation given by equation (IV.71). The solution of Maxwell's equation will give the fields at the next point in space. Simultaneous solution of Maxwell-Bloch equation will generate fields at all space time points.

The above formalism described in this chapter gives the complete picture of a FPR system under coherent excitation.

The multilevel FPR system is converted into an equivalent two level system. This gives an unique opportunity to understand the complicated multiphoton process by a simple two level system. The dynamic Stark shift and ionisation have appeared automatically in the formalism. Finaly the explicit expression of the polarisation will provide all important and interesting harmonic generation processes that could occur in such complicated system.

From the self consistent Maxwell-Bloch equation we can derive an energy conservation equation. As the light pulses at ω, 3ω and 5ω propagate through the medium, their energies are distributed in various processes. Due to multiphoton absorption and ionisation part of the electromagnetic energy will be left in the atom.

The electromagnetic energy density,

$$U = U(1) + U(3) + U(5) \qquad -(IV.72)$$

U(i) = energy density in the i^{th} harmonic field

$$U(i) = 2c\epsilon_0 \int_{-\infty}^{+\infty} |\mathcal{E}_i|^2 \, dt \qquad -(IV.73)$$

$$U = 2c\epsilon_0 \int_{-\infty}^{+\infty} (|\mathcal{E}_1|^2 + |\mathcal{E}_3|^2 + |\mathcal{E}_5|^2)\, dt \qquad -(IV.74)$$

$$\frac{dU}{dz} = 2c\epsilon_0 \int_{-\infty}^{+\infty} \left(\frac{\partial}{\partial z}|\mathcal{E}_1|^2 + \frac{\partial}{\partial z}|\mathcal{E}_3|^2 + \frac{\partial}{\partial z}|\mathcal{E}_5|^2\right) dt$$

$$-(IV.75)$$

From Maxwell's equation (IV.71),

$$\frac{\partial |\mathcal{E}_m|^2}{\partial z} = \frac{m\omega N}{c\epsilon_0} \; Im\left\{\mathcal{E}_m^* \mathcal{P}_m\right\}$$

$$-(IV.76)$$

$$m=1,3,5$$

From equations (IV.75) and (IV.76), using expressions (equations (IV.66) to (IV.70)) for the polarisations, and four photon Bloch equations (equations (IV.53) to (IV.55)) we get the following energy conservation equations.

$$\frac{dU}{dz} = -N\hbar\omega \left[9\sigma_{22}(\infty) + 4\int_{-\infty}^{+\infty} \frac{\sigma_{22}}{T_1}\, dt \right.$$

$$\left. + \int_{-\infty}^{+\infty} \left(5\gamma_1^{5\omega}\sigma_{11} + 5\gamma_2^{\omega}\sigma_{22} + 6\gamma_2^{2\omega}\sigma_{22} + 7\gamma_2^{3\omega}\sigma_{22} + 9\gamma_2^{5\omega}\sigma_{22}\right) dt \right]$$

$$-(IV.77)$$

Equation (IV.77) states that the energy lost by the field is partly stored by the atom due to resonant absorption, partly lost to an intermediate level due to relaxation, or has been used to ionise the atom.

$4\hbar\omega\,\sigma_{22}(\infty)$ = Energy left in the upper level of the FPR atom.

$4\hbar\omega \int_{-\infty}^{+\infty} \frac{\sigma_{22}}{T_1}\,dt$ = Energy lost due to relaxation to an intermediate level.

$$\hbar\omega \int_{-\infty}^{+\infty} \left(5\,\gamma_1^{5\omega}\,\sigma_{11} + 5\,\gamma_2^{\omega}\,\sigma_{22} + 6\,\gamma_2^{2\omega}\,\sigma_{22} + 7\,\gamma_2^{3\omega}\,\sigma_{22} + 9\,\gamma_2^{5\omega}\,\sigma_{22}\right) dt$$

= The energy used to ionise the atom. The coefficients 5,6,7,9 reflect the number of photons needed to reach the final state in the ionisation continuum. In a coherent excitation the major loss will be due to FPR absorption and ionisation.

Four Photon Vector Model

To demonstrate the four photon analogue of single photon vector model first developed by Feynmann et al.[6] we make the following simplifying assumptions:

1. No ionisation
2. No harmonic generation
3. No Stark shift
4. Square pulse excitation

Under the above four assumptions the four photon Bloch equations become:

$$\frac{\partial \sigma_{12}}{\partial t} = i(\sigma_{22} - \sigma_{11}) \frac{\gamma_{12} \mathcal{E}_1^4}{\hbar^4} \qquad -(IV\cdot 78)$$

$$\frac{\partial \sigma_{22}}{\partial t} = -2\, \mathrm{Im}\left\{ \gamma_{12} \frac{\mathcal{E}_1^*}{\hbar^4} \sigma_{12} \right\} \qquad -(IV\cdot 79)$$

$$\frac{\partial}{\partial t}(\sigma_{22} + \sigma_{11}) = 0 \qquad -(IV\cdot 80)$$

We have also assumed that the pulse duration is shorter than the T_1 and T_2 . Let us assume that the square pulse has a real amplitude $\mathcal{E}$. The four phaton Bloch equation becomes:

$$\frac{\partial}{\partial t}\left(\frac{\sigma_{12}}{i}\right) = \left(\sigma_{22} - \sigma_{11}\right)\frac{\gamma_{12}\mathcal{E}^4}{\hbar^4} \qquad -(IV.81)$$

$$\frac{\partial}{\partial t}\left(\sigma_{22} - \sigma_{11}\right) = -4\frac{\gamma_{12}\mathcal{E}^4}{\hbar^4}\,Im\left\{\sigma_{12}\right\} \qquad -(IV.82)$$

From equation (IV.81) with a real amplitude $\mathcal{E}$, σ_{12} is imaginary.

$$Im\left\{\sigma_{12}\right\} = \frac{\sigma_{12}}{i} \qquad -(IV.83)$$

we define,

$$\Omega = 2\frac{\gamma_{12}\mathcal{E}_1^4}{\hbar^4} \qquad -(IV.84)$$

$$\frac{\partial}{\partial t}\left(\frac{\sigma_{12}}{i}\right) = \left(\frac{\sigma_{22}-\sigma_{11}}{2}\right)\Omega \qquad \text{-(IV.85)}$$

$$\frac{\partial}{\partial t}\left(\frac{\sigma_{22}-\sigma_{11}}{2}\right) = -\Omega\left(\frac{\sigma_{12}}{i}\right) \qquad \text{-(IV.86)}$$

We define,

$$W = \frac{\sigma_{22}-\sigma_{11}}{2} \qquad \text{-(IV.87)}$$

$$Q = \frac{\sigma_{12}}{i} \qquad \text{-(IV.88)}$$

$$\vec{R} = W\hat{e}_1 + Q\hat{e}_2 \qquad \text{-(IV.89)}$$

$$\vec{\Omega} = \Omega\hat{e}_3 \qquad \text{-(IV.90)}$$

$\hat{e}_1$, $\hat{e}_2$, $\hat{e}_3$ span a three dimensional orthogonal pseudo space. With the above definition, equations (IV.85,IV.86) can be described by the equation of motion of a rotating vector $\vec{R}$ under the influence of a torque $\vec{\Omega}$.

$$\frac{d\vec{R}}{dt} = \vec{\Omega} \times \vec{R}$$

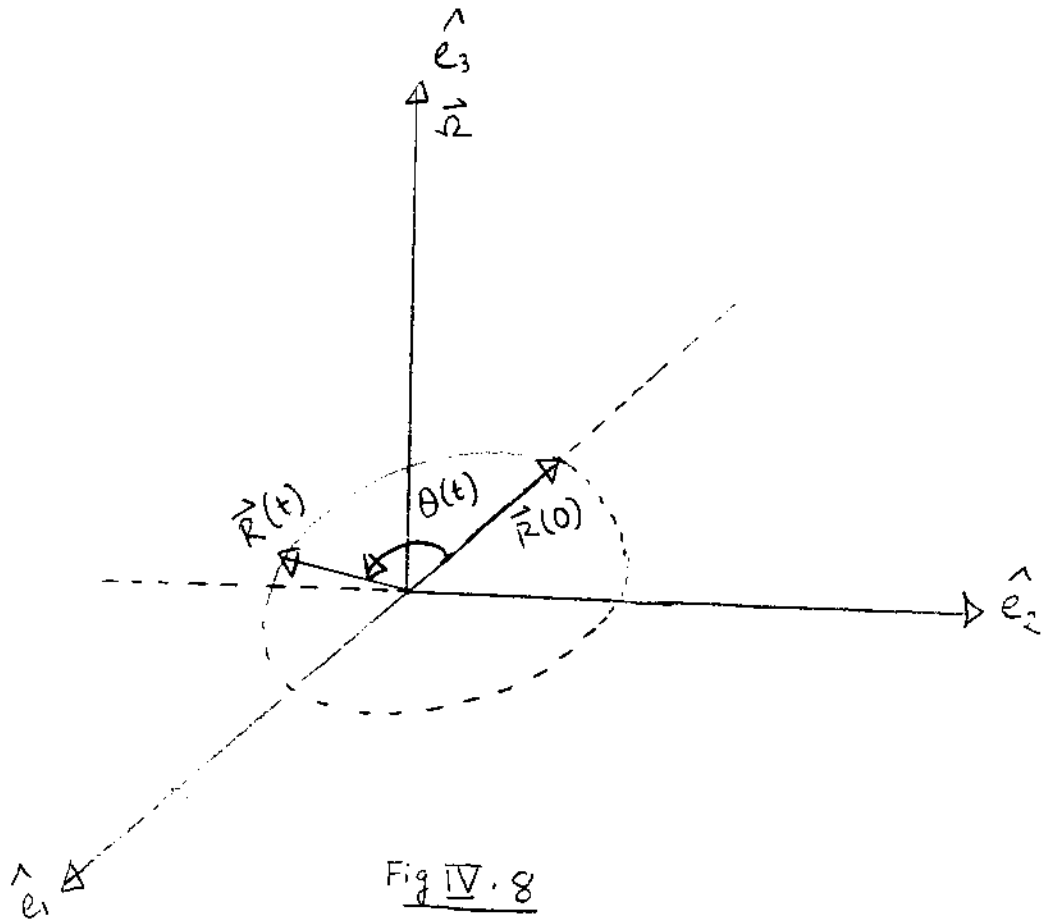

Fig IV.8

$\vec{R}$ is called the "four photon Bloch vector". The rotation of $\vec{R}$ in the pseudospace spanned by $\hat{e}_1$, $\hat{e}_2$, $\hat{e}_3$ describes four photon equation of motion of the density matrix elements (eqn. IV.81, IV.82).

Fig.(IV.9) shows the motion of the vector $\vec{R}$ in the pseudo space. At time t=0, $\sigma_{12}=0$, $\sigma_{22}=0$, $\sigma_{11}=1$, and $\vec{R}=-\hat{e}_3$. With time as the atom interacts with the incident pulse, $\vec{R}$ rotates, σ_{22} and σ_{12} grows with time.

The angle of rotation $\theta(t) = \int_0^t \Omega \, dt'$

or, $$\theta(t) = \frac{2\gamma_{12}}{\hbar^4} \int_0^t \mathcal{E}_1^4 \, dt \qquad - (IV.92)$$

we can define the four photon area of the pulse

$$\theta_4 = \frac{2\gamma_{12}}{\hbar^4} \int_{-\infty}^{+\infty} \mathcal{E}_1^4 \, dt \qquad - (IV.93)$$

where γ_{12} has been defined in equation IV.42.

when $\theta_4 = \pi$, we get the complete population inversion corresponding to W= 1/2. From the four photon vector model we can see that the absorption is determined by the four photon area of the pulse. The four photon area depends on the exact intensity profile of the pulse. For the same energy we will have more four photon absorption with shorter pulse duration. When we include ionisation, the length of four photon Bloch vector $\vec{R}$ will shrink in time. The ionisation will lead to a dephasing effect. Due to the dephasing, the vector component along $\hat{e}_2$ will average to zero leaving a pseudovector along $-\hat{e}_1$. Coherent effects are inhibited because of the ionisation rate making $\sigma_{12} \longrightarrow 0$.

Summary of Four Photon Theory

To conclude this chapter we make the following comments about the FPR system. A FPR many level system can be reduced to an equivalent two level system described by a 2 X 2 resonant density matrix ρ. The four photon Bloch equations (IV.53) to (IV.55) describe ρ as a function of time and field strengths. These equations result from an expansion up to fourth power in the electric field. With intensity and intensity square dependent ionisation, quadratic and quartic Stark shifts, harmonic generation, the interaction becomes extremely complex. A simple minded vector model drawn in analogy with two photon vector model in absence of ionisation, harmonic generation and Stark shift is no longer a true picture of a real atom. The entire four photon process is strongly intensity dependent. The four photon "area" of the pulse is defined as the integral of the square of the power density. From equation (IV.93) the four photon "area" is given by:

$$\theta_4 \propto \int_{-\infty}^{+\infty} \mathcal{E}^4 \, dt \qquad -(IV.94)$$

The four photon "area" should be compared with the two

The four photon "area" should be compared with the two photon "area" described in Chapter II:

$$\theta_2 \propto \int_{-\infty}^{+\infty} \mathcal{E}^2 \, dt \qquad -(IV.96)$$

Two photon "area" is determined by the total energy of the pulse. Since the pulse energy is proportional to the net absorption for the same pulse energy two photon absorption is independent of the pulse duration while four photon absorption increases with decreasing pulse duration. As the four photon absorption demands larger power density the intensity dependent level shift and ionisation become overwhelming and four photon coherent condition ceases. Due to the intensity dependent Stark shift the resonance condition will change as a function of intensity and the pulse will not remain tuned to resonance over the complete pulse duration. For most practical cases a relatively low intensity required for two photon absorption keeps both ionisation and the Stark shift low. A two photon coherence is maintained more easily. Besides ionisation and Stark shift all kinds of higher order Raman processes tend to enhance the complexity in a FPR system. A situation like coherent lossless propagation can hardly be expected. The multiphoton ionisation will inhibit the four photon Bloch oscillation (the oscillation of σ_{12}) and $\sigma_{12} \longrightarrow 0$. The intensity dependent susceptibility will introduce strong phase

modulation of the pulse. The medium index is also changed by the transfer of population (σ_{22} and σ_{11}). The intensity dependent tuning changes the phase by modulating the population (by absorption). Strong ionisation can cause a very big index change by depleting the ground state population. These intensity dependent index changes will eventually cause self focussing or defocussing effect in a beam with an initial gaussian intensity profile. With all these complex processes in a FPR system "self induced transparency" will not be possible.

CHAPTER BIBLIOGRAPHY

1. Dinev et al. Opt. Quantum Electron .12,183(1980).

2. Arlee.V.Smith." Four photon resonant third harmonic generation in Hg." Optics letter,10, 341 (1985).

3. Normand. et al. "Resonant multiphoton interaction and third harmonic generation in Hg vapor.",J.Phys.B:At.Mol.Phys. 16(1983) L227-L232.

4. Milonni P. W. & Eberly J. H., "Temporal coherence in multiphoton absorption. Far off resonance intermediate states", J. Chem.Phys., 68(4), (15 February, 1978), 1602-1613.

5. Georges .A. T. Ph.D Thesis. USC.(1976).

6. Feynmann et al. J. Appl. Phys., 28,49,1957.

CHAPTER V

APPLICATION OF THE FOUR PHOTON THEORY TO MERCURY ATOM

In this chapter we discuss an application of the theory developed in Chapter IV. We apply the theory to the $(6^1S_0 - 6^1D_2)$ transition in mercury (Hg) atom. The energy level diagram of the Hg atom is shown in Fig.(V.1). The ionisation threshhold for Hg is at λ = 118.78 nm, which shows a possibility of very short wavelength harmonic generation by coupling to a continuum state through multiphoton excitation. We study the harmonic generation in the four photon resonant (FPR) transition $(6^1S_0 - 6^1D_2)$ in Hg vapor. Third harmonic generation, ionisation and dynamic Stark shifts are particularly interesting. Fig.(V.2) shows the various $6^1S_0 - 6^1D_2$ resonance processes.

The fifth harmonic level lies in the continuum. The autoionising levels are far above in the continuum, so their effect is negligible. The four photon resonant wavelength for the $6^1S_0 - 6^1D_2$ transition is λ = 560.75 nm, and the third harmonic wavelength is λ = 186.92 nm. All wavelengths are taken from Ref.(V.5). The atom can be ionised from the upper excited state by absorbing one photon. The final state for the ionisation could be either a "p" state or a "f" state.

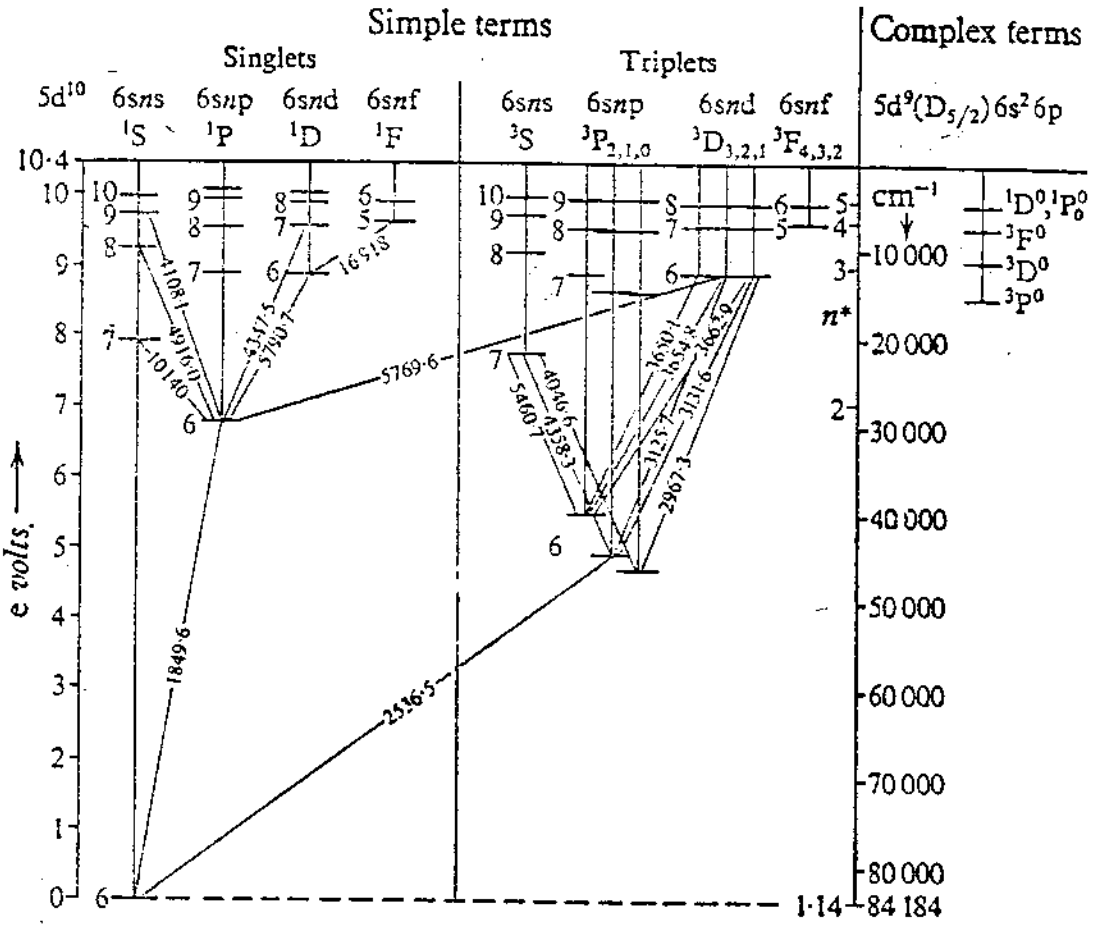
Simple terms
Complex terms
Singlets
Triplets
5d10 6sns 6snp 6snd 6snf
1S 1P 1D 1F
6sns 6snp 6snd 6snf
3S 3P2,1,0 3D3,2,1 3F4,3,2
5d9(D5/2)6s2 6p
cm−1
1D0,1P0
3F0
3D0
3P0
n*
e volts
10·4
10
9
8
7
6
5
4
3
2
1
0
10 000
20 000
30 000
40 000
50 000
60 000
70 000
80 000
84 184
1·14
4108·1
4916·0
10140
4345·5
5790·7
16518
5769·6
1849·6
2536·5
5460·7
4046·6
4358·3
16301
16548
16650
3131·6
3125·7
2967·3

FIG V.1

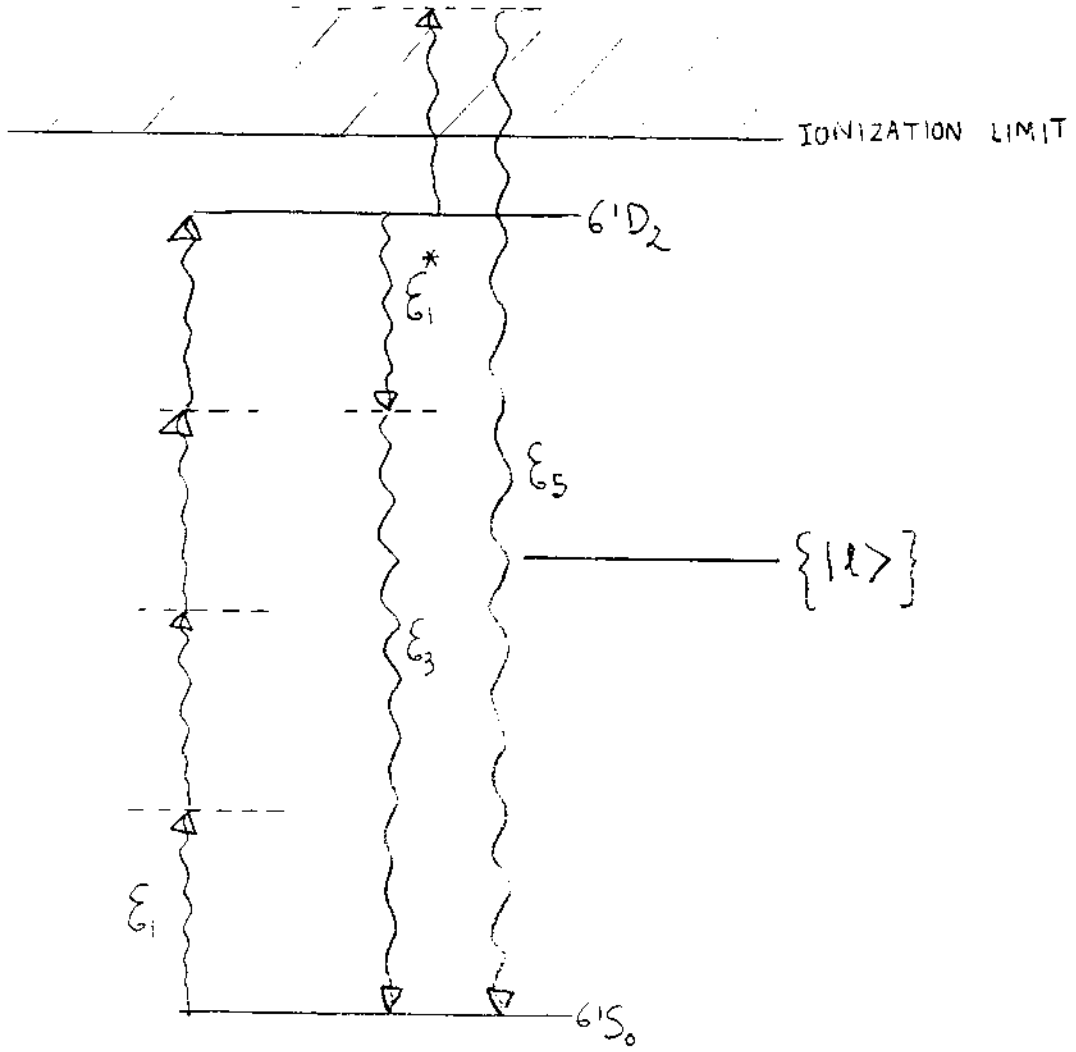
IONIZATION LIMIT
6^1D_2
ε_1^*
ε_5
$\{|l\rangle\}$
ε_3
ε_1
6^1S_0

Fig V·2

The fifth harmonic level on the other hand will coincide with a "p" state. Due to this reason ionisation will be more and fifth harmonic will be much weaker as we have seen in the case of two photon resonant transition 2S - 3D in Li vapor.

The wavefunctions and oscillator strengths were not available for Hg. In order to calculate the atomic parameters we had to make some reasonable estimates for the dipole matrix elements.

Estimate of the Dipole matrix Elements

Line intensities of different transitions in Hg were compared with the line intensity of the H_α line of hydrogen atom. When both the line intensities are normalised (Ref.V.1) we can write,

$$\frac{I_{Hg}}{I_H} = \frac{W_{Hg}}{W_H} \qquad (V.1)$$

I_{Hg} = line intensity of a transition in Hg.

I_H = line intensity of H_α line in hydrogen.

W_{Hg} = transition rate for the same line corresponding to I_{Hg} in Hg.

W_H = transition rate of H_α line in hydrogen.

$$W_{Hg} = \left(\frac{W_H}{I_H}\right) I_{Hg} \qquad (V.2)$$

H_α line in hydrogen corresponds to the transition $3\,^2D_{5/2} \rightarrow 2\,^2P_{3/2}$ corresponding to $\lambda_H = 656.285$ nm

$W_H = 0.64 \times 10^8\ s^{-1}$ .....Ref.(V.2)

$I_H = 1995.26$ .....Ref.(V.1)

$$W_{Hg} = 32076.02\ I_{Hg} \qquad (V.3)$$

Some of the transition rates calculated from equation (V.3) were compared with the experimental value found by Faisal et

al.[4] The comparison is shown in Table III . Since a cosiderable discrepancy was found we took an average estimate for W_{Hg}.

The transition rate $n\ J \longrightarrow n'\ J'$, where $n\ J$ and $n'\ J'$ are the initial and final principal and total angular momentum quantum numbers, is given in Ref.(V.3)

$$W(nJ, n'J') = \frac{4\omega^3}{3\hbar c^3}\left(\frac{1}{2J+1}\right)|\langle nJ \| D \| n'J'\rangle|^2 \tag{V.4}$$

ω = angular frequency of transition

D = dipole moment operator

Equation (V.4) can be rewritten in the following form:[3]

$$W_{Hg}(nJ \rightarrow n'J') = \frac{4\omega^3}{\hbar c^3}\left(\frac{2J_{min}+1}{2J+1}\right)\overline{|\langle nJm'|D_z|n'J'm'\rangle|^2} \tag{V.5}$$

J_{min} = The smallest one between J and J'.

where the bar denotes averaging over M.

$\langle n\ J\ M|\ D_z\ |\ n'\ J'\ M'\rangle$ in the calculation will be replaced by $\left[\overline{|\langle n\ J\ M\ \ D\ \ n\ J\ M\rangle|^2}\right]^{1/2}$. The error of this approximation may be equal to or even less than the error coming from the poor knowledge of the wavefunctions or oscillator strengths.

TABLE III

Comparison of Transition Rates

Transitions	W_{Hg} From Eqn(V.3) (s^{-1}) × 10^8	W_{Hg} From Ref3 (s^{-1}) × 10^8
$6\,^1D_2 \rightarrow 6\,^1P_1$	0.317	0.17
$6\,^1P_1 \rightarrow 6\,^1S_0$	32	7.63
$6\,^3P_1 \rightarrow 6\,^1S_0$	0.638	0.085

This is a fast way of obtaining an estimate of the various coupling constants that are needed in the calculation. A true evaluation of these coefficients should come from experiments. With the above approximation we can write,

$$\langle nJ|\mu_z|n'J'\rangle = \left[\frac{\hbar c^3}{4\omega^3}\left(\frac{2J+1}{2J_{min}+1}\right) W_{Hg}(nJ;n'J')\right]^{1/2} \qquad (V.6)$$

using equation (V.3) we get,

$$\langle nJ|\mu_z|n'J'\rangle = \left[\frac{\hbar c^3}{4\omega^3}\cdot\frac{(2J+1)}{(2J_{min}+1)} \times 32076.02\, I_{Hg}\right] \qquad (V.7)$$

An average estimate of W_{Hg} was used for the transitions mentioned in Table III. Table IV shows $\langle n\ J|\mu_z|n'\ J'\rangle$ for the various transitions. It is important to point out that here we are merely interested in obtaining some meaningful physical parameters for the computation which will provide a deeper meaning to the physical phenomena in a real FPR

TABLE IV

Dipole Matrix Elements

$\lvert n\ell JS\rangle \equiv n\,^{2S+1}\ell_J$	$\lvert n'\ell'J'S'\rangle \equiv n'\,^{2S'+1}\ell'_{J'}$	λ_{Hg} (A°)	$\langle n\ell JS\lvert M_z\rvert n'\ell'J'S'\rangle$ (MKS) $\times 10^{-30}$
$6\,^3P_1$	$6\,^1S_0$	2537.281	4
$6\,^1P_1$	$6\,^1S_0$	1849.6	13
$8\,^1S_0$	$6\,^1P_1$	4917.408	1.5
$9\,^1S_0$	$6\,^1P_1$	4109.225	0.7
$6\,^1D_2$	$6\,^1P_1$	5792.26	10
$7\,^1D_2$	$6\,^1P_1$	4348.718	3.2
$6\,^3D_2$	$6\,^1P_1$	5771.19	9
$6\,^3D_2$	$6\,^3P_1$	3126.569	2
$7\,^1S_0$	$6\,^1P_1$	10140	5
$5\,^1F_3$	$6\,^1D_2$	16918	10
$6\,^3D_1$	$6\,^3P_1$	3132.454	2
$6\,^3D_2$	$6\,^3P_2$	3655.874	2

system.

From the estimated values of μ_2 we calculated the atomic parameters at the resonant wavelength λ =560.75 nm. From now on the resonant levels 6^1S_0 & 6^1D_2 will be denoted by $|1\rangle$ & $|2\rangle$ respectively. The estimated parameters (in MKS Units)for the 6S - 6D FPR transition in Hg vapor are as follows,

FPR wavelength λ = 560.75 nm. ($\omega = 33.615 \times 10^{14}\ s^{-1}$)

Third harmonic λ_3 = 186.92 nm.

Population relaxation time[6] T_1 = 10.5 ns

The pressure dependent phase relaxation time $T_2 \simeq$ 1 ns at about 10 torr pressure.

The various polarisabilities and other coupling constants were estimated using the dipole matrix elements given in Table IV .

The Polarisabilities in MKS units are:

$$\alpha_1'(\omega) = 3.7 \times 10^{-40}$$

$$\alpha_1''(\omega) = 0$$

$$\alpha_2'(\omega) = 5 \times 10^{-39}$$

$$\alpha_2''(\omega) = 7 \times 10^{-40}$$

$$\alpha_1'(3\omega) = 5 \times 10^{-39}$$

$$\alpha_1''(3\omega) = 0$$

$$\alpha_2'(3\omega) = 10^{-40}$$

$$\alpha_2''(3\omega) = 10^{-41}$$

FPR transition matrix element $r_{12} = 3 \times 10^{-163}$ (M.K.S)

On resonant third harmonic generation $\xi_{21} = 10^{-72}$ (M.K.S)

Off resonant third harmonic generation $\alpha_3 = 3 \times 10^{-163}$ (M.K.S)

Note that we have neglected $\alpha_1^{(1)}(\omega)$ and $\alpha_2^{(1)}(\omega)$ and assumed,

$$\alpha_1(\omega) = \alpha_1^{(0)}(\omega)$$

$$\alpha_2(\omega) = \alpha_2^{(0)}(\omega)$$

[see equations (IV.32),(IV.33),(IV.34)]

Calculation of $\alpha_2''(\omega)$ or $\alpha_2''(3\omega)$ involves integration over the continuum states.

$$\alpha_2''(\omega) = -\mathrm{Im}\,\alpha_2(\omega) = -\mathrm{Im}\left\{\frac{1}{\hbar}\sum_{\ell}\frac{|\mu_{\ell 2}|^2}{(\omega_{\ell 2}-\omega)}\right\}$$

$$\alpha_2''(\omega) = -\frac{1}{\hbar}\,\mathrm{Im}\left\{\int\frac{|\langle q|\mu_z|2\rangle|^2}{(\omega_{\ell 2}-\omega)}\,g(E)\,dE\right\}$$

where,

$|\vec{q}\rangle = |\ell\rangle = \frac{1}{(2\pi)^{3/2}}e^{-i\vec{q}\cdot\vec{r}}$ = the free electron wavefunction,

and $E = \frac{\hbar^2 q^2}{2m}$ = the free electron energy as shown in Fig.(V.3),

$$\hbar\omega_{\ell 2} = E + I_2 \qquad (V.8)$$

$g(E)\,dE$ = number of free electron states between E & E + dE

$$\alpha_2''(\omega) = -\mathrm{Im}\left\{\int\frac{|\langle\vec{q}|\mu_z|2\rangle|^2}{(E+I_2-\omega\hbar)}\,g(E)\,dE\right.$$

Instead of calculating $\alpha_2''(\omega)$ explicitly we made an estimate of $\alpha_2''(\omega)$ from the ionisation crossection[3,7]. The crude estimate of the parameters will help us getting closer to a far more complex system.

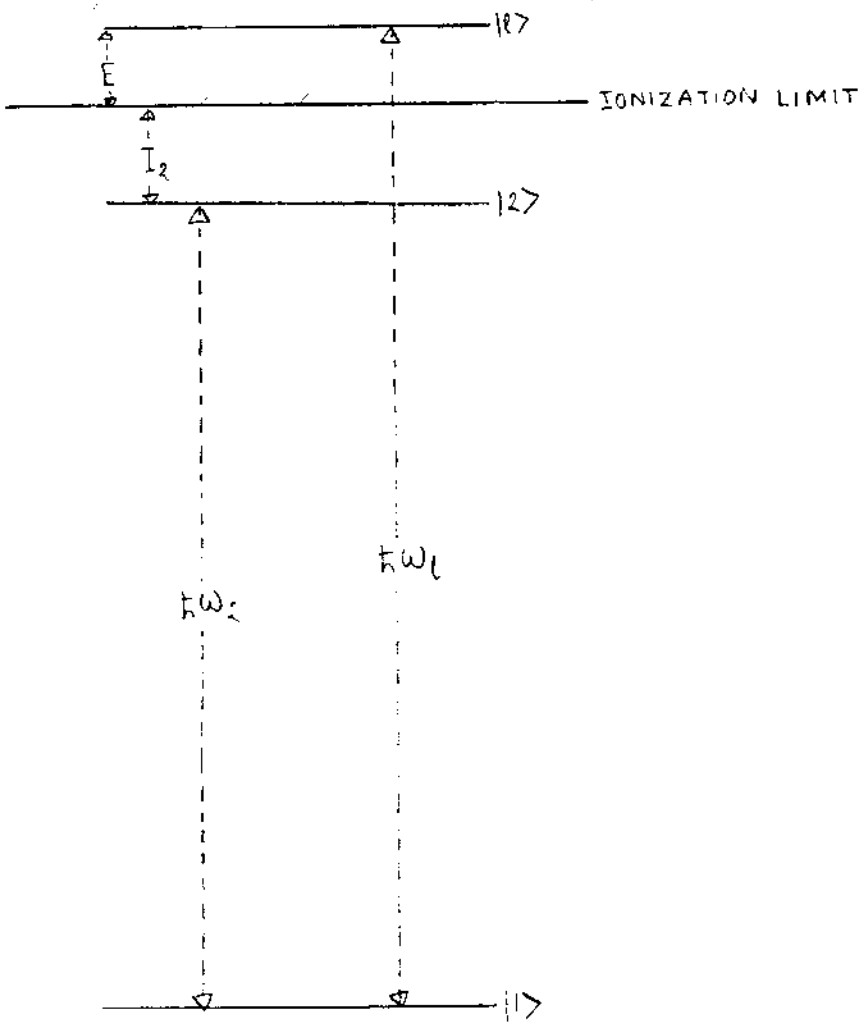

Fig V·3

Power density estimate for FPR excitation

Estimate of the energy density and pulse duration required to excite the FPR transition, is found from the four photon "area" given by equation (IV.93).

$$\theta_4 = \frac{2\gamma_{12}}{\hbar^4}\int_{-\infty}^{+\infty}\mathcal{E}_1^4\,dt$$

For a square pulse of amplitute $\mathcal{E}$ and duration τ_p we can write,

$$\theta_4 = \frac{2}{\hbar^4}\gamma_{12}\,\mathcal{E}^4\tau_p$$

The energy density of the pulse is given by

$$U = 2c\epsilon_0\mathcal{E}^2\tau_p$$

$$\theta_4 = \frac{2}{\hbar^4}\gamma_{12}\frac{U^2}{\tau_p}\frac{1}{4c^2\epsilon_0^2}$$

Using the estimated value of r_{12} for 6S - 6D transition,

$$\theta_4 = 1.75 \times 10^{-22} \frac{U^2}{\tau_p} \qquad (V.9)$$

For 100 mJ/cm^2 and 5 ps pulse we have, $\theta_4 = 3.5 \times 10^{-5}$ this represents the absorption by one atom in 10^5 !

For 10 J/cm^2 and 5 ps pulse we have, $\theta_4 = 0.35$ which corresponds to almost a 20° rotation of the Bloch vector, and about 10% absorbing atoms.

For 2 J/cm^2 and 200 fs pulse we have, $\theta_4 = 0.35$.

This shows that with shorter pulse length we can have stronger absorption. While we need intense pulse for appreciable FPR absorption, the intensity induced Stark shift in a real atom tends to destroy the resonance condition resulting in a very weak or no absorption at all. Our calculation shows that no absorption occurs even with "area" as big as 1.4. For shorter pulses with the same "area" the Stark shift goes from positive to negative values as a function of pulse time and tuning becomes impossible.

Redimensioning Maxwell - Bloch's equations

A complete picture of FPR absorption and harmonic generation demands solution of Maxwell-Bloch's equations. This requires considerable computer calculation which will be discussed in the following sections. To carry out the computer calculation we need to redimension the

equations. For clarity we rewrite the equations (IV.53) to (IV.55). We neglect the fifth harmonic field and higher order effects.

$$\frac{\partial \sigma_{12}}{\partial t} + i\left(4\omega - \omega_{21} - \delta\omega\right)\sigma_{12} + \left(\frac{\gamma_2}{2} + \frac{1}{T_2}\right)\sigma_{12}$$

$$= i\left(\sigma_{22} - \sigma_{11}\right)\left[\gamma_{12}\left(\frac{\mathcal{E}_1}{\hbar}\right)^4 + \frac{\xi_{21}}{\hbar^2}\mathcal{E}_1\mathcal{E}_3\right] \qquad \text{(V.10)}$$

$$\frac{\partial \sigma_{22}}{\partial t} + \left(\frac{1}{T_1} + \gamma_2\right)\sigma_{22}$$

$$= -2\,\mathrm{Im}\left[\left\{\gamma_{12}\left(\frac{\mathcal{E}_1^*}{\hbar}\right)^4 + \xi_{21}\frac{\mathcal{E}_1^*\mathcal{E}_3^*}{\hbar^2}\right\}\right] \qquad \text{(V.11)}$$

$$\frac{\partial\left(\sigma_{22} + \sigma_{11}\right)}{\partial t} = -\gamma_2\,\sigma_{22} \qquad \text{(V.12)}$$

in equations (V.10) to (V.12) all times are in s and all frequencies are in s^{-1} scale. Since the interaction takes place in ps or subpicoseconds time scale we would like to have all times in ps and all frequencies in ps^{-1} scale.

We divide the equation (V.10) by 10^{12} to get the rates in ps^{-1} scale.

$$\frac{\partial \sigma_{12}}{\partial E} + i\left(4\omega - \omega_{2,1} - \delta\omega\right)\sigma_{12} + \frac{\gamma_2}{10^{12}}\sigma_{12} + \frac{\sigma_{12}}{T_2}$$

$$= i\left(\sigma_{22} - \sigma_{11}\right)\left[\frac{r_{12}}{10^{12}}\left(\frac{\xi_i}{\hbar}\right)^4 + \frac{\xi_{T21}}{10^{12}}\frac{\xi_1 \xi_3}{\hbar^2}\right] \qquad \text{(V.13)}$$

We define $$\frac{r_{12}}{10^{12}}\left(\frac{\xi_i}{\hbar}\right)^4 = \underset{\sim}{\xi}_i^4 \qquad \text{(V.14)}$$

$i = 1, 3$

$\underset{\sim}{\xi}_i^4$ is in ps^{-1} scale.

$$\frac{\gamma_2}{10^{12}} = \frac{2}{\hbar}\left[\alpha_2''(\omega)\,|\xi_1|^2 + \alpha_2''(2\omega)\,|\xi_1|^2\right] \times \frac{1}{10^{12}}$$

From now on we write γ_2 as the ionisation rate in ps^{-1}.

$$\gamma_2 = 2\left[A_2''(\omega)\,|\underset{\sim}{\xi}_1|^2 + A_2''(2\omega)\,|\underset{\sim}{\xi}_3|^2\right] \qquad \text{(V.15)}$$

where

$$A_2''(m\omega) = \frac{\alpha_2''(m\omega) \times \hbar}{10^6 \sqrt{r_{12}}} \qquad \text{(V.16)}$$

where $A_2''(m\omega)$ is the reduced polarisability in $ps^{-\frac{1}{2}}$ scale.

Also,

$$\delta\omega(ps^{-1}) = \frac{1}{\hbar \times 10^{12}} \left[\alpha_1'(\omega) - \alpha_2'(\omega)\right] |\underset{\sim}{\varepsilon}_1|^2 + \frac{1}{\hbar \times 10^{12}} \left[\alpha_1'(3\omega) - \alpha_2'(3\omega)\right] |\underset{\sim}{\varepsilon}_3|^2$$

or,

$$\delta\omega(ps^{-1}) = \left[A_1'(\omega) - A_2'(\omega)\right] |\underset{\sim}{\varepsilon}_1|^2 + \left[A_1'(3\omega) - A_2'(3\omega)\right] |\underset{\sim}{\varepsilon}_3|^2 \qquad (V.17)$$

where,

$$A_i(m\omega) = A_i'(m\omega) - i\, A_i''(m\omega) \qquad (V.18)$$

$$A_i(m\omega) = \frac{\alpha_i(m\omega) \times \hbar}{10^6 \sqrt{\gamma_{i2}}} \qquad (V.19)$$

where $A_i(m\omega)$ is in ps^{-1} scale.

Using all the above reduced quantities we can rewrite equation (V.13) as,

$$\frac{\partial \sigma_{12}}{\partial t} + i\left(\Delta\omega - \omega_{21} - \delta\omega\right)\sigma_{12} + \gamma_2 \sigma_{12} + \frac{\sigma_{12}}{T_2}$$

$$= i\left(\sigma_{22} - \sigma_{11}\right)\left[\operatorname{sign}(\gamma_{12})\,\underset{\sim}{\xi}_1^4 + Z_{21}\,\underset{\sim}{\xi}_1\,\underset{\sim}{\xi}_3\right] \qquad (V.20)$$

where

$$Z_{21} = \frac{\xi_{21}}{10^6\sqrt{\gamma_{12}}} \qquad (V.21)$$

In the same way we redimension all the Maxwell-Bloch's equations. We express all fields in terms of the redimensioned field amplitude given by equation (V.14). Maxwell's equation (IV.76) together with the expressions of polarisation given by equations (IV.66) - (IV.69) are redimensioned in terms of the newly defined parameters.

For 6S - 6D trasition we have $\operatorname{sign}(\gamma_{12}) = 1$

$$\frac{\partial \sigma_{12}}{\partial t} + i\left(\Delta\omega - \omega_{21} - \delta\omega\right)\sigma_{12} + \gamma_2 \sigma_{12} + \frac{\sigma_{12}}{T_2}$$

$$= i\left(\sigma_{22} - \sigma_{11}\right)\left[\underset{\sim}{\xi}_1^4 + Z_{21}\,\underset{\sim}{\xi}_1\,\underset{\sim}{\xi}_3\right] \qquad (V.22)$$

$$\frac{\partial \sigma_{22}}{\partial t} + \frac{\sigma_{22}}{T_1} + \gamma_2 \sigma_{22} = -2\,\mathrm{Im}\left[\left\{\underset{\sim}{\xi}_1^{*4} + Z_{21}\,\underset{\sim}{\xi}_1^{*}\,\underset{\sim}{\xi}_3^{*}\right\}\sigma_{12}\right] \quad \text{(V.23)}$$

$$\frac{\partial}{\partial t}\left(\sigma_{22} + \sigma_{11}\right) = -\gamma_2 \sigma_{22} \quad \text{(V.24)}$$

$$\frac{\partial \underset{\sim}{\xi}_1}{\partial x} = -iC_1 \underset{\sim}{P}_1 \quad \text{(V.25)}$$

$$\frac{\partial \underset{\sim}{\xi}_3}{\partial x} = -i3C_1 \underset{\sim}{P}_3 \quad \text{(V.26)}$$

$$\underset{\sim}{P}_1 = \left[A_1(\omega)\sigma_{11} + A_2(\omega)\sigma_{22}\right]\underset{\sim}{\xi}_1 + 4\,\underset{\sim}{\xi}_1^{*3}\sigma_{12} + Z_{21}\sigma_{12}\underset{\sim}{\xi}_3^{*3} + 3\chi_3\,\underset{\sim}{\xi}_3\,\underset{\sim}{\xi}_1^{*3}\sigma_{11} \quad \text{(V.27)}$$

$$\underset{\sim}{P}_3 = \left[A_1(3\omega)\sigma_{11} + A_2(3\omega)\sigma_{22}\right]\underset{\sim}{\xi}_3 + Z_{21}\sigma_{12}\,\underset{\sim}{\xi}_1^{*} + \chi_3\sigma_{11}\,\underset{\sim}{\xi}_1^{3} \quad \text{(V.28)}$$

Where all frequencies are in ps^{-1}, all times are in ps, all fields amplitudes are in $ps^{-1/4}$ and distances are in

cms.

γ_2, $\delta\omega$ are defined in equations (V.15) and (V.17)

Z_{21} is defined in equation (V.21)

$$C_1 = \frac{\omega N 10^4 \sqrt{r_{12}}}{2C\epsilon_0 k} \qquad (V.29)$$

C is in $ps^{\frac{1}{2}}\ cm^{-1}$.

$$\chi_3 = \frac{\alpha_3}{|r_{12}|} \qquad (V.30)$$

The newly dimensioned atomic parameters are:

$A_1'(\omega) = 71$

$A_1''(\omega) = 0$

$A_2'(\omega) = 958$

$A_2''(\omega) = 134$

$A_1'(3\omega) = 958$

$A_1''(3\omega) = 0$

$A_2'(3\omega) = 19$

$A_2''(3\omega) = 2$

$Z_{21} = 1.8 \times 10$

$\chi_3 = 1$

The redimensioning of the equations is essential for numerical calculations. All the redimensioned numbers are finite and can be handled by the computer. Before we present the results of the computer calculation, we need to point out some of the subtle features of this FPR system.

Four Photon Rabi Oscillation versus Raman Process

From equations (V.22) & (V.23) we see that there are two driving terms for the FPR transition namely,

$\underset{\sim}{\mathcal{E}}_1^4$ = The four photon Rabi rate

$Z_{21}\, \underset{\sim}{\mathcal{E}}_1\, \underset{\sim}{\mathcal{E}}_3$ = Raman transition rate

These two terms can compete with each other and can appear in opposite phases to completely stop the FPR interaction. The two competing processes are shown in Fig.(V.4).

The four photon absorption pumped by $\underset{\sim}{\mathcal{E}}_1^4$, decays via ionisation and stimulated Raman emission. In presence of third harmonic field, Raman scattering can be stronger than ionisation. As soon as the atom is pumped into the excited state, it decays via Stimulated Raman Scattering, before it has a chance to be ionised. This vanishing of ionisation in presence of a third harmonic signal was experimentally observed both by Arlee V. Smith[9] and by Normand et al.[10] The vanishing of ionisation could either be due to the stopping of FPR interaction or due to the enhanced Raman emission.

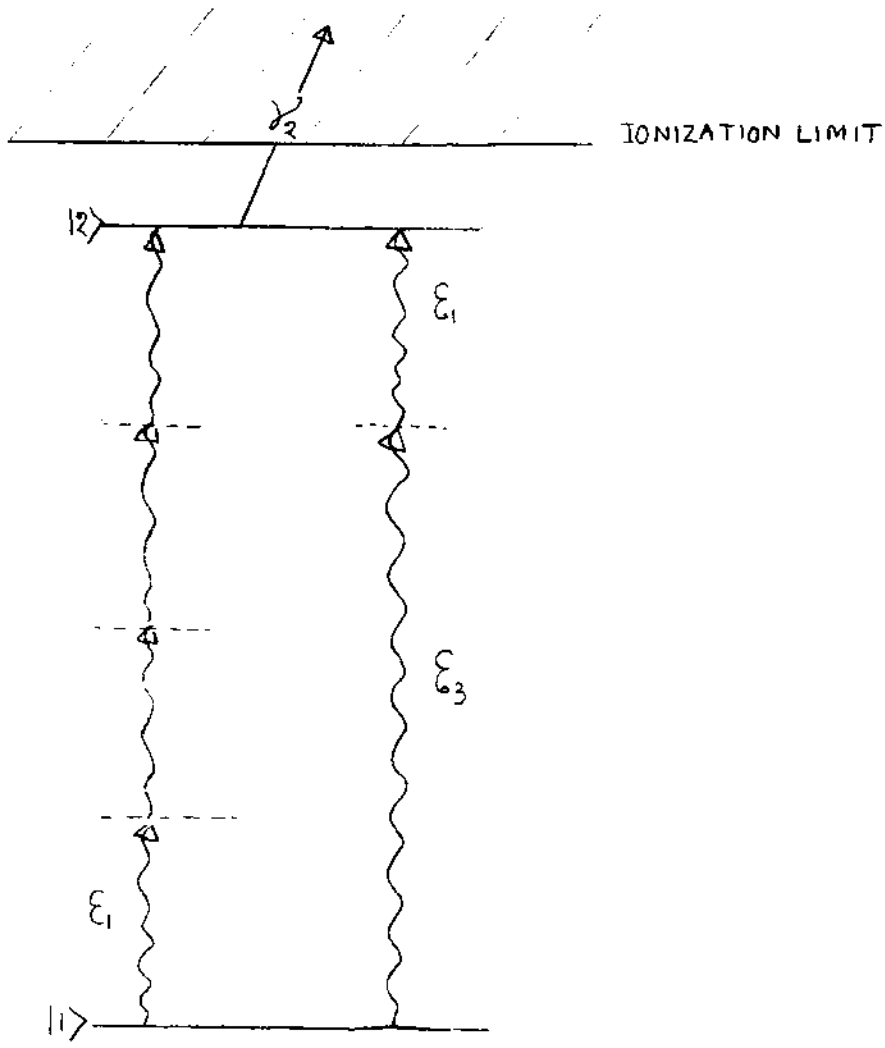
IONIZATION LIMIT
γ_2
$|2\rangle$
ε_1
ε_3
ε_1
$|1\rangle$

Fig V.4

Off-resonant versus on-resonant third harmonic generation:

From equation (V.28)

$\mathcal{Z}_{21}\sigma_{12}\underset{\sim}{\mathcal{E}}_1^*$ = The FPR third harmonic polarisation

$\chi_3\sigma_{11}\underset{\sim}{\mathcal{E}}_1^3$ = The off-resonant third harmonic polarisation

$\mathcal{Z}_{21}\sigma_{12}\underset{\sim}{\mathcal{E}}_1^*$ involves the FPR interaction with four photon absorption. Whereas $\chi_3\sigma_{11}\underset{\sim}{\mathcal{E}}_1^3$ involves no multiphoton absorption where the field energy flows between the fundamental and the third harmonic fields, sharing nothing with the atom.

For an example, let us consider the four photon vector model. From equation (IV.88)

$$\sigma_{12} = -\frac{i}{2}\sin\theta(t)$$

$$\simeq -\frac{i}{2}\theta(t) \qquad \text{for } \theta(t) \ll 1$$

using equation (IV.92)

$$\sigma_{12} = \left(-\frac{i}{2}\right)\frac{2\gamma_{12}}{\hbar^4}\mathcal{E}_1^4\tau_p$$

$$= -i\,\frac{\gamma_{12}}{\hbar^4}\mathcal{E}_1^4\tau_p \qquad \text{(V.31)}$$

Using the redimensioned field equation (V.14) and

$$\sigma_{12} = -i \underset{\sim}{\mathcal{E}}_1^4 \tau_p \qquad \text{(V.32)}$$

The on resonant part of $\underset{\sim}{P}_3$ is given by

$$\chi_{on} = Z_{21}\, \sigma_{12}\, \underset{\sim}{\mathcal{E}}_1^*$$

$$= (-i)\, Z_{21} |\underset{\sim}{\mathcal{E}}_1|^2 \tau_p\, \underset{\sim}{\mathcal{E}}_1^3 \qquad \text{(V.33)}$$

The off resonant part of $\underset{\sim}{P}_3$ is given by (assuming $\sigma_{11} \simeq 1$)

$$\chi_{off} = \chi_3\, \underset{\sim}{\mathcal{E}}_1^3 \qquad \text{(V.34)}$$

From equations (V.33) & (V.34) it follows that the on resonant part is enhanced by the energy of the pulse. Using the four photon "area" = 0.005 and pulse duration = 5 ps (ie. a case of very weak interaction, 5 out of 1000 atoms are absorbing!) we have

$$2\ \underset{\sim}{\mathcal{E}}_1^4 \tau_p = 0.005$$

$$\underset{\sim}{\mathcal{E}}_1^2 \tau_p = 0.118$$

using the value of $Z_{21} = 1.8 \times 10^3$ and $\chi_3 = 1$

$$\chi_{ON} = (-i)\ 1.8 \times 10^3 \times 0.118 \times \underset{\sim}{\mathcal{E}}_1^3$$

$$\chi_{ON} = (-i)\, 212\ \underset{\sim}{\mathcal{E}}_1^3$$

$$\chi_{off} = \underset{\sim}{\xi}^{3}$$

This shows that the on resonant part is at least two orders of magnitude larger than the off resonant part even in the case of very low absorption (a factor of 100 was estimated, only with $1 J/cm^2$ and 5 ps pulse width). This shows a very pronounced resonance enhancement. There is no intermediate two photon resonance here (like in the Li experiment) and the third harmonic is enhanced due to the four photon resonance. Being so weak the off resonant part hardly shifts the phase of the third harmonic polarisation.

Computer Integration of Maxwell - Bloch Equation

The computer solution provides a complete picture of the third harmonic generation of the FPR atom in presence of the dynamic Stark shift and ionisation. Atomic equations (V.22) to (V.24) were solved for each z-position ie. at each step of propagation, with a given incident fundamental field. Then the polarisations $\underset{\sim}{P}_1$ and $\underset{\sim}{P}_3$ were calculated using equations (V.27) & (V.28). With the calculated polarisations $\underset{\sim}{P}$ and $\underset{\sim}{P}_3$ Maxwell's equations (V.25) & (V.26) were integrated to generate fields at $Z + \Delta Z$. For integration of the two sets of partial differential equations (the atomic & Maxwell's equations), Butcher's approach[8] was used with order =5. The computer program is given in Appendix B. Because of high non-

linearity (ξ^4- type) both in Bloch equation & Maxwell's equation while many methods (like Adams-Bashforth) failed to converge, Butcher's method converged though the step size had to be made as small as 0.001 cm while the total distance of propagation was 0.05 cm. The 5ps time scale was broken into 2000 small steps for the integration of Bloch's equation. The space time propagation of atomic and Maxwell's equations give a clear picture of the harmonic generation, saturation and ionisation as a function of distance.

Results of Computer Calculation

The results of computer integration of Maxwell - Bloch equations will be described here. The incident pulse has a gaussion profile and has no chirp. Mercury vapor pressure was assumed to be about 10 torr. The incident laser pulse at λ =560.7 nm was tuned to four photon resonance with the $6^1S_0 - 6^1D_2$ transition in mercury atom. With the intensity level giving appreciable four photon "area", a very big Stark shift of the four photon transition line was observed. The Stark shift was big enough to throw the interaction completely out of resonance. From equation IV.30 Stark shift $\delta\omega$ of the resonance transition is

$$\delta\omega = \frac{1}{\hbar}\left[\alpha_1'(\omega) - \alpha_2'(\omega)\right]|\mathcal{E}_1|^2 \qquad \text{(V.35)}$$

[the third and fifth harmonic fields are neglected]

Stark shift of level I1> is

$$\delta\omega_1 = -\frac{\alpha_1'(\omega)}{\hbar}|\mathcal{E}_1|^2 \qquad \text{(V.36)}$$

Stark shift of level I2> is

$$\delta\omega_2 = -\frac{\alpha_2'(\omega)}{\hbar}|\mathcal{E}_1|^2 \qquad (V.37)$$

repeating equation IV.33 for the polarisability of the i^{th} level,

$$\alpha_i(\omega) = \frac{1}{\hbar}\sum_{\ell}\left[\frac{|\mu_{\ell i}|^2}{(\omega_{\ell i}-\omega)} + \frac{|\mu_{\ell i}|^2}{(\omega_{\ell i}+\omega)}\right] \qquad (V.38)$$

From equation (V.38) it follows that $\alpha_i(\omega)$ increases if there is a nearby one - photon (ω) level ℓ . Due to the absence of any nearby one - photon level the polarisability of the 6^1S_0 level is one order of magnitude smaller than that of 6^1D_2 . The presence of 6^1P_1 and 5^1F_3 levels enhances the polarisability of the 6^1D_2 level. From equation (V.36) and (V.37) Stark shift of the 6^1S_0 level being proportional to the polarisability is at least one order of magnitude smaller than the Stark shift of 6^1D_2 level. From now on we will write 6S for 6^1S_0 and 6D for 6^1D_2. The net Stark shift of the four photon resonant transition is mainly due to the shift of 6D level. In order to follow the Stark shifted resonance we had to detune the wavelength of the incident light so much that the polarisability of the 6D level changed (due to the change of wavelength) giving rise to an entirely different Stark shift. The closer we want to tune to the resonance the wavelength

dependent polarisability moves it further away. Fig V.5 shows α_2' (the real part of the polarisability of 6D level) as a function of wavelength λ . α_2' jumps from a very big positive value to a very big negative value about the 6D - 6^1P_1 resonance at λ = 579 nm. Fig V.6 shows the Stark shift of the four photon resonance wavelength as a function of the incident light wavelength. Stark shift shows similar jump about λ = 579 nm. This Stark shift was calculated for the intensity 3.8 X 10^{12} Watts/cm^2, which is close to the peak intensity of a 5 ps (FWHM) pulse with 20 J/cm^2 energy density. At about λ = 560.7 nm the Stark shift is about 10 nm, ie. the four photon resonance shifts from zero field resonance at λ = 560.7 nm to the field induced resonance at λ =570.7nm. When the laser is tuned to λ =570.7nm, the induced Stark-shift changes (due to change in the polarisability) and moves the resonance even further away. While the resonance tuning is difficult with a fixed intensity it gets even worse in presence of a short pulse having all kinds of intensity levels. Fig V.7 shows the shift of 6D level and α_2' as a function of time in presence of a 5 ps pulse with 20 J/cm^2 energy density. As the 6D level is shifting down with increasing pulse intensity it sees a different polarisability and α_2' changes. The changed α_2' in turn changes the level shift. Such self induced time dependent shift of the resonant levels destroys the resonance condition. In this case the incident laser pulse was tuned to zero - field resonance at λ = 560.7 nm.

FIG V.5 Real part of the polarizability α_2' of 6^1D_2 level in (MKS) unit versus wavelength λ(nm)

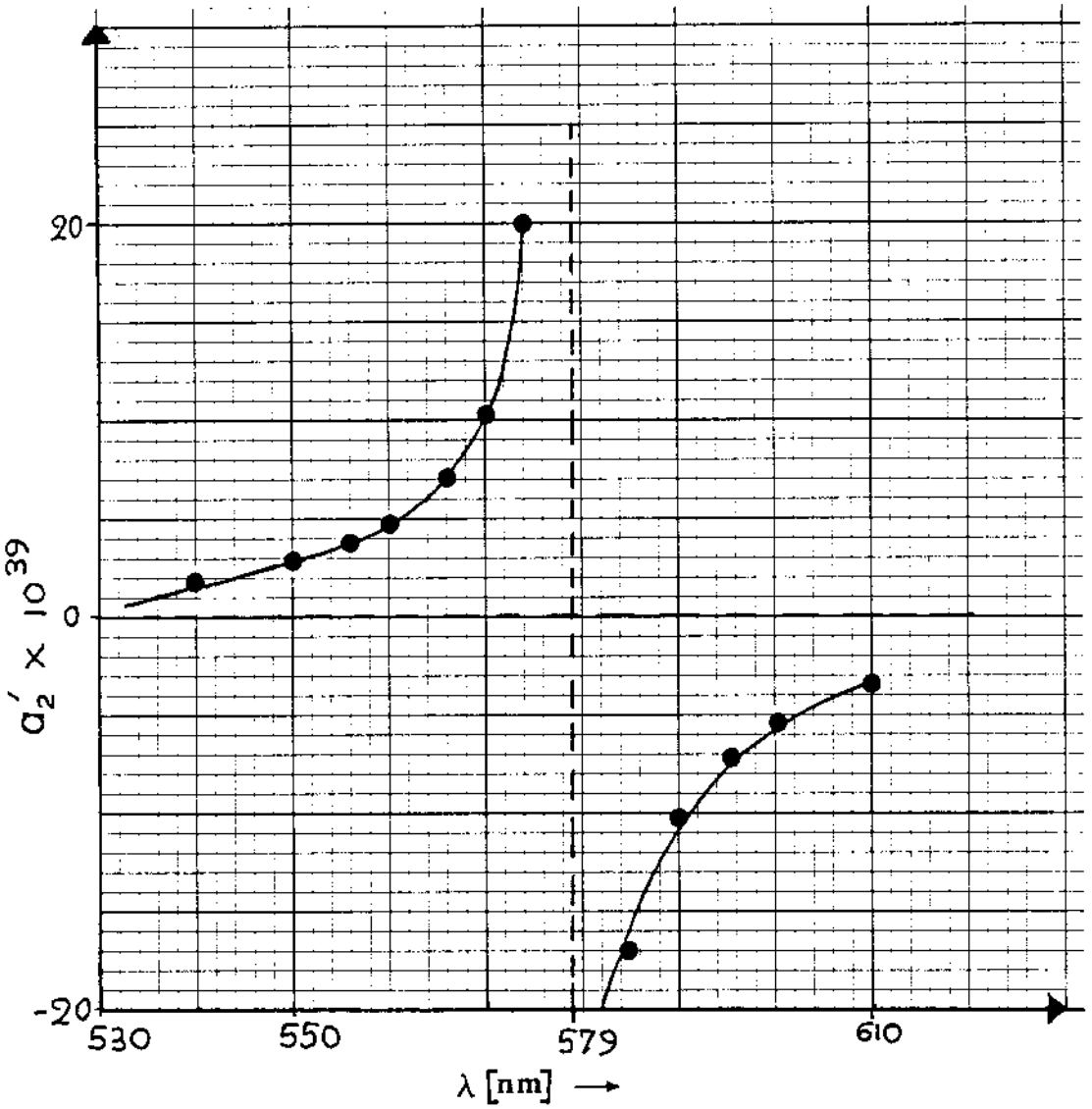

FIG V.5

FIG V.6 Stark Shift $\delta\lambda$ in nm of the Four Photon Resonant wavelength versus the wavelength $\lambda(nm)$ of the incident Light of Intensity 3.3×10^{12} W/cm^2

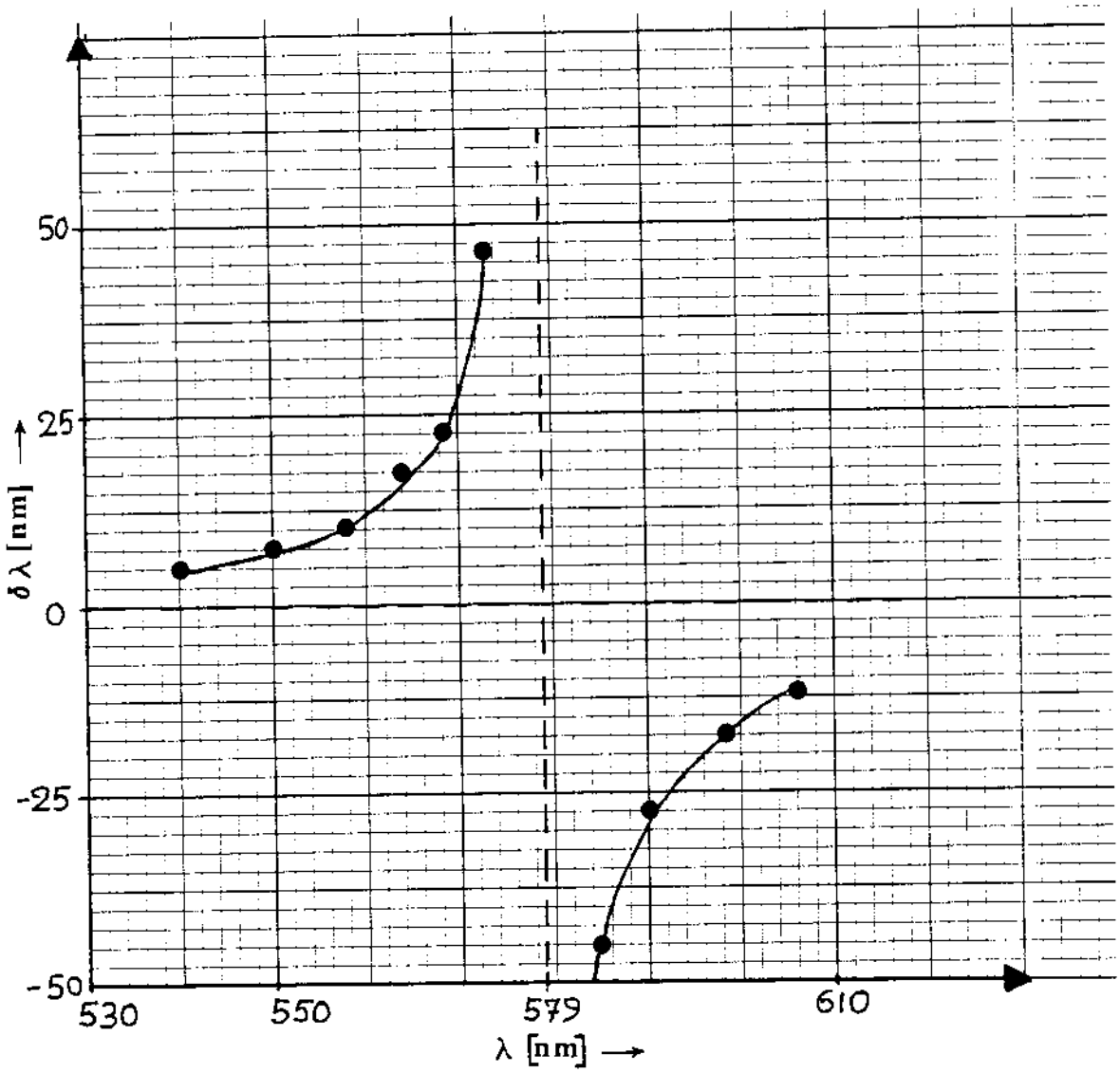

FIG V.6

FIG V.7 Stark Shift $\Delta\lambda_2$ (-⊙-) of 6^1D_2 level and polarizability α'_2 (MKS) (—•—) versus time in picosecond in presence of an 5ps (FWHM) pulse of 20 J/cm^2 energy density. The incident pulse has the form

$$\mathcal{E}(t) = \mathcal{E}_0 \, e^{-(t/\tau_p)^2}$$

τ_p = half-width at 1/e max = 3 ps.

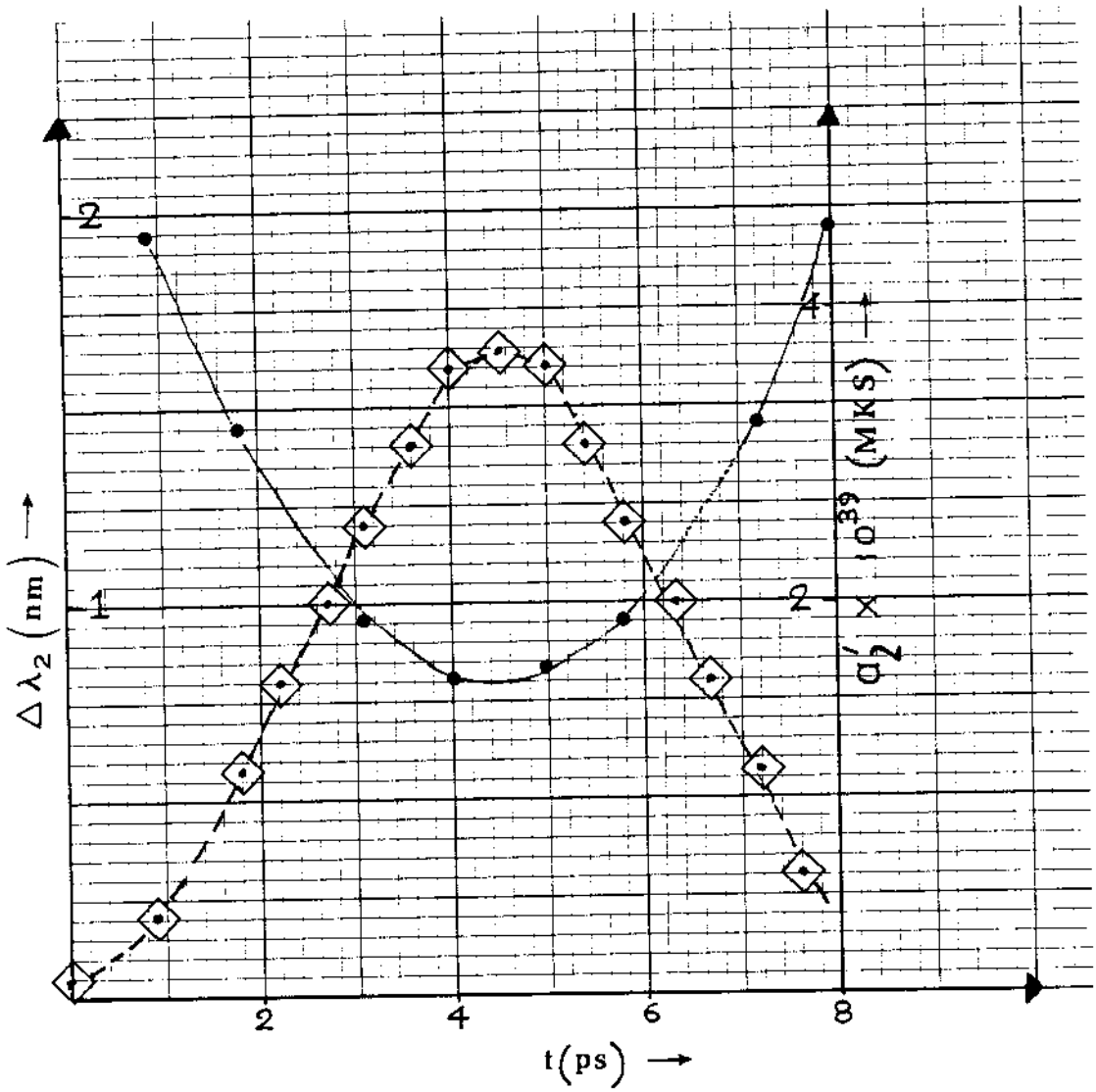

FIG V.7

FIG V.8 Stark Shift $\Delta\lambda_2(nm)$ of 6^1D_2 level versus time in picosecond in presence of an input pulse of 200 femtosecond (FWHM) duration having $4J/cm^2$ energy density.

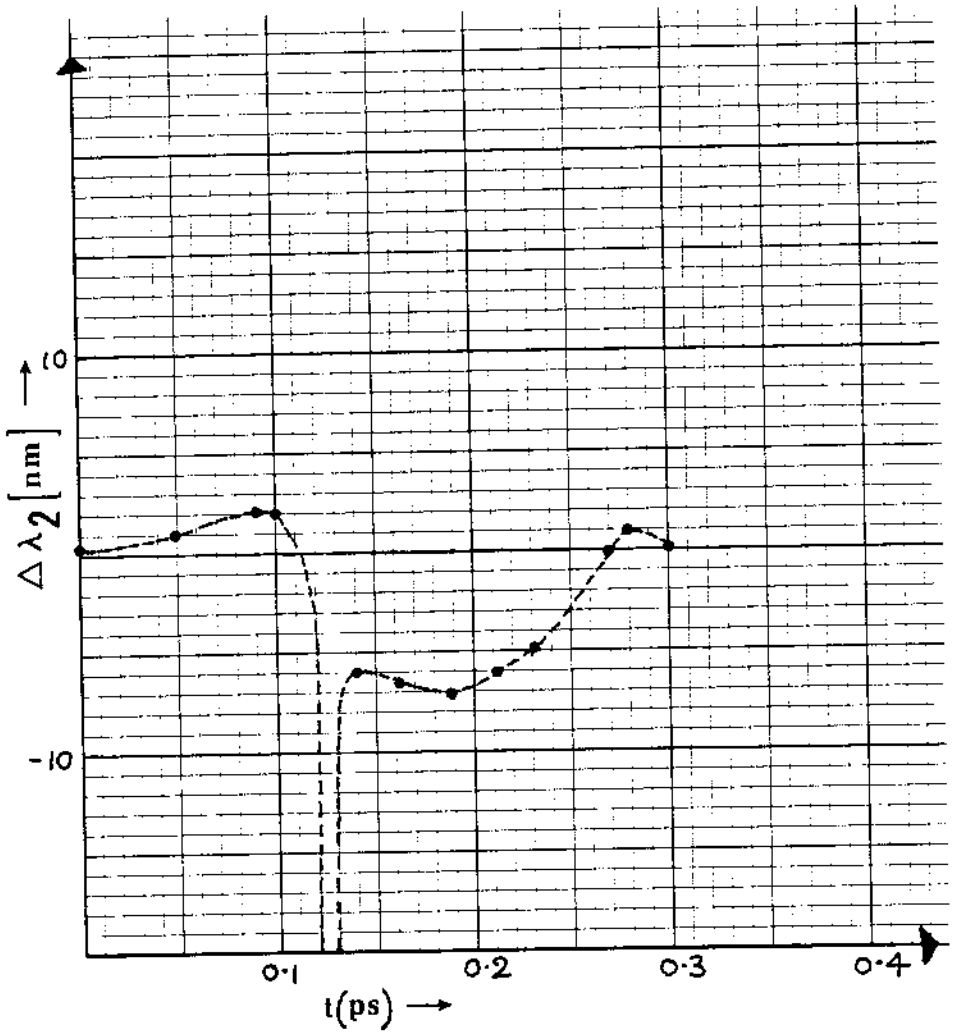

FIG V.8

FIG V.9 Polarizability α_2' (MKS) versus time (ps) in presence of a 200 fs(FWHM) Gaussian pulse with 4J/cm^2 energy density.

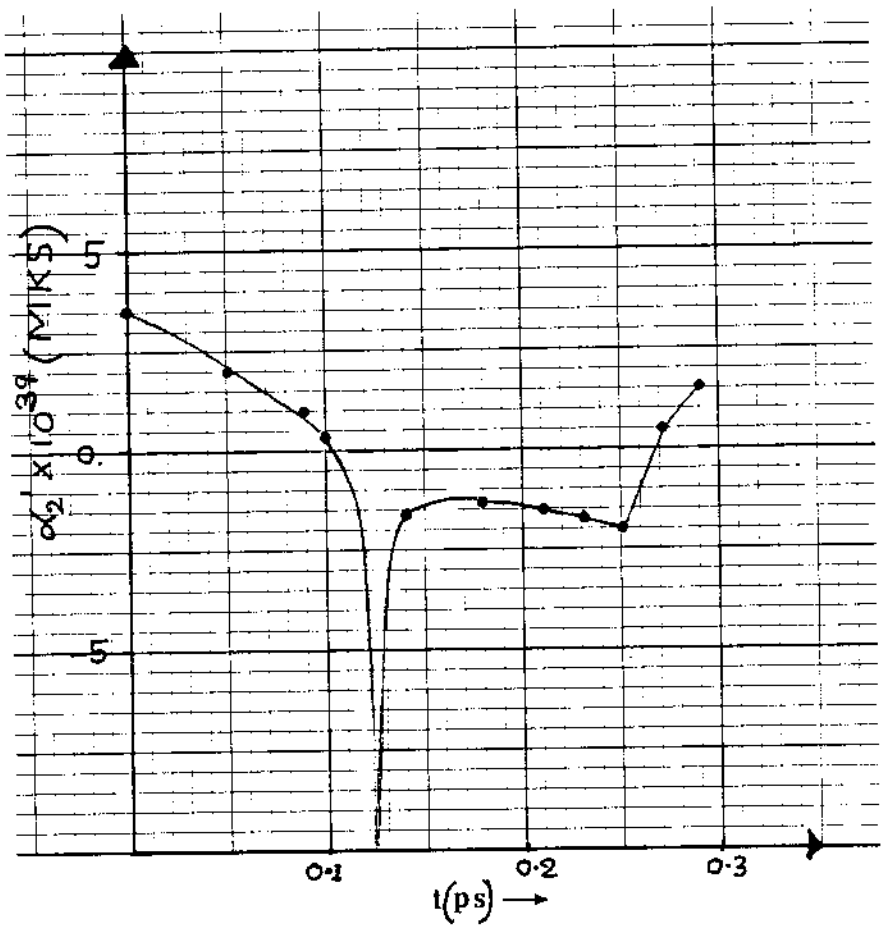

FIG V.9

A shift of 1.6 nm of the 6D level near the peak of the pulse corresponds to about 6 nm shift of the FPR wavelength. With shorter pulse (having even higher peak intensity) the time dependent level shift is even more dramatic. Fig V.8 shows the Stark shift of 6D level in nm in presence of a 200 fs (FWHM) pulse of 4 J/cm^2 energy density at λ = 560.7 nm. At about 120 fs (near the peak of the pulse) the Stark shift goes fast from a positive value to a large negative value. Fig V.9 shows a similar behaviour of α_2^1 in presence of the fs pulse. The 6D level first goes down in frequency and then near the peak intensity it moves up fast and goes far beyond its zero - field value, stays there for a short time (10 fs) and then again moves down back to its zero - field value at the end of the pulse. Evidently no resonance condition could exist in this self induced detuning process. Laser induced Stark shift broadens the multiphoton resonance linewidth.

Five ps pulse with 20 J/cm^2 energy density was propagated through the medium. The shift of the FPR transition was about 6 nm. Both α_2^1 and Stark shift were dynamically corrected in the four photon Bloch equation in the following way. First the shift of the level was calculated using the zero field α_2^1 (corresponding to the detuned wavelength) and then α_2^1 was recalculated (for the next step of the integration) using the new shifted levels. Such dynamic correction of the level provided a real picture of the interaction. The computer

program for the numerical analysis is given in APPENDIX B. The incident pulse is in the form

$$\mathcal{E}_1(t) = \mathcal{E}_0 e^{-(t/\tau_p)^2}$$

τ_p = half width at 1/e maximum = 3 ps

Four photon "area" of the pulse is approximately 1.4.

The zero field FPR wavelength of the 6S - 6D transition = 560.7 nm.

The incident light wavelength = 566.7 nm.

The incident wavelength was adjusted for maximum absorption.

Maximum third harmonic energy conversion = 4.5×10^{-8}

Maximum peak field conversion = 2.7×10^{-4}

Maximum ionisation (% of ionised atoms) = 0.15 %

The third harmonic saturation distance is about 200 microns.

Fig V.10 shows third harmonic peak field conversion and ionisation versus the distance. Ionisation of 0.15 % near z =0 dropped to 0.1×10^{-3} % at about z = 200 micron. Such sharp fall of ionisation with the rise of the third harmonic field confirms the experimental observation of Ref IV.2 & IV.3. Fig V.11 shows the fundamental and the third harmonic amplitude and phase at two distances as a function of time. At z = 0, it shows the incident pulse of 5 ps (FWHM) duration as a function of time. At z =300 micron the third harmonic amplitude and phase as well as the incident fundamental amplitude are shown as a function of time in ps. The third harmonic pulse has a duration of 3 ps (FWHM). The third harmonic phase stays at $-\pi$

FIG V.10 Percentage Ionization (-⊕-⊕-) and Third Harmonic Peak Field Conversion η (—△—) versus distance (in μm).

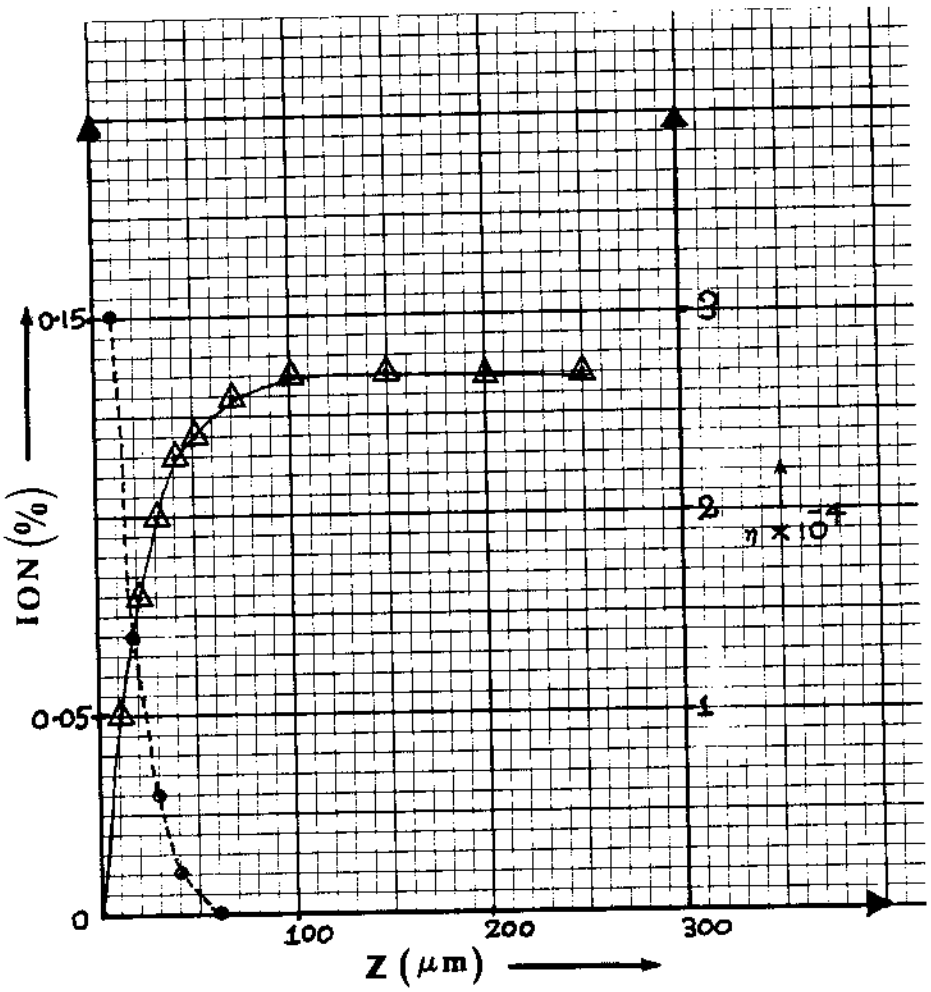

FIG V.10

FIG V.11 Propagation of a 5ps (FWHM) Gaussian pulse with 20J/cm^2 energy density through Hg vapor at 10 Torr. At z=0 redimensioned field amplitude $\mathcal{E}_1$ at fundamental frequency is shown as a function of time (ps) (—•—). At z=300 μm fundamental and 3rd harmonic field amplitudes ($\mathcal{E}_1$ —•— and $\mathcal{E}_3$ —›—) as well as the third harmonic phase ϕ_3 (---) is shown as a function of time (ps).

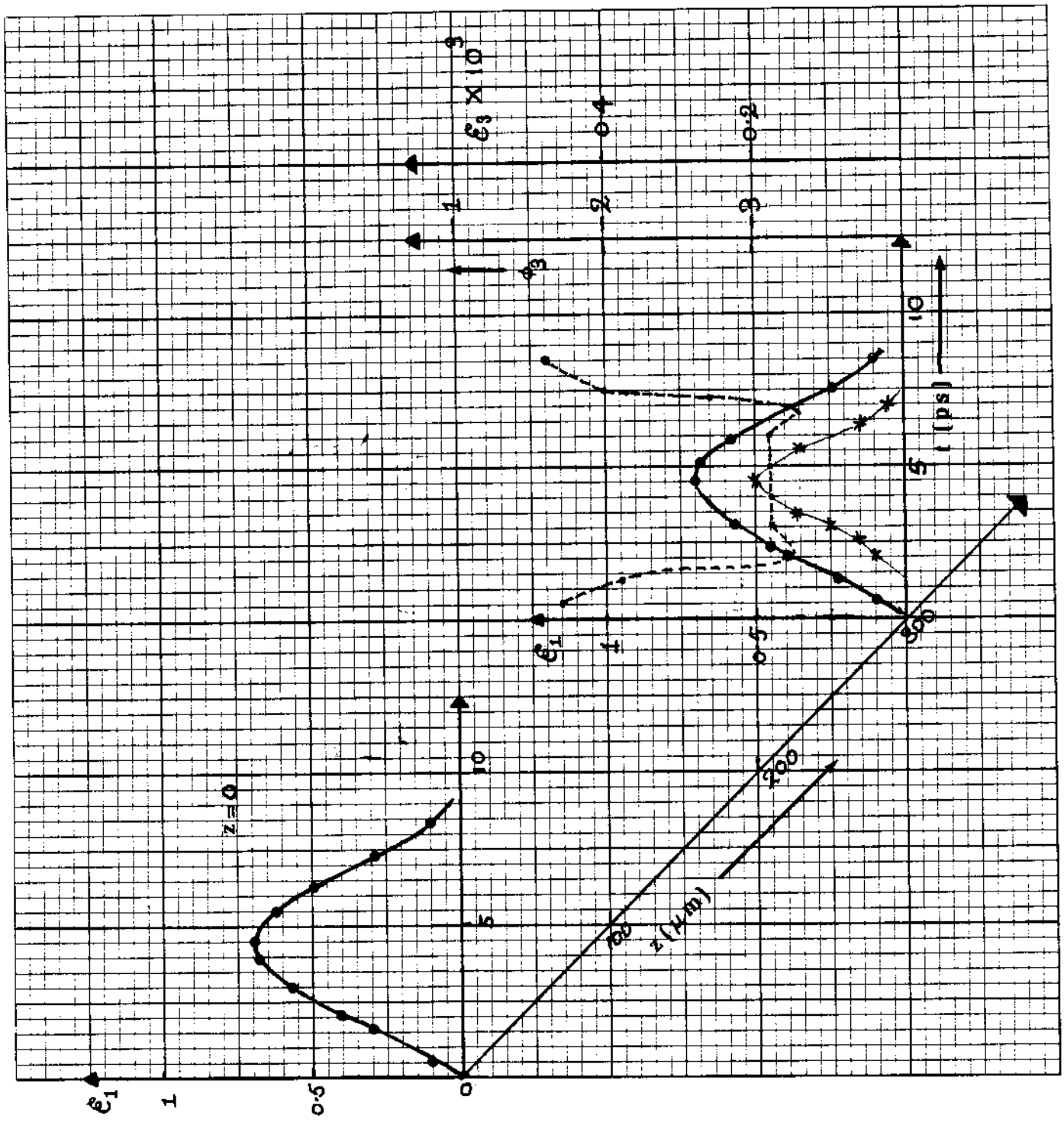
$\varepsilon_3 \times 10^3$
0·4
0·2
3
2
1
ϕ_3
10
σ_1 (psi)
ε_{11}
4
0·5
300
ε_1
z = 0
10
5
200
100
x (μm)
0
1
0·5

FIG V.11

over the FWHM of the incident 5 ps pulse. The phase of the fundamental pulse stays at zero. The peak field amplitude of the fundamental = 0.7. The peak field amplitude of the third harmonic = 0.19×10^{-3}, using $z_{21} = 1.8 \times 10^{3}$ we have,

$$\underset{\sim}{\mathcal{E}}_1^4 = 0.24 \qquad \text{and} \qquad z_{21}\, \underset{\sim}{\mathcal{E}}_1\, \underset{\sim}{\mathcal{E}}_3 = 0.24 \times e^{-i\pi}$$

$$\underset{\sim}{\mathcal{E}}_1^4 + z_{21}\, \underset{\sim}{\mathcal{E}}_1\, \underset{\sim}{\mathcal{E}}_3 = 0$$

From equation (V.22)

$$\frac{\partial \sigma_{12}}{\partial t} \sim i(\sigma_{22} - \sigma_1)\left(\underset{\sim}{\mathcal{E}}_1^4 + z_{21}\, \underset{\sim}{\mathcal{E}}_1\, \underset{\sim}{\mathcal{E}}_3\right) = 0$$

In the situation mentioned above all interaction stops, and ionisation goes to zero. A large ionisation was observed at the input end of the medium, where third harmonic was weak. The FPR pumping term $\underset{\sim}{\mathcal{E}}_1^4$ and stimulated resonant Raman scattering term $z_{21}\, \underset{\sim}{\mathcal{E}}_1\, \underset{\sim}{\mathcal{E}}_3$ work together in opposite phases to prevent a population of level I2>. For the third harmonic it is a self induced saturation effect. With increasing pressure, there will be more THG in a shorter distance, and Rabi oscillation will be stopped instantly, resulting in a saturation of THG.

In the above results the off resonant part of third harmonic polarisation $\chi_3\, \underset{\sim}{\mathcal{E}}_1^3$ in equation (V.28) was neglected. When we added the off resonant part no significant difference was observed. The THG is enhanced by the FPR (a higher order

resonance) condition.

This calculation gives a clear physical interpretation of the experimantal observation in Ref 9 & in Ref 10. It predicted a dramatic Stark shift in presence of short pulses which are subject to experimental tests. People have measured a red shift of 6S - 6D transition, but the Stark shift was negligible for the nanosecond pulses that they have used for the excitation.

CHAPTER BIBLIOGRAPHY

1. MIT Wavelength table. vol 2.,The MIT Press.

2. "Quantum mechanics of one and two electron atoms". Bethe and Salpeter.

3. I.I Sobelman. "Atomic Spectra and Radiative Transition" Springer Verlag.1979.

4. Faisal et al."Time Resolved Fluorescence spectroscopy ... " J.Phys B: Atom.Molec. Phys. 13(1980) 2027-2035.

5. NSRDS-NBS 35 Vol-I Atomic Energy Levels as Derived From The Analysis of Optical Spectra.

6. Borisov et al. "Measurement of Lifetimes of 6D Mercury Levels...." Optic Spectrosk 47(1), 109 (1979).

7. Johnson et al. Physical Rev A,25, 337(1982).

8. Leon Lapidus and John .H.Seinfeld.,"Numerical solution of ordinery differential equations. Academic Press,NY 1971.

9. Arlee.V.Smith." Four photon resonant third harmonic generation in Hg." Optics letter,10, 341 (1985).

10. Normand. et al. "Resonant multiphoton interaction and third harmonic generation in Hg vapor.",J.Phys.B:At.Mol.Phys. 16(1983) L227-L232.

CHAPTER VI

SUMMARY AND CONCLUSION

A detailed experimental study on third harmonic generation (THG) in two photon resonant (TPR) coherent interaction and a theoretical study on four photon resonant (FPR) coherent interaction has been conducted. The experiment has verified the following ideas.

1. Anomalous transmission of 90° phase shifted pulses through TPR medium (lithium 2S - 4S and 2S - 3D transitions).

2. Enhancement of THG in presence of TPR coherent excitation with a pair of 90° phase shifted pulses.

3. A TPR S - S transition is more efficient than a TPR S - D transition.

4. Tuning in multiphoton resonance is determined by the intensity of the input pulse.

Two photon coherence has been studied in detail as a function of phase and delay of the interacting pulse sequence. This experiment shows that phase correlated pulse sequence can be used to control multiphoton coherent resonant effects.[1] The coherent interaction has been found to be the key point for efficient harmonic generation.

An accurate (to at least 0.5 $\mathring{A}$) measurement of intensity dependent Stark shift has been done with the newly developed "interferometric wavemeter". Stark shifts as big as

several pulse bandwidths (of picosecond pulses) result in a poor tuning of multiphoton resonance and becomes a limiting factor of resonant harmonic generation.

A complete theory has been developed for harmonic generation in a FPR coherent interaction. A numerical application of the theory to Hg atom successfully interprets the experimental observations[2,3] in terms of the stimulated Raman scattering. The FPR excitation and phase dependent stimulated Raman scattering (in presence of third harmonic field) work together in opposite phases to stop the multiphoton interaction. The accurate modeling of such complex systems is important. Accurate control of the pulse shape is becoming possible in the femtosecond domain. It may be possible to find a particular shape of excitation (amplitude and phase versus time) which would defeat the "depopulation" effect (stopping of resonant interaction) mentioned above. With the intensity required for FPR transition, the calculation predicts a dramatic Stark shift effect which completely destroys the resonance condition. Because of the Stark shift, an intense pulse suffers a "self detuning" effect. With an intense pulse the FPR medium behaves like an off resonant medium and no absorption takes place. Such time dependent Stark shifts are the most important limitting factors in resonant multiphoton processes.

The theory can be applied to many different FPR systems. For example in Zn vapor $4\,^1S_0 - 6\,^1S_0$ transition can be

tuned to four photon resonance at λ_ω = 605.7 nm and third harmonic at $\lambda_{3\omega}$=201.9 nm and fifth harmonic at $\lambda_{5\omega}$=121.1 nm can be generated. In Neon atom the $3\,P\left(1\,\frac{1}{2}\right)$ J=2 level can be tuned to FPR (λ_ω=265.15 nm) and third harmonic at $\lambda_{3\omega}$=88.4 nm and fifth harmonic as low as $\lambda_{5\omega}$=53 nm can be generated.

As we have just begun to understand coherent resonant multiphoton processes there lies many difficult questions to be answered. We have treated the FPR system by assuming a FPR condition. In a real FPR system under the influence of short pulses the resonance condition changes in time. Questions like, how to handle such time dependent resonance condition, are yet to be answered.

CHAPTER BIBLIOGRAPHY

1. Besnainou et al." Molecular multiphoton excitation by phase coherent pulse pairs" J.Chem.Phys., 81, 143(1984).

2. Arlee.V.Smith." Four photon resonant third harmonic generation in Hg." Optics letter,10, 341 (1985).

3. Normand. et al. "Resonant multiphoton interaction and third harmonic generation in Hg vapor.",J.Phys.B:At.Mol.Phys. 16(1983) L227-L232.

APPENDIX A

ADIABATIC EXPANSION OF THE OFF RESONANT DESITY MATRIX ELEMENT

To give an example let us consider $\sigma_{1\ell}(3)$ appearing in equation of σ_{12} . From equation (IV.24) for $\ell \neq 1,2$

$$\sigma_{1\ell}(3) = -\alpha_{\ell_1}(3) \sum_{P_1=2,4} \left[\sigma_{ij}(P_1)\Omega_{j\ell} - \Omega_{ij}\sigma_{j\ell}(P_1)\right] e^{i\left(\frac{3-P_1}{3-P_1}\right)\phi_1}$$

$$-\alpha_{\ell_1}(3) \sum_{P_3=0,6} \left[\sigma_{ij}(P_3)\beta_{j\ell} - \beta_{ij}\sigma_{j\ell}(P_3)\right] e^{i\left(\frac{3-P_3}{3-P_3}\right)\phi_3}$$

$$-\alpha_{\ell_1}(3) \sum \left[\sigma_{ij}(P_5)\delta_{j\ell} - \delta_{ij}\sigma_{j\ell}(P_5)\right] e^{i\left(\frac{3-P_5}{3-P_5}\right)\phi_5}$$

(A.1)

For simplicity let us ignore the third and fifth harmonic fields.

$$\sigma_{1\ell}(3) = -\alpha_{\ell_1}(3) \sum_{P_1=2,4} \left[\sigma_{ij}(P_1)\Omega_{j\ell} - \Omega_{ij}\sigma_{j\ell}(P_1)\right] e^{i(3-P_1)\phi_1}$$

(A.2)

$$\sigma_{1\ell}(3) = -\alpha_{\ell_1}(3)\,\sigma_{12}(4)\,\Omega_{2\ell}\,e^{-i\varphi_1} - \alpha_{\ell_1}(3)\,\sigma_{1j}(2)\,\Omega_{j\ell}\,e^{i\varphi_1}$$

$$+ \alpha_{\ell_1}(3)\,\Omega_{1j}\sum_{P_1=2,4}\sigma_{j\ell}(P_1)\,e^{i(3-P_1)\varphi_1}$$

(A.3)

Note that $\sigma_{1j}(P_1)$ for j=2 and p =4 has generated the resonant element, which must not be expanded by adiabatic approximation. Expanding $\sigma_{1j}(2)$ by adiabatic approximation

$$\sigma_{1j}(2) = -\alpha_{j_1}(2)\sum_{q=1,3}\left[\sigma_{1k}(q)\,\Omega_{kj} - \Omega_{1k}\,\sigma_{kj}(q)\right]e^{i(2-q)\varphi_1}$$

In equation (A.3) we can see contribution from the first two terms and ignore the contribution from the third term. Later on we can add its contribution.

$$\sigma_{1\ell}(3) = -\alpha_{\ell_1}(3)\,\sigma_{12}(4)\,\Omega_{2\ell}\,e^{-i\varphi_1}$$

$$+ \alpha_{\ell_1}(3)\,\Omega_{j\ell}\,\alpha_{j_1}(2)\,e^{i\varphi_1} \times \left(\sigma_{1k}(q)\,\Omega_{kj} - \Omega_{1k}\sigma_{kj}(q)\right)e^{i(2-q)\varphi_1}$$

$$q=1,3$$

(A.4)

by further expanding

$$\sigma_{1k}(q) = -\alpha_{k_1}(q)\sum_{r=q-1,q+1}\left[\sigma_{1g}(r)\,\Omega_{gk} - \Omega_{1g}\,\sigma_{gk}(r)\right]e^{i(q-r)\varphi_1}$$

and similar expansion for $\sigma_{kj}^{(q)}$.

$q = 1,3 \qquad r = 0,2,2,4$

$$\sigma_{1\ell}^{(3)} = -\alpha_{1\ell}(3)\,\sigma_{12}(4)\,\Omega_{2\ell}\,e^{-i\varphi_1}$$

$$+\alpha_{\ell_1}(3)\,\alpha_{j1}(2)\,\Omega_{j\ell}\,e^{i\varphi_1}\Omega_{kj}\Big[-\alpha_{k_1}(1)\,\sigma_{11}\Omega_{1k}\,e^{i\varphi_1}e^{i\varphi_1}$$

$$-\alpha_{k_1}(3)\,\sigma_{12}(4)\,\Omega_{2k}\,e^{-i\varphi_1}\,e^{-i\varphi_1}\Big] + \cdots$$

or,

$$\sigma_{1\ell}^{(3)} = -\alpha_{\ell_1}(3)\,\sigma_{12}(4)\,\Omega_{2\ell}\,e^{-i\varphi_1}$$

$$-\alpha_{\ell_1}(3)\,\alpha_{j1}(2)\,\alpha_{k1}(1)\,\Omega_{1k}\Omega_{kj}\Omega_{j\ell}\,e^{i2\varphi_1}\sigma_{11}$$

$$-\alpha_{\ell_1}(3)\,\alpha_{j1}(2)\,\alpha_{k1}(3)\,\Omega_{2k}\,\Omega_{kj}\,\Omega_{j\ell}\,e^{-i\varphi_1}\sigma_{12}(4) + \cdots$$

(A.5)

In equation (A.5) $\sigma_{1\ell}^{(3)}$ is expanded in powers of Ω or $\mathcal{E}_1$. In order to generate equation for σ_{12} till the fourth power of $\mathcal{E}_1$ and expansion of $\sigma_{1\ell}^{(3)}$ till the third power of $\mathcal{E}_1$ is sufficient. Since equation (A.5) contains terms upto third power of $\mathcal{E}_1$, no further expansion of $\sigma_{1\ell}^{(3)}$ will be needed. Note that in the last expansion we have neglected all off resonant terms. The above procedure shows a very little portion of an elaborate expansion procedure. The various terms of the expansion are due to verious scattering processes. We rewrite

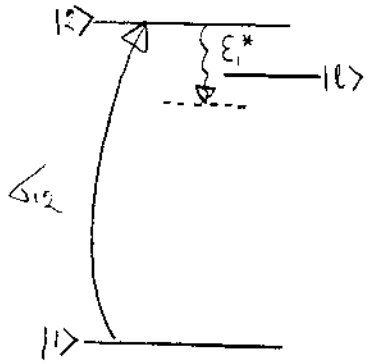

$\sigma_{12}\,\varepsilon_1^*$

Fig A.1

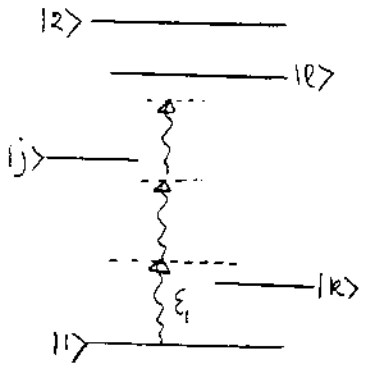

$\sigma_{11}\,\varepsilon_1^3$

Fig A.2

equation (A.5) as

$$\sigma_{1\ell}(3) = -\frac{\mu_{2\ell}\,\mathcal{E}_1^{*}\,\sigma_{12}}{\hbar(3\omega-\omega_{\ell 1})} - \frac{\mu_{ik}\,\mu_{kj}\,\mu_{j\ell}\,\mathcal{E}_1^{3}\,\sigma_{11}}{\hbar^3(3\omega-\omega_{\ell 1})(2\omega-\omega_{j1})(\omega-\omega_{k1})}$$

$$+ \cdots \qquad (A.6)$$

Fig (A.1) & (A.2) shows two of the scattering processes generating $\sigma_{1\ell}^{(3)}$. Drawing pictures in the intermediate steps helps to understand the expansion procedure and to neglect the unphysical terms. In this example we did not show the effect of third and fifth harmonic fields which were included in the actual derivation to generate the various mixing terms.

APPENDIX B

COMPUTER INTEGRATION OF MAXWELL-BLOCH EQUATION

```
      COMPLEX ALFA2,ALFA13,ALFA23,TQ,E1,E3,ALFA1,AK1,AK3
      COMPLEX PRE1,PE1,PRDE1,PDE1,DE1,DE12,PRE3,PE3,PRDE3
      COMPLEX PDE3,DE3,DE32,P1,P3
      COMMON/JC/ALFA1,ALFA2,ALFA13,ALFA23,ZI,AK1,AK3,DISP
     1,DOM0,H1,H2,H3,H4,T1INV,T2INV,XH1,XH2,XH3
     2,XH4,XH5,XH6,XH7,XH8,XH9,WL0,H5,H6,H7,H8,H9
     3,IS,NS,MS,AION,DIST,PI,DX,NST
      COMMON/ARYS/E1(2024),E3(2024),TQ(2024),TL(2024)
     1,TW(2024),TU(2024),P1(2024),P3(2024)
      COMMON/OTHER/AMP,CENTER,M,DT,MT,WIDTH,WD2,R12
      COMMON/ARAY/EN1(2000),EN3(2000),E1P(2000),E3P(2000)
     1,ECON(2000),CONVER(2000),ARION(2000)
      DIMENSION PRE1(2024),PRE3(2024),PE1(2024),PE3(2024)
      DIMENSION PRDE1(2024),PRDE3(2024),PDE1(2024),PDE3(2024)
      DIMENSION DE1(2024),DE3(2024)
      LOGICAL L1
      LOGICAL L3

        IS=1
      DIST=0.0
      CALL DEFINE
      CALL PULSE
      ECON(IS)=0.0
      ECON is the energy conversion
      IS is the distance index
       CONVER(IS)=0.0
      CONVER stores the peak-field conversion
      as a funtion of distance
       AION=0.0
      CALL OUTPUT
evios &present funtions and derivatives:
      DO 1 I=1,M
      PRE1(I)=E1(I)
      PE1(I)=E1(I)
      PRE3(I)=E3(I)
      PE3(I)=E3(I)
      PRDE1(I)=(0.0,0.)
      PRDE3(I)=(0.0,0.)
      PRE & PE are the previous and present FIELDS
      PRDE & PDE are the previous and present derivatives
      CALL BLOCH
      DO 2 IS=2,NS
      DO 3 I=1,M
lculation of present derivatives
      PDE1(I)=-AK1*P1(I)
```

```
    PDE3(I)=-AK3*P3(I)
redictionof funtion at half point
    E1(I)=PRE1(I)+XH1*PDE1(I)+XH2*PRDE1(I)
    E3(I)=PRE3(I)+XH1*PDE3(I)+XH2*PRDE3(I)
    IF(CABS(E1(I)).LT..1E-10) E1(I)=(0.0,0.)
    IF(CABS(E3(I)).LT..1E-10) E3(I)=(0.0,0.)
    CONTINUE
alculation of derivatives at half point
    CALL BLOCH
    DO 4 I=1,M
    DE1(I)=-AK1*P1(I)
    DE3(I)=-AK3*P3(I)
rediction of funtion at next point
    E1(I)=(28.*PE1(I)-23.*PRE1(I))/5.+(XH3*DE1(I)-XH4*PDE1(I)
  1-XH5*PRDE1(I))
    E3(I)=(28.*PE3(I)-23.*PRE3(I))/5.+(XH3*DE3(I)-XH4*PDE3(I)
  1-XH5*PRDE3(I))
    IF(CABS(E1(I)).LT..1E-10) E1(I)=(0.0,0.)
    IF(CABS(E3(I)).LT..1E-10) E3(I)=(0.0,0.)
    CONTINUE
alculation of derivatves at next points
    CALL BLOCH
    SEN1=0.0
    SEN3=0.0
    E1MAX=0.0
    E3MAX=0.0
    DO 5 I=1,M
    DE12=-AK1*P1(I)
    DE32=-AK3*P3(I)
orrecting funtion at next point
    E1(I)=(32.*PE1(I)-PRE1(I))/31.+(XH6*DE1(I)+XH7*DE12+XH8*PDE1(I)
  1-XH9*PRDE1(I))
    E3(I)=(32.*PE3(I)-PRE3(I))/31.+(XH6*DE3(I)+XH7*DE32+XH8*PDE3(I)
  1-XH9*PRDE3(I))
    IF(CABS(E1(I)).LT..1E-10) E1(I)=(0.0,0.)
    IF(CABS(E3(I)).LT..1E-10) E3(I)=(0.0,0.)
    SES1=E1(I)*CONJG(E1(I))
        SES3=E3(I)*CONJG(E3(I))
    E1M=SQRT(SES1)
    E3M=SQRT(SES3)
     L1=E1M.GT.E1MAX
     L3=E3M.GT.E3MAX
     IF(L1) E1MAX=E1M
     IF(L3) E3MAX=E3M
     SEN1=SEN1+SES1
     SEN3=SEN3+SES3
```

```
aifting the present point to the next point
    PRE1(I)=PE1(I)
    PE1(I)=E1(I)
    PRE3(I)=PE3(I)
    PE3(I)=E3(I)
    PRDE1(I)=PDE1(I)
    PRDE3(I)=PDE3(I)
    EN1(IS)=SEN1*DT
    EN3(IS)=SEN3*DT
    EN1 & EN3 store the 1st & 3rd harmonic energy
    as a funtion of distance
    E1P(IS)=E1MAX
    E3P(IS)=E3MAX
    E1P & E3P store the 1st & 3rd harmonic
    PEAK field as funtion of distance
    ECON(IS)=EN3(IS)/EN1(1)
    CONVER(IS)=E3MAX/E1P(1)
    CALL BLOCH
    ARION(IS)=AION
istance propagated
    DIST=(IS-1)*DX
    IOUT=(IS-1)/MS
    AOUT=FLOAT(IOUT)
    EOUT=FLOAT(IS-1)/FLOAT(MS)
    IF(AOUT.NE.EOUT)GO TO 2
    CALL OUTPUT
     CONTINUE
     WRITE(6,10)
    FORMAT(/,2X,4HDIST,15X,3HEN1,20X,3HEN3,15X,3HION)
     DO 11 K=1,NS,NST
     DIST=(K-1)*DX
     WRITE(6,12)DIST,EN1(K),EN3(K),ARION(K)
     FORMAT(E12.5,3X,E15.5,2X,E15.5,2X,E15.5)
     CONTINUE
    STOP
    END
```

```
C*****************************************************************
      SUBROUTINE DEFINE
      ******************
      COMPLEX ALFA2,ALFA13,ALFA23,TQ,E1,E3,ALFA1,AK1,AK3
      COMMON/JC/ALFA1,ALFA2,ALFA13,ALFA23,ZI,AK1,AK3,DISP
     1,DOM0,H1,H2,H3,H4,T1INV,T2INV,XH1,XH2,XH3
     2,XH4,XH5,XH6,XH7,XH8,XH9,WL0,H5,H6,H7,H8,H9
     3,IS,NS,MS,AION,DIST,PI,DX,NST
      COMMON/ARYS/E1(2024),E3(2024),TQ(2024),TL(2024)
     1,TW(2024),TU(2024),P1(2024),P3(2024)
      COMMON/OTHER/AMP,CENTER,M,DT,MT,WIDTH,WD2,R12
      COMMON/ARAY/EN1(2000),EN3(2000),E1P(2000),E3P(2000)
     1,ECON(2000),CONVER(2000),ARION(2000)
       PI=3.14159205359
       DOM0=-100.
       DOM0 is the 0-field detuning
      WIDTH =5.
      WIDTH0=WIDTH
      WIDTH IS THE FWHM OF THE PULSE IN PS.
      ALL TIMES ARE IN PS. AND ALL FREQUENCIES IN PS E-1
          PSE-1 STANDS FOR RADIANS/PSEC.
      T2 = 1000.
         PHASE RELAXATION TIME IN PS.
      T1 = 10000.
         ENERGY RELAXATION TIME IN PS.
      T2INV = 1./T2
      T1INV = 1./T1
      ALFA1=(71.,0.0)
      ALFA2=(958.,-134.)
      ALFA13=(958.,0.0)
      ALFA23=(19.,-2.0)
      AK1=(0.,.006)
      AK1=.006 crresponds to 10 TORR pressure
      AK3=3.*AK1
      ABS1=AIMAG(AK1)
        ZI=1.8E03
        DISP=0.
      DISP is the additional dispersion needed to phase match
          OMEGA=33.615+(DOM0/400.)
          R12=.3
          AL2=(57./(OMEGA-32.543))+(115./(11.137-OMEGA))
          AL1=(16./(74.29-OMEGA))+(169./(101.92-OMEGA))
          AL1=AL1/1.05
          AL1=AL1*10.5/SQRT(R12)
          AL2=AL2*10.5/SQRT(R12)
          ALI2=AIMAG(ALFA2)
          ALFA1=CMPLX(AL1,0.)
          ALFA2=CMPLX(AL2,ALI2)
]]]]]]]]]]]]]]]]]]]]]]]]]]]]]]]]]]]]]]]]]]]]]]]]]]]]]]]]]]]]]]]]]]]]]
```

```
                T2INV = 0.
                 T1INV = 0.
      FOR TESTING T1INV & T2INV ARE SET = 0
JJJJJJJJJJJJJJJJJJJJJJJJJJJJJJJJJJJJJJJJJJJJJJJJJJJJJJJ
       NS=40
       N1S=NS
       NS=NS+1
       MS=1
    MS is the gap in the space interval for taking output
    DX=.0001
  NS=no. of step length & DX is the step length in cm
         NST=2
  NST IS THE GAP IN DISTANCE for the final output
         WIDTH = WIDTH/2*SQRT(ALOG(2.))
         TWO=ALOG(2.)
         TWO=2*SQRT(TWO)
         WIDTH=WIDTH/TWO
    write(6,300)WIDTH
)   format(10X,'width=',E15.5)
         ENGY=20000.
      ENGY IS THE PULSE ENERGY IN MJ/CM2
   CON=2.23E-10
   WRITE(6,90) CON
)       FORMAT(10X,'CON=',E15.6)
   SOME2=(ENGY*3770.)/2.
   SQ=(SOME2*1.E12)/(WIDTH*SQRT(PI/2.))
   AMP = SQRT(SQ)
      SO FAR AMP IS IN MKS
   AMP=(AMP*CON)
     IS THE AMP OF THE ELECTRIC FIELD
    AMP FROM NOW ON IS IN PS-1/4 AND CORRESPONDS TO
     AMP OF EACH SPLIT PULSE
   WD2 = WIDTH**2
      M=2000
   IS THE NUMBER OF POINTS (IN TIME) THAT CONSTITUTES A PULSE.
   CENTER = (1.5)*WIDTH
      IS THE PULSE CENTER.
)T     IS THE TIME INCREMENT (IN THE RETARDED TIME FRAME OF REFERENCE).
       DT=(2*CENTER)/FLOAT(M)
        H2=(3.*DT)/8
```

```
      H1=3*H2
      H3=(32./15.)*DT
          H4=4.*DT
         H5=(26./15.)*DT
         H9=DT/93.
         H6=64*H9
         H7=15*H9
         H8=12*H9
           XH2=(3.*DX)/8
         XH1=3*XH2
         XH3=(32./15.)*DX
         XH4=4.*DX
         XH5=(26./15.)*DX
         XH9=DX/93.
         XH6=64*XH9
         XH7=15*XH9
         XH8=12*XH9
         MT=M/20
   MT is the gap in time interval
   WL0=1.
WL0 is the initial population of the initial level
  WRITE(6,6)ENGY,WIDTH0,DOM0
  FORMAT('       INPUT PULSE PARAMETER(1ST HARMONIC FIELD)',
 1/,'-------------------------------------------------------',/,
 23X,'INPUT ENERGY DENSITY(MJ/CM2)=',E12.2,/,10X,'pulse width
 3IN PS (FWHM)=',E10.4,/,10X,'DETENUING=',E15.3)
  WRITE(6,7)N1S,DX,ABS1
  FORMAT(/,5X,'NO. OF PROPAGATION STEPS=',I5,/,5X,'STEP
 1LENGTH IN CM=',E10.4,/,5X,'REDIMENSIONED FIELD ABSORPTION COEF=',
 2E10.4)


   WRITE(6,8)
   FORMAT(/,'         REDIMENSIONED FIELD PARAMETERS')
  WRITE(6,9)AMP,CENTER,WIDTH
  FORMAT(/,'   PEAK FIELD AMPLITUDE=',E10.4,/,'  CENTER='
 1,F8.5,/,2X,'PULSE WIDTH(HW at 1/e maximum)=',E10.3)
  WRITE(6,10)
  FORMAT(/,10X,'MEDIUM PARAMETERS',/,
 1'-----------------------------------------')
  WRITE(6,4) ALFA1,ALFA2,ZI
  FORMAT(' ALFA1=',2(E10.3,1X),2X,' ALFA2=',2(E10.3,2X),/,
 16X,' ZI =',E15.9,/)
  WRITE(6,20)ALFA13,ALFA23
  FORMAT(/,1X,'ALFA13=',2(E10.3,2X),'ALFA23=',2(E10.3,2X))
  WRITE(6,21)DISP
  FORMAT(/,2X,'ADDITIONAL DISPERSION ADDED TO 3RD-HARMONIC=',
 1E10.3,/)
```

```
      WRITE(6,5) T2INV,T1INV
    5 FORMAT(' RELAXATIONS:  1/T2 = ',F8.7,/,13X,' 1/T1 =',F8.7)
      WRITE(6,56)
   56 FORMAT(///,'
     1___________',/,19X,'PROPAGATION STARTS',/,'-----------------
     2------------------------------------')
      RETURN
      END

*****************************************************************
```

```
   SUBROUTINE BLOCH
**************************
   COMPLEX E14,E1C4,Q,PQ,Q1,QD,QD1,E2Q,DQ2,QM,CQ,FE1,DQ,E1Q,E3Q
   COMPLEX ALFA2,ALFA13,ALFA23,TQ,E1,E3,ALFA1,AK1,AK3
   COMPLEX P1,P3,FE3,FE13,CFE13,PL1,PL3,CFEQ
   COMMON/JC/ALFA1,ALFA2,ALFA13,ALFA23,ZI,AK1,AK3,DISP
  1,DOM0,H1,H2,H3,H4,T1INV,T2INV,XH1,XH2,XH3
  2,XH4,XH5,XH6,XH7,XH8,XH9,WL0,H5,H6,H7,H8,H9
  3,IS,NS,MS,AION,DIST,PI,DX,NST
   COMMON/ARYS/E1(2024),E3(2024),TQ(2024),TL(2024)
  1,TW(2024),TU(2024),P1(2024),P3(2024)
   COMMON/OTHER/AMP,CENTER,M,DT,MT,WIDTH,WD2,R12
   COMMON/ARAY/EN1(2000),EN3(2000),E1P(2000),E3P(2000)
  1,ECON(2000),CONVER(2000),ARION(2000)
   THE INPUT TO THIS SUBROUTINE IS A COMPLEX ELECTRIC FIELD
   GIVEN BY THE ARRAYS E1(2024),  (DIMENSION SET
   TO M). THE PARAMETERS ARE THE FREQUENCY MISMATCH FROM
   RESONANCE DOM0 = OMEGA0 - 2*OMEGALIGHT, AND ALL THE MEDIUM
   PARAMETERS SPECIFIED IN SUBROUTINE DEFINE.
      CCL = 0.
      CCU = 0.
   THESE TWO VARIABLES WILL BE USED TO MEASURE THE ENERGY ABSORPTION.
   Q=(0.,0.)
   WL=WL0
   WU=0.
                    QD=(0.,0.)
                    WLD=0.
                    WUD=0.
   Q1=(0.,0.)
   WL1=WL0
   WU1=0.
                     QD1=(0.,0.)
                     WLD1=0.
                     WUD1=0.
                   K21=1
        OMEGA=33.615+(DOM0/400.)
     RAL2=REAL(ALFA2)
     RAL1=REAL(ALFA1)
```

```
   R1=10.5/SQRT(R12)
  DO 1 I=1,M
  FE1=E1(I)
  E1M2=(REAL(FE1))**2+(AIMAG(FE1))**2
  E14=FE1**4
  E1C4=(CONJG(FE1))**4
  IF (ABS(E1M2).LT..1E-20) E1M2=0.
  IF(CABS(E14).LT..1E-20) E14=(0.,0.)
  IF(CABS(E1C4).LT..1E-20) E1C4=(0.,0.)
  FE3=E3(I)
  E3M2=(REAL(FE3))**2+(AIMAG(FE3))**2
  IF(ABS(E3M2).LT..1E-20) E3M2=0.0
      PQ=Q1+H1*QD+H2*QD1
        PU=WU1+H1*WUD+H2*WUD1
          PL=WL1+H1*WLD+H2*WLD1
          PW=PU-PL
  IF(CABS(PQ).LT..1E-20) PQ=(0.,0.)
  IF(ABS(PU).LT..1E-20) PU=0.
    E1Q=E1C4*PQ
   GAM2=-AIMAG(ALFA2)*E1M2-AIMAG(ALFA23)*E3M2
   FE13=FE1*FE3
   IF(CABS(FE13).LT..1E-20) FE13=(0.0,0.)
   CFE13=CONJG(FE13)
   STKS=(RAL1-RAL2)*E1M2+(REAL(ALFA13)-REAL(ALFA23)
1)*E3M2
 STKS=stark-shift in ps-1
   CFEQ=CFE13*PQ*ZI
          DWU2=-(2*GAM2)*PU-2*AIMAG(E1Q)-2*AIMAG(CFEQ)
          DWL2=2*AIMAG(E1Q)+2*AIMAG(CFEQ)
  DQ2=(-(0.,1.)*(DOM0-STKS)-T2INV-GAM2)*PQ+(0.,1.)*(E14+
1ZI*FE13)*PW
           QM=(28.*Q-23.*Q1)/5.+(H3*DQ2-H4*QD-H5*QD1)
      WUM=(28.*WU-23.*WU1)/5.+(H3*DWU2-H4*WUD-H5*WUD1)
         WLM=(28.*WL-23.*WL1)/5.+(H3*DWL2-H4*WLD-H5*WLD1)
         IF(CABS(QM).LT..1E-20) QM=(0.,0.)
         IF(ABS(WUM).LT..1E-20) WUM=0.
        E2Q=E1C4*QM
        CFEQ=CFE13*QM*ZI
    DWU=-(2*GAM2)*WUM-2*AIMAG(E2Q)-2*AIMAG(CFEQ)
    DWL=2*AIMAG(E2Q)+2*AIMAG(CFEQ)
  CU=(32.*WU-WU1)/31.+(H6*DWU2+H7*DWU+H8*WUD-H9*WUD1)
  CL=(32.*WL-WL1)/31.+(H6*DWL2+H7*DWL+H8*WLD-H9*WLD1)
 IF(ABS(CU).LT..1E-20) CU=0.
```

```
      CW=CU-CL
        DQ=(-(0.,1.)*(DOM0-STKS)-T2INV-GAM2)*QM+(0.,1.)*(E14
     1+ZI*FE13)*CW
      CQ=(32.*Q-Q1)/31.+(H6*DQ2+H7*DQ+H8*QD-H9*QD1)
        E3Q=E1C4*CQ
        CFEQ=CFE13*CQ*ZI
           DWU=-(2*GAM2)*CU-2*AIMAG(E3Q)-2*AIMAG(CFEQ)
            DWL=2*AIMAG(E3Q)+2*AIMAG(CFEQ)
            DQ=(-(0.,1.)*(DOM0-STKS)-T2INV-GAM2)*CQ+(0.,1.)*(E14
     1+ZI*FE13)*CW
         QAB=CABS(CQ)
        IF(QAB.LE.1.) GO TO 800
        IF(K21.NE.1) GO TO 801
        WRITE(6,802)
2       FORMAT(3HREQ,12X,3HIMQ,15X,4HE1M2,15X,4HE3M2)
          K21=2
01                WRITE(6,803) CQ,E1M2,E3M2
3          FORMAT(2(E12.5,3X),5X,E12.5,5X,E12.5)
0         IF(CABS(CQ).LT..1E-20) CQ=(0.,0.)
          OMEGA0=32.543-(RAL2*E1M2/100.)
          OMEGA1=11.137+(RAL2*E1M2/100.)
          RAL2=(57./(OMEGA-OMEGA0))+(J15./(OMEGA1-OMEGA))
          RAL2=RAL2*R1
     Q1=Q
     WL1=WL
     WU1=WU
                 QD1=QD
                 WLD1=WLD
                 WUD1=WUD
        QD=DQ
        WLD=DWL
        WUD=DWU
                              Q=CQ
                              WL=CL
                              WU=CU
       TQ(I)=CQ
     TL(I)=WL
     TU(I)=WU
     TW(I)=CW
     PL1=(ALFA1*(TL(I)-1.))+ALFA2*TU(I)
     PL3=(ALFA13*(TL(I)-1.))+ALFA23*TU(I)+DISP
     P1(I)=PL1*FE1+4.*((CONJG(FE1))**3)*TQ(I)+
    1ZI*(CONJG(FE3))*TQ(I)+3.*TL(I)*FE3*((CONJG(FE1)**2))
     P3(I)=PL3*FE3+ZI*(CONJG(FE1))*TQ(I)+TL(I)*(FE1**3)
     P1(I)=PL1*FE1+4.*((CONJG(FE1))**3)*TQ(I)+
    1ZI*(CONJG(FE3))*TQ(I)
```

```
 P3(I)=PL3*FE3+ZI*(CONJG(FE1))*TQ(I)
P1 and P3 are the 1st and 3rd harmonic polarizations.
 CCL=CCL+DWL
    CCU=CCU+DWU

 CCL=CCL*DT
 CCU=CCU*DT
     AION=1.-(TU(M)+TL(M))
         AION=-(CCU+CCL)

 RETURN
 END
```

```
*************************************************************
      SUBROUTINE PULSE
     COMPLEX ALFA2,ALFA13,ALFA23,TQ,E1,E3,ALFA1,AK1,AK3
     COMMON/JC/ALFA1,ALFA2,ALFA13,ALFA23,ZI,AK1,AK3,DISP
    1,DOM0,H1,H2,H3,H4,T1INV,T2INV,XH1,XH2,XH3
    2,XH4,XH5,XH6,XH7,XH8,XH9,WL0,H5,H6,H7,H8,H9
    3,IS,NS,MS,AION,DIST,PI,DX,NST
     COMMON/ARYS/E1(2024),E3(2024),TQ(2024),TL(2024)
    1,TW(2024),TU(2024),P1(2024),P3(2024)
     COMMON/OTHER/AMP,CENTER,M,DT,MT,WIDTH,WD2,R12
     COMMON/ARAY/EN1(2000),EN3(2000),E1P(2000),E3P(2000)
    1,ECON(2000),CONVER(2000),ARION(2000)
     LOGICAL L2

     ESG1 = 0.
     E1MAX=0.

       DO 1 I=1,M
        EF1 = EXP(-((I*DT-CENTER)**2)/WD2)
     IF(EF1.LT..1E-6) EF1=0.
           E1(I)=AMP*EF1
     ESGM=E1(I)*CONJG(E1(I))
      E1M=SQRT(ESGM)
     ESG1=ESG1+ESGM
       L2=E1M.GT.E1MAX
       IF(L2) E1MAX=E1M
            E3(I)=(0.0,0.)
            TU(I)=0.
            TL(I)=1.
        CONTINUE
     ESG1 = TOTAL ENERGY OF SUPERPOSITION PULSE GOING TO THE
     HEAT PIPE;
                  EN1(IS)= ESG1*DT
                  E1P(IS)=E1MAX
                  EN3(IS)=0.0
                  E3P(IS)=0.0
     RETURN
     END
*************************************************************
```

```
*****************************************************************************
   SUBROUTINE OUTPUT
   ******************
   COMPLEX ALFA2,ALFA13,ALFA23,TQ,E1,E3,ALFA1,AK1,AK3
   COMMON/JC/ALFA1,ALFA2,ALFA13,ALFA23,ZI,AK1,AK3,DISP
  1,DOM0,H1,H2,H3,H4,T1INV,T2INV,XH1,XH2,XH3
  2,XH4,XH5,XH6,XH7,XH8,XH9,WL0,H5,H6,H7,H8,H9
  3,IS,NS,MS,AI0N,DIST,PI,DX,NST
   COMMON/ARYS/E1(2024),E3(2024),TQ(2024),TL(2024)
  1,TW(2024),TU(2024),P1(2024),P3(2024)
   COMMON/OTHER/AMP,CENTER,M,DT,MT,WIDTH,WD2,R12
   COMMON/ARAY/EN1(2000),EN3(2000),E1P(2000),E3P(2000)
  1,ECON(2000),CONVER(2000),ARION(2000)
   DIMENSION PH(2024),PH3(2024)
    STEP=FLOAT(IS-1)
    WRITE(6,20)STEP
    FORMAT(2X,'CURRENT STEP IN PROPAGATION=',F10.2)
    WRITE(6,1)DIST
   FORMAT(2X,'DISTANCE OF PROPAGATION IN CM=',F6.3)
   WRITE(6,2)EN1(IS)
   FORMAT(/,2X,'1ST HARMONIC ENERGY=',E10.5)
   WRITE(6,3)EN3(IS)
   FORMAT(/,2X,'3RD HARMONIC ENERGY=',E10.5)
   WRITE(6,19)ECON(IS)
   FORMAT(/,5X,'ENERGY CONVERSION=',E15.10)
   WRITE(6,4)
   FORMAT(2X,4HTIME,11X,6HRE(E1),9X,6HIM(E1),9X,7HABS(E1))
   DO 5 I=1,M,MT
   E1R=REAL(E1(I))
   E1I=AIMAG(E1(I))
   ABE1=E1R**2+E1I**2
   ABE1=SQRT(ABE1)
   TIME=I*DT
   WRITE(6,6)TIME,E1R,E1I,ABE1
   FORMAT(2X,E10.5,3(2X,E13.5))
   CONTINUE
    phase calculation
   DO 7 I=1,M
   PH(I)=0.
   CONTINUE
   E12=0.
   DET=0.
```

```
DO 8 I=1,M
E11=E12
E12=REAL(E1(I))
E1I=AIMAG(E1(I))
IF(ABS(SIGN(1.,E11)*SIGN(1.,E12)-1.).LT..1) GO TO 9
DET=DET+PI*SIGN(1.,E11)*SIGN(1.,E1I)
IF(ABS(E12).GT..1E-9)PH(I)=ATAN(E1I/E12)+DET
IF(ABS(E12).LT..1E-9)PH(I)=PH(I-1)
CONTINUE
WRITE(6,10)
FORMAT(/,8X,4HTIME,16X,5HPHASE)
DO 11 I=1,M,MT
TIME=I*DT
WRITE(6,12)TIME,PH(I)
FORMAT(2X,E10.5,3X,E15.5)
CONTINUE
third harmonic field
WRITE(6,15)
FORMAT(/,2X,4HTIME,11X,6HRE(E3),9X,6HIM(E3),9X,7HABS(E3))
DO 13 I=1,M,MT
 E3R=REAL(E3(I))
 E3I=AIMAG(E3(I))
ABE3=E3R**2+E3I**2
ABE3=SQRT(ABE3)
TIME=I*DT
WRITE(6,14)TIME,E3R,E3I,ABE3
FORMAT(2X,E10.5,3(2X,E13.5))
CONTINUE
 3RD harmonic phase calculation
DO 50 I=1,M
PH3(I)=0.
 CONTINUE
E32=0.
DET3=0.
DO 52 I=1,M

E31=E32
E32=REAL(E3(I))
E3I=AIMAG(E3(I))
```

```
   IF(ABS(E32).LT..1E-20) E32=0.
   IF(ABS(E3I).LT..1E-20) E3I=0.
   IF(ABS(SIGN(1.,E31)*SIGN(1.,E32)-1.).LT..1) GO TO 51
   DET3=DET3+PI*SIGN(1.,E31)*SIGN(1.,E3I)
    IF(ABS(E32).GT..1E-9)PH3(I)=ATAN(E3I/E32)+DET3
   IF(ABS(E32).LT..1E-9)PH3(I)=PH3(I-1)
    CONTINUE
   WRITE(6,53)
   FORMAT(/,4X,4HTIME,5X,18H3RD HARMONIC PHASE)
   MTM=MT
   IF(IS.LT.16)GO TO 58
   MTM=MT/5
     DO 54 I=1,M,MTM
   TIME=I*DT
   WRITE(6,55)TIME,PH3(I)
   FORMAT(2X,E10.5,3X,E15.5)
   CONTINUE
   population vs. time
   WRITE(6,29)
   FORMAT(/,2X,'POPULATION VS. TIME',/)
   WRITE(6,26)
   FORMAT(2X,4HTIME,11X,5HTL(I),10X,5HTU(I),7X,10HLOST ATOMS)
   DO 27 I=1,M,MT
   TLOS=1.-(TU(I)+TL(I))
   TIME=I*DT
   WRITE(6,28)TIME,TL(I),TU(I),TLOS
   FORMAT(2X,E10.5,3(2X,E13.5))
   CONTINUE
   WRITE(6,16)AION
   FORMAT(/,5X,'ION PRODUCED=',E15.5)

   peak field of 1st and 3rd harmonic field
   WRITE(6,17)E1P(IS),E3P(IS)
   FORMAT(/,2X,'FUDAMENTAL PEAK FIELD=',E15.5
  1,/,2X,'3RD HARMONIC PEAK FIELD=',E15.5)
  peak field conversion
    WRITE(6,18)CONVER(IS)
    FORMAT(/,5X,'PEAK FIELD CONVERSION=',E15.10,//)
    WRITE(6,25)
    FORMAT('----------------------------------------')
   RETURN
   END

***************
```

REFERENCES

Abella et al.,"Photon echoes," Physical Review 141, 391 (1966).

Belenov et al.,"Coherent effects in propagation of ultrashort light pulses in a medium with two-photon resonance absorption." Soviet Physics JEPT 29 , 754 (1969).

Besnainou et al., "Molecular multiphoton excitation by phase coherent pulse pairs." J.Chem. Phys. 81, 143 (1984).

Bethe and Salpeter, "Quantum mechanics of one and two electron atoms."

Borisov et al., "Measurement of Lifetimes of 6D Mercury Levels...." Optic Spectrosk, 47(1), 109 (1979).

Diels et al.,"intracavity pulse compression with glass," Optics Letters 8, 4 (1983).

Diels et al.,"Control and measurement of ultrashort pulse shapes," Applied Optics 24, 1270 (1985).

Diels.J.C., "Two-photon coherent propagation ,transmission of 90 phase shifted pulses.", Optical and Quantum Electronics 8, (1976) 513-522.

Diels et al.,"Coherent two photon resonant third and fifth harmonic generation in metal vapors." Physical Review A 19, 1589 (1979).

Diels J-C. and Hahn E.L., "Carrier-frequency distance

dependence ...." Physical Review A 8, 1084 (1973).

Diels J-C., "Coherent propagation and harmonic generation," Proceeding of the VI Vavilov Conference on Coherence and Nonlinear Optics, Novosibirsk, (June, 1979).

Dinev et al., Opt. Quantum Electron. 12, 183 (1980).

Faisal et al., "Time resolved fluorescence spectroscopy " J.Phys B: Atom. Molec. Phys. 13, (1980) 2027-2035.

Feynmann et al., J.Appl.Phys. 28 ,49 (1957).

Georges et al.,"Theory of third harmonic generation in metal vapor under two photon resonant conditions." Physical Review A, 15, 300 (1977).

Georges. A.T. Ph.D Thesis USC. (1976).

Grischkowsky et al.,"Adibatic following model for two photon transition." Physical Review A 12, 2514 (1975).

Johnson et al., Physical Review A 25, 337 (1982).

Kuhn.H.G., " Atomic Spectra," Academic Press, NY, 1969.

Lapidus Leon and Seinfeld John.H., "Numerical solution of ordinery differential equations." Academic Press, NY 1971.

McCall S. L. and Hahn E. L.,"Self-induced transparency by pulsed coherent light," Physical Review Letter 18, 908 (1967).

Miles et al., "Optical third harmonic generation in alkali metal vapors," IEEE J.Qn.Elec. QE-9, 470 (1973).

Milonni P.W. and Eberly J.H., "Temporal coherence in multiphoton absorption....", J.Chem.Phys. 68(4), 1602, (1978)

MIT Wavelength Tables. vol 2., The MIT Press.

Moore C.E., "Atomic Energy Levels," National Bureau of Standards. (GPO, Washington, D.C., 1971).

Mukherjee et al.,"Coherent multiphoton interaction using sequence of of picosecond pulses." Technical Digest XIV International Quantum Electronics Conference (IQEC ,'86), p.78.

Mukherjee.A., Ph.D Thesis, North Texas State University, (1987).

Normand et al., "Resonant multiphoton interaction and third harmonic generation in Hg vapor." J.Phys.B: At.Mol.Phys. 16 (1983) L227-L232.

NSRDS-NBS 35 Vol-I "Atomic Energy Levels as Derived From the Analysis of Optical Spectra."

Smith Arlee.V., "Four Photon resonant third harmonic generation in Hg." Optics Letters 10, 341 (1985).

Sobelman I.I. "Atomic Spectra and Radiative Transition" Springer Verlag. 1979.

Vanherzeele et al., "Spatial and Temporal properties of a tunable picosecond dye-laser oscillator amplifier system," Applied Optics 23, 2056 (1984).